

VISCOELASTIC PROPERTIES OF SOFT TISSUES: APPLICATION TO KNEE LIGAMENTS AND TENDONS

THÈSE N° 1643 (1997)

PRÉSENTÉE AU DÉPARTEMENT DE PHYSIQUE

ÉCOLE POLYTECHNIQUE FÉDÉRALE DE LAUSANNE

POUR L'OBTENTION DU GRADE DE DOCTEUR ÈS SCIENCES

PAR

Dominique P. PIOLETTI

Ingénieur physicien diplômé EPF
originaire de Chavannes-près-Renens (VD)

acceptée sur proposition du jury:

Prof. J.-J. Meister, directeur de thèse
Dr A.A. Amis, corapporteur
Prof. J. Botsis, corapporteur
Prof. K. Hayashi, corapporteur
Prof. P.-F. Leyvraz, corapporteur
Dr L.R. Rakotomanana, corapporteur

Lausanne, EPFL
1997

*“... Il n’y a de science que par une école permanente.
La société sera faite pour l’école et non pas l’école pour la société.”*

Gaston Bachelard, 1938

Remerciements

Ce travail de thèse a bénéficié de l'apport et des conseils de nombreuses personnes. Je ne peux les citer toutes ici (la liste serait trop longue!), je leur témoigne par ces lignes ma reconnaissance.

Le Prof. J.-J. Meister a dirigé cette thèse. Son laboratoire m'a offert les conditions idéales pour la réalisation de ce travail de recherche. Je le remercie pour la confiance qu'il m'a témoignée ainsi que pour ses conseils judicieux. Ses suggestions m'ont permis d'approfondir différents points de ma thèse.

Le Prof. P.-F. Leyvraz a supervisé la partie clinique de cette thèse. Je le remercie pour son investissement personnel et pour ses conseils éclairés tout au long de la thèse. Il a toujours su trouver du temps à me consacrer quand j'en avais besoin, malgré un agenda bien rempli ...

J'exprime toute ma gratitude au Dr. L. Rakotomanana. Il m'a fait bénéficier de sa rigueur scientifique, de sa curiosité et de son esprit de synthèse hors du commun tout au long de ma thèse. Je lui dois beaucoup tant sur le plan scientifique que sur le plan humain.

J.-F. Benvenuti m'a supporté comme collègue de bureau pendant 4 ans. Je le remercie pour les intéressantes discussions scientifiques et moins scientifiques que l'on a eues pendant ce travail. Je remercie également P. Beillas, R. Conde, L. Faber, C. Gilliéron, J. Heegaard, F. Lauper, O. Ramambason, N. Ramaniraka, M. Sartirani, A. Terrier et M. Waliszewski pour leurs diverses contributions à ce travail.

Je remercie l'équipe de l'atelier mécanique D. Godat, J. Knoepfli et G. Ney qui, même avec de faux plans, m'ont fourni des pièces correctes!

D'une manière générale, je remercie toute l'équipe du LGM (ancienne et actuelle) pour l'ambiance de travail agréable et sympathique qu'ils ont su créer.

Plus personnellement, je tiens à exprimer toute ma reconnaissance à mes parents et à ma soeur pour leur soutien et encouragements pendant toute la durée de mes études.

Finalement, je remercie Myriam pour sa patience et compréhension durant toute la durée de cette thèse et plus spécialement pour les derniers mois où le genre de phrase "il faut juste que je change un petit truc dans la thèse" a été très utilisé.

Ce travail a bénéficié du soutien financier de l'Hôpital Orthopédique de la Suisse Romande.

Abstract

Ligaments play a central role in the stability of the knee. Due to the increase in sport activities of the young population, rupture of the anterior cruciate ligament (ACL) has become a frequent clinical problem. A surgical procedure replacing the deficient ligament is performed to restore the knee's initial stability. Although this surgical technique is widespread and well established, long term clinical results are inconsistent and the stability of the knee is not always restored, leading to premature arthrosis of the knee. This inconsistency of ACL replacement motivated the present study. "Optimal" ACL replacement only can be performed if the static and dynamic properties of the ligament are precisely known.

In order to investigate these mechanical properties, an experimental set-up was developed to test human cruciate ligaments, as well as patellar tendon, which is commonly used for cruciate ligament replacement. Traction tests at different constant rates of elongation and stress relaxation tests were performed at controlled temperature (37°C) and humidity (100%). Results showed that cruciate ligaments and patellar tendons exhibit a non-linear elastic behavior in addition to a viscous behavior. The viscous behavior encompassed two phenomena: first a behavior where stress depended on strain rate (short term memory effects) and second a behavior where stress relaxed on a longer time scale (long term memory effects).

In order to describe the different mechanical behaviors of the specimens in a general mechanical framework, a theoretical model was developed by simultaneously taking into account the non-linear elastic behavior, the short term memory effects and the long term memory effects. This proceeding satisfied the basic mechanical and thermodynamical requirements. The originality of the present model is based on the fact that the different mechanical behaviors are described in one framework allowing a compact description of the biomechanical properties of different soft tissues. The description of the short term memory effects is new in situations involving large deformations. The model is restricted by considering the specimens as isotropic, homogeneous and incompressible.

The identification process of the different mechanical behaviors was facilitated with the proposed model. The non-linear elasticity was described with two parameters, the short term memory effects with one parameter and the long term memory effects with six parameters. No statistical differences were found between the parameters used for the anterior cruciate ligaments, the posterior cruciate ligaments and patellar tendons. The non-linear elastic behavior was implemented in a finite element code. The stress field in an ACL was calculated during a knee flexion and a tibial drawer test. The calculated stress field was inhomogeneous, with the highest stress in the anteriomedial part of the ACL. It was found that internal rotation of the knee generally increased the calculated stress in the ACL. These numerical results agree with *in vitro* studies given in the literature. The numerical results yielded a stress field in the ligament which was complementary to *in vitro* studies, where only the resultant ligament force can be measured.

Several useful clinical conclusions can be drawn from the present biomechanical study. Diagnosis of an ACL rupture is generally performed by a contralateral comparison of antero-postero knee laxity (tibial drawer test) using a quasi-static load. However, diagnosis of an injured knee would be more accurate if the antero-postero load was dynamically applied to the knee: in this case, a knee with a rupture ACL would not show any effect, whereas a knee with an intact ACL would become stiffer with increasing the strain rate. In case of ACL replacement, the graft should be preconditioned in order to diminish the effects of stress relaxation. During the rehabilitation program after an ACL suture or replacement, flexion of the knee in an internal position should be omitted because internal rotation increases the stresses in the ligament.

Résumé

Les ligaments croisés jouent un rôle essentiel dans la stabilité du genou, où ils sont soumis à des efforts importants. De part l'activité sportive croissante dans notre société, des accidents impliquant une rupture du ligament croisé antérieur (LCA) sont devenus courants. Afin de remédier à l'instabilité qui suit cette rupture, une intervention chirurgicale consistant à remplacer le ligament déficient par une greffe peut être effectuée. Bien que cette technique soit relativement ancienne et courante, les résultats à long terme sont inconsistants. La restauration de la stabilité du genou n'est pas toujours assurée et des problèmes d'arthrose précoce sont alors possibles. Cet état de fait a motivé la présente étude. Le remplacement "optimal" du LCA lésé ne peut être obtenu que si les propriétés biomécaniques statiques et dynamiques de ce ligament sont précisément connues et décrites.

Dans ce but, un banc expérimental a été développé afin d'effectuer des tests mécaniques sur des ligaments croisés et tendons rotuliens humains, ce dernier tissu étant couramment utilisé comme greffe de LCA. Ce banc expérimental permet des tests de tractions à vitesses constantes, ainsi que des mesures de relaxation des contraintes, ceci dans un environnement contrôlé à 37°C et 100% de taux d'humidité. Les résultats ont montré que les ligaments croisés et tendons rotuliens ont un comportement élastique non linéaire en plus d'un comportement visqueux. Ce comportement visqueux regroupe en fait deux phénomènes, un comportement où la contrainte dépend du taux de la déformation (viscosité à mémoire courte) et un comportement où la contrainte diminue au cours du temps (viscosité à mémoire longue).

Afin de décrire dans un cadre unique les différents comportements mécaniques des spécimens, un modèle théorique est développé. Il permet de tenir compte à la fois du comportement élastique non linéaire, de la viscosité à mémoire courte et de la viscosité à mémoire longue. Ce modèle satisfait les lois de conservations mécaniques ainsi que les principes de la thermodynamique. L'originalité du modèle réside dans le fait que les différents comportements mécaniques sont décrits dans un cadre unique, permettant ainsi une description concise du comportement biomécanique des tissus mous considérés. La description de la viscosité à mémoire courte dans le cas de déformations finies est également originale. Le modèle est limité au cas où les spécimens sont considérés comme isotropes, homogènes et incompressibles. L'identification expérimentale des différents comportements mécaniques est de plus facilitée par la modélisation proposée. Ainsi, le modèle a deux paramètres pour décrire l'élasticité non linéaire, un paramètre pour la viscosité à mémoire courte et finalement 6 paramètres pour décrire la viscosité à mémoire longue. De part la diversité des comportements mécaniques des spécimens, les paramètres obtenus n'ont pas montré de différence statistique entre ligaments croisés antérieurs, ligaments croisés postérieurs et tendons rotuliens.

La partie du modèle décrivant le comportement élastique non linéaire a été implémentée dans un code d'éléments finis. La distribution des contraintes a pu être calculée dans un LCA lors d'une flexion ainsi que lors d'un test clinique de mesure du

tiroir antérieur du genou. Cette distribution s'est révélée inhomogène. Les contraintes les plus élevées se trouvent sur la partie antéro-médiale du LCA près de l'insertion fémorale. D'une manière générale, la valeur des contraintes calculées augmentent lors de rotation interne du genou. Ces résultats sont confirmés par des études expérimentales de la littérature. En donnant accès au champ des contraintes dans le LCA, l'étude numérique présentée apporte des informations complémentaires aux études *in vitro* où seule la force résultante dans le LCA peut être mesurée.

De cette modélisation biomécanique, quelques résultats utiles aux cliniciens ont pu être obtenus. Dans le cas de diagnostic de rupture du LCA, il serait plus aisé de mettre en évidence une laxité inter-genoux si les tests étaient faits de manière dynamique. En effet, les tests dynamiques augmenteraient les contraintes dans le genou avec LCA rendant ce genou plus rigide, alors qu'ils n'auraient aucun effet sur la laxité du genou lésé. Lors d'un remplacement de LCA par une greffe biologique, celle-ci devrait être préconditionnée afin de diminuer la relaxation de la contrainte. Finalement, les programmes de réhabilitation à la suite de sutures ou de remplacements du LCA, devraient éviter tous mouvements impliquant une rotation interne du genou (au moins immédiatement après l'opération), la valeur des contraintes étant augmentée lors de tel mouvement.

Table of contents

1 Introduction and motivations	1
1. 1 Anatomy of the knee.....	1
1. 2 Rupture situations	4
1. 3 Research motivations	6
1. 4 State of the art in experiments	6
1. 5 State of the art in theory.....	10
1. 6 Summary	13
1. 7 Thesis objectives.....	13
2 Continuum based theory	15
2. 1 General principles.....	15
2. 2 Viscoelastic constitutive laws.....	19
3 Mechanical tests	25
3. 1 Material and methods.....	25
3. 2 Experimental results.....	33
3. 3 Discussion	40
4 Identification of the constitutive laws	43
4. 1 Elastic identification	43
4. 2 Viscous identification	49
4. 3 Viscoelastic constitutive law	56
4. 4 Discussion	56

Table of contents

5 Numerical simulations of the ligament stress field	61
5.1 Numerical model	61
5.2 Numerical results.....	66
5.3 Discussion	73
6 Conclusions and perspectives	75
6.1 Conclusions.....	75
6.2 Perspectives.....	76
Bibliography	79
Appendix A Mathematical background of the long term memory effects	91
A.1 Three general principles	91
A.2 Mathematical interpretation of the fading memory principle.....	92
Appendix B Elastic potentials tested in the compressible case	95
Appendix C Elastic, short term memory effects and long term memory effects identification	97
C.1 Elastic and short term memory effects identification.....	97
C.2 Relative relaxation	100
C.3 Long term memory effects identification	103

CHAPTER 1 *Introduction and motivations*

The ligaments play a central role in the stability of the knee. Due to the increase in sport activities of the young population, rupture of the anterior cruciate ligament has become a frequent clinical problem. However, the success of surgical treatments is inconsistent. Therefore, biomechanical studies were performed in order to understand the stabilizing role of the ligaments inside the knee. Mechanical behavior was demonstrated in non-linear stress-strain curves, stress dependence on the strain rate and stress relaxation. The different mechanical behaviors were generally identified with distinct theories.

The first objective of this thesis is to develop a general mechanical framework to describe the different mechanical behaviors of the soft tissues as ligaments. This framework satisfies the basic mechanical and thermodynamical requirements. The second objective is to create an experimental model and to identify the experimental data with the developed theory. The final objective is to perform numerical simulations of the stress in the ligament under different mechanical situations.

1. 1 Anatomy of the knee

The knee joint consists of three pieces of bone: the femur, the tibia and the patella. This articulation has six degrees of freedom. However, it mainly works in flexion-extension. The knee is principally charged in compression under the force of gravity. This joint allows an internal-external rotation (i.e. the rotation of the leg along its longitudinal axis). This rotation occurs only when the knee is flexed.

From a mechanical point of view, the knee has two contradictory functions:

- to have a good stability in full extension, position in which the knee supports large stresses due to the body weight and to the length of the arm lever;
- to get a large mobility from a certain flexion angle, mobility necessary for running and for the optimum orientation of the foot.

The knee combines these contradictory functions thanks to some ingenious mechanical systems. One of these is the ligament system. Four main ligaments can be

found in the knee, the two medial and lateral ones at the periphery of the joint and the two cruciate ligaments (anterior and posterior) inside the joint.

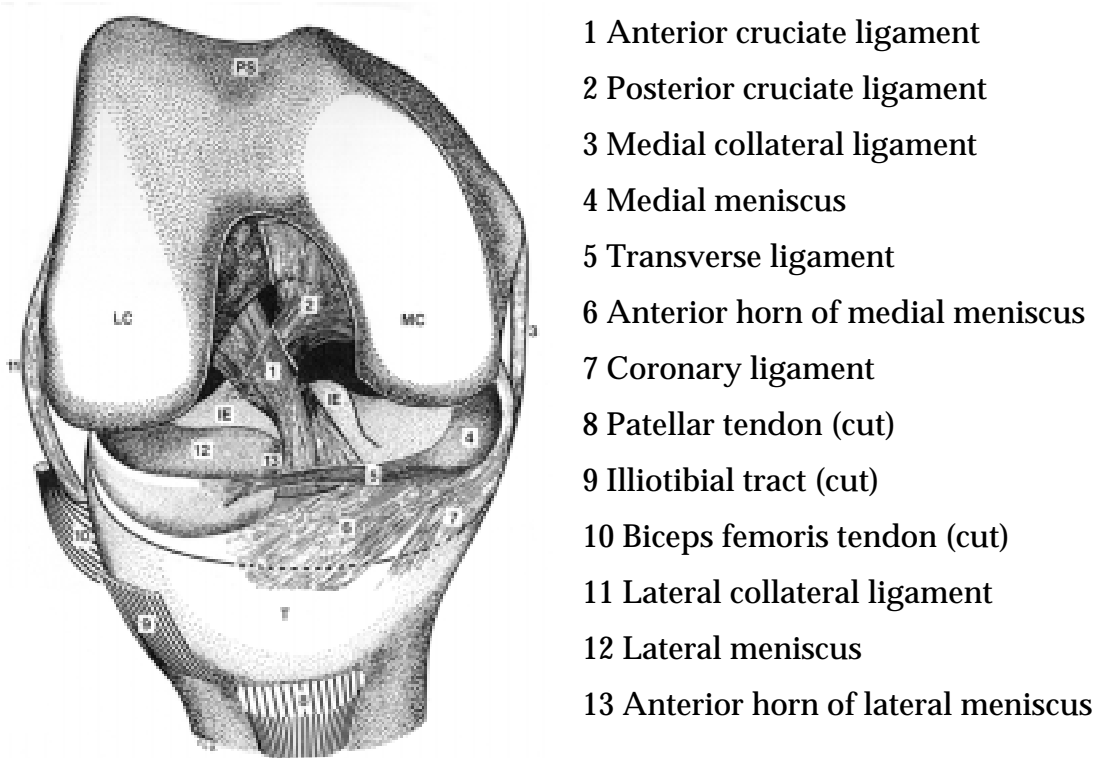


Figure 1.1 Anatomy of the knee with the joint at 90° of flexion.

1. 1. 1 Ligaments function

The main function of the ligaments is to avoid injury by limiting the motion of the joint. Each ligament has a particular function due to its position and shape. Generally, the collateral ligaments give a lateral stability of the knee in extension. The cruciate ligaments stabilize the antero-posterior motion and keep the articular areas in contact during flexions. Moreover, the collateral ligaments limit the external rotation while the cruciate ligaments limit the internal one.

The ligaments are not the only structures working for the stability of the knee. There is a combination of different related elements: the ligaments, the capsulo-ligament elements, the musculature and the shape of the tibial tray and distal femur (Figure 1.1.). The ligaments also function to transmit information to the central nervous system.

1. 1. 2 Ligaments structure

The lateral ligaments are stretched when the knee is in extension and relaxed during flexion. The fibers of the cruciate ligaments have not all the same length.

Consequently, they are not stretched at the same flexion angle. Similar to muscles, there is fiber recruitment [Blankevoort, 1991]. The cruciate ligaments are in contact with each other. They are not free inside the joint cavity but are covered by the synovial membrane. It is interesting to note that the ligaments can sustain stress until rupture without external evidence e.g. [Kennedy, 1974]. The ACL can be divided in a posterior and an anterior bundle. The posterior bundle is composed of small fascicles embedded in a loose alveolar tissue, whereas the anterior bundle is formed of dense, thick collagen fascicles. The ACL fascicles approximately follow an helical path along the ligament axis. *In situ* observations show that the anterior bundles are loaded more frequently and more heavily than the posterior bundles [Hollis, 1993].

Water represents 65 to 70% of the total weight of an ACL [Woo, 1986]. The dry weight of a normal ACL is 70 to 80% type I collagen. This collagen is supposed to be relatively inactive from a metabolic point of view and has a half life of 300 to 500 days. The maximum collagen molecule length and diameter are 300nm and 1.5nm respectively. The collagen molecules have a screwlike shape. Three of these screws fit together to build a super screw which is called tropocollagen and four or five tropocollagen fit together to create a microfibril.

The fibers are bound to each other and the surrounding matrix by several different bonds (covalent, ionic, etc.). The matrix is composed of proteoglycan and glycosaminoglycan. It represents 1% of the dry weight of the ligaments. The lateral ligament fibers are in parallel with each other and the cruciate ligament fibers are interlaced. However at high magnification, the ACL fibers are parallel [Kennedy, 1974; Oakes, 1993] (Figure 1.2.).



Figure 1.2 Scanning electron micrographs of normal human ACL, demonstrating the wave-like configuration and parallel arrangement of groups of collagen fibrils from [Kennedy, 1974].

The ACL is irrigated by blood. The only elastin fibers found in the ACL come from the blood vessels. As previously mentioned, the ACL are innervated [Kennedy, 1974; Madey, 1993] and can play a sensor role for the knee [Brand, 1986].

1. 2 Rupture situations

A review of sport related injuries reveals a high percentage of knee ligament injuries. Of the four main ligaments, the anterior cruciate is the one most frequently damaged [Fetto, 1980]. It has been estimated that there are almost 75,000 ACL ruptures annually in the United States [Brown, 1993].

ACL injuries generally occur during dynamic loading. ACL injuries that occur due to skiing are described as a violent rotation of the tibia on the femur [Speer, 1995]. In soccer, the collision of one player with another and being kicked by an opposing player were the most frequent causes of ACL injuries [Lindenfeld, 1994]. The most common mode of injury in volleyball occurs during the landing phase of a jump [Ferreti, 1992]. In summary, the majority of the ACL ruptures arises during sudden motion of the tibia relative to the femur. This observation was already made e.g. [Crowninshield, 1976] as it was noticed that sport-related injuries occur at strain rates estimated to vary from relatively slow rates to as much as 500%/s.

ACL instability is associated with a high rate of concomitant injuries [Duncan, 1995]. Meniscal lesions are especially common [Bray, 1989]. Degenerative changes in the articular cartilage are then possible [McDaniel, 1980]. Despite the fact that ACL rupture is common, the clinical treatment is not straightforward.

1. 2. 1 Conservative treatment

In some cases, ruptures of ACL are not surgically treated. Non-surgical treatment is called conservative treatment. It has been shown that physiotherapy can help increase stability in a deficient knee [Fridén, 1991]. Knee instability can also be reduced with the use of tape or a brace [Anderson, 1992].

The non-operative treatment is recommended in cases where part of the injured ACL remains functional in the initial stability examination. Even in athletes, partial injuries can be successfully treated without surgery [Kannus, 1992]. The only alarming factor is the high rate of cartilage degeneration [Sommerlath, 1992]. This remark highlights the limit of the conservative treatment.

1. 2. 2 Surgical treatment

According to the literature, the surgical repair of an intrasubstance tear of the ACL is clinically inferior to the reconstructive option [Fu, 1993]. Clinical and experimental studies have consistently shown a lack of repair or healing of the ACL after injury. This has been confirmed by *in vitro* studies where ACL cells exhibit lower rates of cell division, growth and migration than lateral ligament cells [Nagineni, 1992].

Consequently, extensive surgical procedures have been developed for ACL replacement. Although this procedure has been in existence for a long time e.g. [Robson, 1903], there is not a consensus on the surgical technique. Two main options

are available: intra-articular or extra articular positioning of the graft. Based on biomechanical studies, there has been no motivation for using the extra-articular procedure e.g. [Amis, 1993].

With the intra-articular option, the orientation and position of the tunnels into the bones play a significant role on the amplitude of the flexion-extension that a patient can reach post-operatively [Djian, 1994; Graf, 1993; Romano, 1993]. It has been proposed e.g. [Fu, 1996] that the insertions sites for the graft should be identical to those of the ACL.

The graft type is another important parameter. The central one-third of the patellar tendon (PT) is the most commonly used graft in an ACL reconstruction [Jackson, 1993]. In fact, this tissue has been used in ACL replacement since 1939 [Campbell, 1939]. Comparisons between the use of PT, doubled semitendinous, gracilis tendon and quadriceps tendon grafts show that the PT gives better clinical results [Aglietti, 1994]. In addition to natural material, a composite collagenous prosthesis was developed [Dunn, 1992].

There are two different types of grafts: autograft (tissue taken from the patient) and allograft (tissue taken from a bank). The latter needs to be sterilized in order to avoid transmission of diseases. Obviously, this sterilization should not decrease the mechanical properties of the grafts. For example, gamma irradiation (for sterility) followed by solvent drying (for preservation) has been found to be a good procedure for the preservation of tendon graft [Maeda, 1993]. The motivation for using an allograft is to avoid the patellar pain that frequently occurs following the harvesting of the central part of the patella for ACL replacement [O'Brien, 1991].

The tensioning of the graft during the surgical procedure is critical e.g. [Amis, 1989]. Its value not only influences the laxity of the knee repair, but also affects the healing and remodelling process e.g. [Beynon, 1993; Hayashi, 1996]. Upon extensive literature review of the isometric problem of graft placement, several contradictions are found e.g. [Amis, 1995].

Biologic grafts exhibit an initial loss of strength [Bosch, 1992]. Consequently synthetic augmentation has been used to increase the initial strength of the graft. Some investigators have judged the results to be satisfactory e.g. [Amendola, 1992] while others have found this technique to be unconvincing e.g. [Kerboull, 1993].

Despite the existence of biological grafts, synthetic materials are also used for the entire graft. The materials used vary from polyester fibers [Amis, 1994], carbon fibers [Demmer, 1991], Gore-Tex [Paulos, 1992] to Dacron [Andersen, 1992; Barrett, 1993]. The clinical results were not satisfactory for most of the synthetic materials. The failures were mostly due to high frequency ruptures, wear, plasticity or post-operative infections.

The determination of the “optimal” ACL reconstruction has involved many clinical studies. However, long term results of the ACL replacement have been classified satisfactory for only 66% of the cases e.g. [Aglietti, 1992]. Rehabilitation difficulties,

patello-femoral problems and loss of motion all contribute to the lower success rate. After 2 years, the PT graft differs structurally and mechanically from a ligament suggesting that this graft may never approach normal ligament characteristics [Bosch, 1992]. Moreover, a disturbing finding showed that there is an increase incidence of degenerative joint disease in the reconstructed patients, compared to the patient treated without ACL surgery e.g. [Daniel, 1993].

1. 3 Research motivations

All the clinical inconsistencies yield inconstant long term results which further establish the fact that the ACL mechanical behavior of a normal knee is not well understood. The diversity of proposed treatments in case of ACL rupture reflects this lack of understanding. Moreover, many surgical parameters such as insertion zones, initial tensioning of the graft or even the position of the knee during the drilling of the tunnels hole are not uniquely defined. Therefore, an increased understanding of the mechanical properties of the ACL and graft function is required to improve ACL surgical repair. One method of developing further knowledge about ACL function is through biomechanical studies.

Biomechanics is a general term for the mechanical concepts that are used to describe the properties of a living tissue. From these mechanical concepts, experimental, theoretical and numerical studies are developed to better understand the role of the ligaments and grafts in knee stability.

The following section is a review of the main biomechanical results from experimental, theoretical and numerical studies found in the literature.

1. 4 State of the art in experiments

There are two different approaches to describe the mechanical behavior of the knee ligaments:

- 1) force or elongation measurements during a flexion of the knee;
- 2) force and elongation measurements during traction tests.

The first test furnishes general information useful in understanding rupture situations. From a surgical point of view, this test provides a method for determining some critical values that a ligament graft should meet. Comparisons of mechanical behavior between the ligaments and their grafts during physiological loading situations are possible. However, these results are difficult to translate into a theoretical mechanical formulation. The theoretical model is attainable when the two principal variables (force and elongation) are measured simultaneously. The second

kind of tests is then performed. Traction tests are used to determine relationship between force and elongation (or stress and strain).

1. 4. 1 Force or elongation measurements during a flexion of the knee

1. 4. 1. 1 Elongation measurements

Basic *in vitro* measurements of ligament elongation begin by isolating some fibers and marking their femoral and tibial insertion [Blankevoort, 1991; Hefzy, 1986; Sidles, 1988]. The position of these insertions are then measured as a function of knee flexion. If the fiber length is assumed to be the straight line joining the tibial and femoral insertions, then fiber elongation is measured as a function of knee flexion. It has been found that the posterior bundles of the ACL are stretched in extension; whereas, the anterior bundles are mainly stretched during flexion. Qualitative comparisons between specimens or studies are uncertain due to the difficulty of isolating the same fibers. Nonetheless, it is generally accepted that anterior displacements increase the fiber length of the ACL. This type of study assumes that the elongation of the ligament is uniform. However, it has been shown that spatial variations in strain values exist along the ligament length with greater magnitudes occurring at the insertion sites [Beynnon, 1993]. These results were obtained from *in vivo* tests in which an Hall effect transducer was used to directly measure strain on the ligament.

1. 4. 1. 2 Force measurements

There is an indirect and a direct method to perform force measurements. The indirect method is based on reproducible motions. The entire knee is tested under special motions, the corresponding forces and couples are measured. The tests are then repeated with only the ACL (other soft structures are removed). The force acting in this ligament can then be calculated. An uneven force distribution has been found in the ACL during the application of anterior forces. The force transmission was maximal when the knee was flexed at 30° e.g. [Hollis, 1993]. Through universal force measurement device, it was determined that the antero-medial portion of the ACL carries the majority of an anterior applied force e.g. [Fujie, 1995].

The direct method uses force transducers directly placed on the ligaments [Holden, 1994; Lewis, 1982]. Position of the transducer on the ligament can greatly affect the results [Barry, 1986]. Comparisons between ACL and graft force measurements after an intra-articular operation have been performed and the amount of force was more important in the graft than in the ACL. There was no logical explanation [Lewis, 1989]. *In vivo* human force measurements show that the peak force in ACL is reached at full

extension [Roberts, 1994]. This result agree with the *in vitro* study displayed in Figure 1.3.

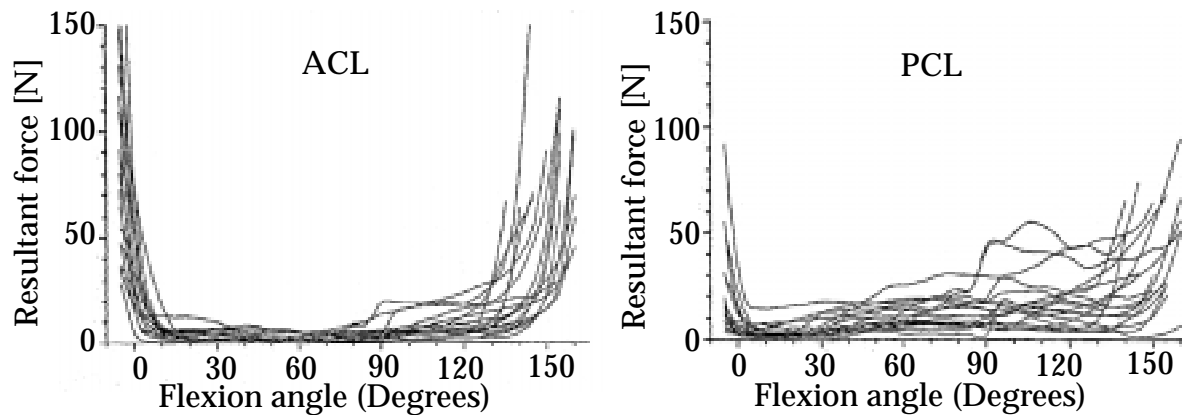


Figure 1.3 Resultant anterior and posterior cruciate ligaments force as a function of the flexion angle for 18 human specimens (*in vitro* study) [Wascher, 1993].

1. 4. 2 Force and elongation measurements during a traction test

Mechanical descriptions of ligaments obtained from traction tests are divided in two classes, the structural and the mechanical properties. The structural properties consider the tensile behavior of the bone-ligament-bone complex as a functional composite. The mechanical properties are the material characteristics of the ligament substance. Many studies have been performed to determine the mechanical properties of the ligament. However, from a surgical point of view, structural properties are more important than mechanical properties e.g. [Hayashi, 1996]. It is the whole structure (bone-ligament-bone) which mechanically stabilizes the knee and not only the ligament itself. As noted e.g. [Woo, 1993], surprisingly little research has been done on the tensile properties of the human ACL. For the rest of this study, only structural properties will be considered.

Several parameters can influence the mechanical behavior of the ligaments during a traction test. Some have been identified: the age [Noyes, 1976], the strain rate [Kennedy, 1976], the sex [Goldstein, 1987], the temperature [Lam, 1990], the hydration [Chimich, 1992] and the fiber orientation during the traction tests [Woo, 1993]. Data comparisons among studies should only be performed once these parameters are accounted for.

The stress dependence on the strain rate in ligament biomechanics has a controversial history. It was generally accepted that mechanical behavior of ligaments or tendons are not strain rate dependent e.g. [Fung, 1973] and some others authors e.g. [Dorlot, 1980; Woo, 1981; Yamamoto, 1996] came to the same conclusion. However, if we carefully examine the results of Fung [Fung, 1973], strain rate effects are visible in the stress-strain curves. Furthermore, review of the literature reveals that strain rate effects on the mechanical behavior of soft tissues is not uncommon. It was found that

the maximum load tolerated by isolated human ACL increased by 32% on the average for a fourfold increase in strain rate e.g. [Kennedy, 1976]. Strain rate effects have been demonstrated in tendons [Haut, 1983; Sanjeevi, 1982], intrinsic and extrinsic human wrist ligament [Nowalk, 1991], rat incisor periodontal ligament [Chiba, 1993], canine anterior cruciate ligament [Haut, 1969] rabbit anterior cruciate ligament and patellar tendon [Danto, 1993]. These strain rate effects have been confirmed *in vivo* with a goat model where it was found that faster gait leads to greater ACL forces [Holden, 1994].

1. 4. 2. 1 Uniaxial loading

One dimensional mechanical traction tests are the most common tests performed on ligaments. These tests can be applied to the entire knee or on isolated ligaments.

Tensile tests performed on the entire knee have the advantage that the orientation of the insertion zones are physiologic. This orientation must be precisely controlled, otherwise this advantage vanishes [Woo, 1993]. A video dimensional analyser is used to measure strain [Woo, 1993]. This method requires a regular surface and sufficient space to fix markers on the ligaments. This method is often used with the lateral ligaments. It gives a local representation of the strain which is not necessarily representative of the whole ligament.

Isolated ligament traction tests were performed with either the whole ligament [Kennedy, 1976], different bundles of fibers [Butler, 1992] or groups of fibers [Mommersteeg, 1996]. For example, traction tests performed on the antero-medial bundles of the ACL resulted in a failure load almost four time greater than the posterior bundles e.g. [Butler, 1992].

From the traction tests, one dimensional force-elongation and hence stress-strain curves are obtained. The behavior of these curves was always similar. The initial non-linear portion of the curve was followed by an almost linear stress-strain curve. The assumption of mechanical isotropy of the specimens is necessary for the uniaxial tests used to identify three dimensional constitutive laws. This assumption may be limiting. Transverse isotropy is a more realistic assumption. The identification process requires not only uniaxial testing but also biaxial testing.

1. 4. 2. 2 Biaxial loading

It is difficult to apply biaxial loading to cruciate ligaments because of their geometrical dimensions. Transverse loading is limited by the fact that the transverse load must be anchored to the soft structure of the ligaments. This direct clamping generates artifacts in the stress and strain measurements. The presence of artifacts in measurements could explain the lack of experimental data for biaxially loaded ligaments in the literature. Biaxial loading has been performed on human fascia lata specimens e.g. [Weiss, 1994]. Stress-strain curves obtained along the fiber direction showed the previously mentioned trend (non-linear part following by a linear one),

while stress-strain curves for transverse loading (perpendicular to the fiber direction) show an almost linear behavior. The identified transverse constitutive law has been applied to ligaments and this procedure is questionable because fascia lata and ligament specimens have been demonstrated to have different mechanical properties e.g. [Butler, 1984].

1. 5 State of the art in theory

There are two approaches to describe the mechanical behavior of the soft tissues:

- 1) structural approach which takes into account the tissue structure;
- 2) continuum approach based on continuum mechanics theory.

1. 5. 1 Structural approach

The structural approach starts with a description from the fiber level so that the constitutive relations for the whole tissue can be obtained [Lanir, 1979]. Basically, the macroscopic response of the material is predicted based on the mechanical properties of the constituent materials, the geometric factors describing the microscopic structure and the interactions between the components. This approach enables to understand the mechanical role of the geometrical structure in soft tissues. The fiber orientation can be obtained with scanning electron photomicrographs e.g. [Ault, 1992]. Based on an initial length distribution, expression for the force can be calculated. Comparisons between experimental and theoretical unidimensional stress-strain curves give good results e.g. [Decraemer, 1980]. In the structural approach, it is assumed that the tissue's response is the sum of the responses of its constituents. Even if the constituents are considered to be linearly elastic the combined system can be non-linear due to the nonuniformity in its structures. The constituents can have however different mechanical properties. This concept was used to model flat collagenous tissues and it was found that the nonuniformity in the geometrical structure of the fibers accounted for the non-linear stress-strain relations. It should be noted that mathematical formulations of structural model can be very complex rendering this description intractable [Stouffer, 1983].

The ligaments do not stretch all their fibers at the same knee flexion. Therefore, stiffness characteristic of the ligament is variable. It has been proposed to model the ligament as the addition of non-linear elastic line elements e.g. [Mommersteeg, 1996]. This type of model requires experimental force or displacement measurements during a flexion of the knee as input.

1. 5. 2 Continuum approach

The continuum theory was brought to biomechanics through the work of Fung [Fung, 1973]. The properties of a tissue are known once its constitutive law (stress-strain relation) is determined. Therefore the continuum approach consists of an interpretation of the experimental stress-strain curves obtained with the traction tests. This interpretation is called the identification process. Three different identifications are performed in ligaments biomechanics: linear elasticity, non-linear elasticity and non-linear viscoelasticity.

1. 5. 2. 1 Linear elasticity

The linear elastic identification considers only the linear part of the stress-strain curve. The modulus of elasticity reduces to one number in this case, which facilitates comparison of results from different studies. For the human ACL separated in two bundles, linear identification can be used to determine the modulus of elasticity for the anterior bundle 283.1 [MPa] and for the posterior bundle 154 [MPa] e.g. [Butler, 1992]. The modulus of elasticity of the posterior cruciate ligament has been estimated to be 250 [MPa] e.g. [Race, 1994] and 365 [MPa] for the patellar tendon (PT) in a young population e.g. [Flahiff, 1994]. These values are given as illustration and are not demonstrating the varied values found in the literature. The effects of different parameters (age, strain rate, orientation of the fibers, c.f. section 1. 4. 2) should be considered when comparing the modulus of elasticity between studies.

Linear elastic identification can give an imprecise mechanical description. This identification overestimates the stress-strain curve in the beginning of the curve (which is called the toe region). The toe region usually encompasses the physiological range of normal tissue function [Fung, 1981] and therefore it is important to have a correct description of this region. Linear description considers two different specimens mechanically identical if the linear section of their stress-strain curve are identical, even if the non-linear section of their stress-strain curve are different. A more precise elastic identification is motivated by the deficiencies of the current method.

1. 5. 2. 2 Non-linear elasticity

The modulus of elasticity becomes a function of the strain with the non-linear elastic identification. Consequently, parameters comparison between studies can be performed only if the same function is used. It has been proposed to model the modulus of elasticity as a linear function [Fung, 1973]. The corresponding stress-strain relationship is given by an exponential function in this case. This model accurately represents the mechanical behavior of soft tissue. A more refined model can be obtained if the modulus of elasticity is described by two (or more) linear functions.

In case of finite deformation, a popular approach has been to postulate the form of an elastic potential from which the stress-strain relationship was derived. Different forms of elastic potentials can be found in the literature. A general form of elastic potential W for soft tissue behavior is e.g. [Veronda, 1970]:

$$W = C_1(\exp[\beta(I_1 - 3)] - 1) + C_2(I_2 - 3) + g(I_3)$$

where C_1 , C_2 , β are material constants and g is a function which becomes zero if the material is incompressible. I_1 , I_2 and I_3 represents the strain invariants. The exponential description of the elastic potential accurately describes the experimental stress-strain curves. Good results were found for soft tissue modeling when the elastic potential equation was reduced to the first term of the above equation e.g. [Demiray, 1972].

1. 5. 2. 3 Viscoelasticity

The viscoelasticity of the ligaments is demonstrated through cyclical testing, traction tests performed at different strain rates and relaxation or creep tests. The mechanical time dependence is called viscoelasticity. Basically, viscoelasticity includes two different effects: the short term memory and the long term memory effects.

The short term memory effects are related to the strain rate dependence of the stress. As noted, e.g. [Danto, 1993], few studies have been conducted in this area. In the literature, strain rate effects are usually modeled by expanding elastic models to encompass viscoelasticity. For example, with a linear elastic description, the modulus of elasticity is a function of the strain rate e.g. [Blevins, 1994; Chiba, 1993]. Similarly, with a non-linear elastic description, the parameters appearing in the elastic potentials will be given as a function of strain rate e.g. [Danto, 1993; Haut, 1969]. In this sense, the strain rate is considered to be an implicit variable. When the strain rate is considered as an explicit variable, the viscoelasticity is often modeled by addition of spring element and dashpot element e.g. [Jamison, 1968; Sanjeevi, 1982]. The spring element and dashpot element are represented by $E\varepsilon$ and $\mu'\dot{\varepsilon}$, respectively. ε represents the strain, $\dot{\varepsilon}$ the strain rate, E the modulus of elasticity and μ' a viscous parameter. It is difficult to generalize this approach when large deformations are encountered.

The long term memory effects are determined by stress relaxation or creep tests. In soft tissues biomechanics, the long term memory effects are generally identified with the quasi-linear viscoelastic theory [Fung, 1981]. This theory gives a relation of the integral type between the stress and the history of the strain. This theory was obtained under some special hypothesis. The relaxation function which is generally as a function of time and strain is assumed to be given by two functions, one of time and one of strain. The stress at present time is obtained as the superposition of the stress at all previous time. In fact this superposition principle, first proposed by Boltzmann, has its domain of application enlarged with the quasi-linear viscoelastic theory. This theoretical formulation makes it possible to handle the non-linear

viscoelastic response within the framework of linear theory. It has been well adapted to account for long term memory effects but, does not take into account strain rate effects.

1. 5. 3 Numerical simulations

Numerical models of the knee joint often consider ligaments as linear or non-linear spring elements [Andriacchi, 1983; Loch, 1992; Moeinzadeh, 1983; Mommersteeg, 1996; Wismans, 1980]. With this type of model, it is not possible to calculate the stress distribution in the ligaments. Another proposed model was the four bar linkage model e.g. [O'Connor, 1993], in which the knee with the two cruciate ligaments are represented as four bars. The simplified kinematics and resultant forces in the bars can be calculated.

The stress distributions in the ligaments can be calculate with a finite element model. A few works in this area can be found in the literature. In a recent study e.g. [Harper, 1993], the stress was calculated in the patellar tendon graft. Elastic spring was used for the constitutive law of the patellar tendon and a simplified kinematics was applied. A transverse isotropic constitutive law was numerically implemented to calculate the stress in soft tissues under simulated traction tests e.g. [Weiss, 1994].

1. 6 Summary

Measurements during flexion of the knee and traction testing provide compatible data. A few investigators used these two tests to obtain a global description of the role of the ligaments in the knee. Ideally, both measurements should be combined in order to obtain maximal information. In case of traction tests, the proposed identifications give either a description of the stress relaxation phenomenon or, occasionally, a description of the strain rate dependence. Numerical stress calculations in the cruciate ligaments made using realistic constitutive laws and kinematics seem to be lacking.

1. 7 Thesis objectives

The mechanical behavior of the knee ligaments and their grafts are sophisticated. This behavior has been described by several theories, each of which took into account only part of the mechanical characteristics. The strain rate dependence was not fully and rigorously described in large deformation situations.

The first objective of this thesis is to formulate a general mechanical framework which describes the different mechanical characteristics of the soft tissues and

satisfies the basic mechanical and thermodynamical requirements. This framework must take into account large deformation situations.

The second objective is to create an experimental set-up in which the different mechanical characteristics of the ligaments and tendons will be identified in relation to the general mechanical framework developed.

The third objective is to perform numerical simulations in which the stress in the ligament would be calculated. The identified constitutive laws are used for the material description and the three dimensional kinematics of the knee flexion are used as boundary conditions.

CHAPTER 2 *Continuum based theory*

The stress in a material is determined by the following three steps:

1. equilibrium of the mechanical problem (general mechanical principles)
2. description of the material properties (constitutive laws)
3. resolution of the problem (numerical simulations).

The points 1. and 2. are detailed in this chapter. Description of the numerical resolutions (point 3.) will be done in Chapter 5.

Section 2. 1 provides a formal framework in which the general mechanical principles and thermodynamical requirements are included. Section 2. 2 gives the general principles governing the constitutive laws of materials. An original general viscoelastic law that takes into account non-linear elastic behavior, short term memory effects and long term memory effects and satisfies the general principles of section 2. 2 is presented in subsection 2. 2. 3. The form of the general viscoelastic law is further restricted by thermodynamical and geometrical considerations at the end of the chapter.

2. 1 General principles

The objective is to model the stresses and strains in a soft tissue submitted to large deformation (large rotation and large strain). A coherent mechanical description must be formulated within the theory of finite deformations. Stress and strain tensors have to be carefully defined.

2. 1. 1 Kinematics of a continuum

The initial undeformed configuration occupied by the body is used to define the strain, the strain rate and the stress and to formulate the equilibrium equation. This description is called *total Lagrangian description* (or equally the *material description*) and is summarized in the following equations e.g. [Gurtin, 1981].

The actual position of a material particle \mathbf{x} at time t is given by the map $\mathbf{y} = \mathbf{y}(\mathbf{x}, t)$ called the motion or the *deformation* (Figure 2.1). The *displacement* of \mathbf{x} is defined by

$$\mathbf{u} = \mathbf{u}(\mathbf{x}, t) = \mathbf{y}(\mathbf{x}, t) - \mathbf{x} \quad (2.1)$$

The *velocity* of \mathbf{x} is then given by (dot denoting material time derivative):

$$\mathbf{v} = \mathbf{v}(\mathbf{x}, t) = \frac{\partial}{\partial t} \mathbf{y}(\mathbf{x}, t) = \dot{\mathbf{u}} \quad (2.2)$$

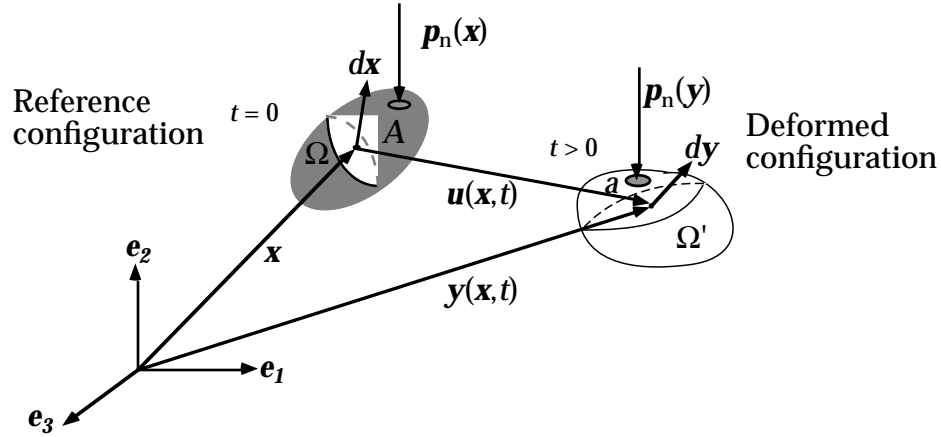


Figure 2.1 Kinematics variables definition of the material description.

The deformation of an infinitesimal material fiber is captured by the *deformation gradient tensor* \mathbf{F}

$$\mathbf{F} = \mathbf{F}(\mathbf{x}, t) = \frac{\partial}{\partial \mathbf{x}} \mathbf{y}(\mathbf{x}, t) \quad (2.3)$$

The (right Cauchy-Green) *material metric tensor* (T for transposition)

$$\mathbf{C} = \mathbf{C}(\mathbf{x}, t) = \mathbf{F}^T \mathbf{F} \quad (2.4)$$

is used as alternative *objective*¹ deformation descriptor.

The *rate of the deformation gradient* is given by

$$\dot{\mathbf{F}} = \dot{\mathbf{F}}(\mathbf{x}, t) = \frac{\partial \mathbf{F}}{\partial t} = \frac{\partial^2 \mathbf{y}}{\partial \mathbf{x} \partial t} = \frac{\partial}{\partial \mathbf{x}} \dot{\mathbf{u}} \quad (2.5)$$

1. Objective is used as synonym for material frame indifference. This concept means that the strain measurement should not be influenced by rigid body motions. As illustration, the deformation gradient \mathbf{F} is not objective as it includes part of the rotation in its formulation (polar decomposition of \mathbf{F} : $\mathbf{F} = \mathbf{R}\mathbf{U}$; \mathbf{R} : rotational tensor \mathbf{U} : stretch tensor). The definition of the material metric tensor \mathbf{C} makes it possible to eliminate the rotational dependence for the strain descriptor: $\mathbf{C} = \mathbf{F}^T \mathbf{F} = \mathbf{U}^T \mathbf{R}^T \mathbf{R} \mathbf{U} = \mathbf{U}^T \mathbf{U}$ with $\mathbf{R}^T \mathbf{R} = \mathbf{I}$.

The *rate of the material metric* tensor then takes the form:

$$\dot{\mathbf{C}} = \dot{\mathbf{C}}(\mathbf{x}, t) = \dot{\mathbf{F}}^T \mathbf{F} + \mathbf{F}^T \dot{\mathbf{F}} \quad (2.6)$$

This rate tensor is objective.

2. 1. 2 Dynamics of a continuum

2. 1. 2. 1 Mass conservation

The system is considered to be closed and then must satisfy the principle of mass conservation expressed here in the reference configuration of the body Ω [Germain, 1986]:

$$\frac{d}{dt} \int_{\Omega} \rho_0 d\Omega = 0 \quad (2.7)$$

This principle is satisfied if we assume that the density ρ_0 , in regard to the reference configuration is independent of time. Actual density ρ and reference density ρ_0 are then related by the relation:

$$\rho_0 = \rho \det \mathbf{F} \quad (2.8)$$

2. 1. 2. 2 Linear and angular momentum conservation

The dynamics of a continuum is governed by two fundamental principles: *the conservation of linear momentum* and *the conservation of angular momentum*. These two principles are expressed by:

$$\begin{aligned} \frac{d}{dt} \int_{\omega} \rho_0 \mathbf{v} dV &= \int_{\Gamma} \bar{\mathbf{p}}_n dA + \int_{\omega} \rho_0 \mathbf{b} dV & \forall \omega \in \Omega \\ \frac{d}{dt} \int_{\omega} \mathbf{x} \wedge \rho_0 \mathbf{v} dV &= \int_{\Gamma} \mathbf{x} \wedge \bar{\mathbf{p}}_n dA + \int_{\omega} \mathbf{x} \wedge \rho_0 \mathbf{b} dV & \forall \omega \in \Omega \end{aligned} \quad (2.9)$$

Γ is the reference boundary. \mathbf{b} is a density body force defined per unit of reference volume. $\bar{\mathbf{p}}_n$ is a contact force characterized by a nominal traction vector defined per unit reference area. The external forces create on the frontier $\partial\omega$ of any part $\omega \subseteq \Omega$, internal nominal stress vector \mathbf{p} [Gurtin, 1981]. The nominal stress vector is assumed to depend only linearly on the unit normal \mathbf{n} outward $\mathbf{n} dA \in \partial\omega$ (Cauchy hypothesis). The existence of a nominal stress tensor \mathbf{P} (Piola-Kirchhoff-1) in every particle of the solid may be demonstrated and is expressed by

$$\mathbf{p}[\mathbf{x}, t, \mathbf{n}(\mathbf{x})] = \mathbf{P}(\mathbf{x}, t) \mathbf{n}(\mathbf{x}) \quad (2.10)$$

The hypothesis that encompasses these principles applied to all parts ω of the reference configuration Ω of the solid is called the *localization*.

Localization of the linear momentum conservation gives (for writing convenience, \mathbf{x} is not explicitly written in equation development):

$$\rho_0 \frac{\partial \mathbf{v}}{\partial t} = \text{Div} \mathbf{P} + \rho_0 \mathbf{b} \quad (2.11)$$

with *Div* the material divergence operator. By combining (2.11) and mass conservation, the local description of conservation of angular momentum is:

$$\mathbf{F} \mathbf{P}^T - \mathbf{P} \mathbf{F}^T = \mathbf{0} \quad (2.12)$$

We define a (symmetric) stress tensor \mathbf{S} by the relation:

$$\mathbf{P} = \mathbf{F} \mathbf{S} \quad (2.13)$$

The conservation of angular momentum (2.12) is then satisfied using the stress tensor \mathbf{S} . This stress is called the material (or Piola-Kirchhoff-2) stress tensor¹ and it is objective. Therefore, used of the stress tensor \mathbf{S} is a convenient way to satisfy both the objectivity and the conservation of angular momentum. The mechanical problem is reduced, in this case, to the conservation of the linear momentum (2.11).

2. 1. 3 Thermodynamics of a continuum

Once the mechanical problem is clearly stated, the *first* and *second principle* of thermodynamics must be satisfied. In this work, temperature was assumed constant (an isothermal process which corresponded to our experimental situation). Therefore, thermodynamics description was for this particular case.

The first principle is concerned with energy conservation. In large deformation theory, this principle is expressed by:

$$\frac{d}{dt} \int_{\omega} \rho_0 e dV = \int_{\omega} \mathbf{S} : \dot{\mathbf{C}} dV \quad \forall \omega \in \Omega \quad (2.14)$$

where e is the specific internal energy. The notation “:” represents the scalar product between second order tensors².

1. The material stress tensor \mathbf{S} is related to the classical Cauchy stress $\boldsymbol{\sigma}$ by the relation: $\boldsymbol{\sigma} = J^{-1} \mathbf{F} \mathbf{S} \mathbf{F}^T$ with $J = \det \mathbf{F}$

2. $\mathbf{A} : \mathbf{B} = \sum_{i,j=1}^3 A^{ij} B_{ij}$

The local description of the first principle takes the form:

$$\rho_0 \frac{\partial e}{\partial t} = S : \dot{C} \quad (2.15)$$

The second principle states that the rate of entropy production is always greater than or equal to zero:

$$\frac{d}{dt} \int_{\omega} \rho_0 s dV \geq 0 \quad \forall \omega \in \Omega \quad (2.16)$$

where s is the specific entropy.

Localization of the second principle results in the following equation:

$$\rho_0 \frac{\partial s}{\partial t} \geq 0 \quad (2.17)$$

This equation can be rewritten incorporating the first principle and the mass conservation. This leads to the Clausius-Duhem inequality e.g. [Truesdell, 1992]:

$$S : \dot{C} - \rho_0 \frac{dW_e}{dt} \geq 0 \quad (2.18)$$

where $W_e = e - \theta s$ is the specific free energy and θ , the absolute temperature.

2.2 Viscoelastic constitutive laws

The mechanical and thermodynamical problems are reduced to equation (2.11) (conservation of linear momentum) and equation (2.18) since the conservation of mass and angular momentum are satisfied by the material description. However, the description of the mechanical behaviour of the material still remains. This is achieved through the formulation of the *constitutive law*, relating the stress to the strain.

Three general principles govern the constitutive laws of materials. The *principle of determinism*, the *principle of local action*, which asserts that the present stress at a particle is determined by the history of an arbitrarily small neighborhood of that particle and the *principle of material frame-indifference* (objectivity), which asserts that the response of a material is the same for all observers [Noll, 1958]. It can be demonstrated e.g. APPENDIX A, that these three general principles are satisfied when considering the following constitutive law:

$$S(t) = S_e(C(t)) + \mathfrak{I}_{s=0}^{\infty} \{G(t-s); C(t)\} \quad (2.19)$$

where \mathfrak{S} is a functional representing *the history* of $\mathbf{G}(t-s) = \mathbf{C}(t-s) - \mathbf{C}(t)$ and $S_e(\mathbf{C}(t))$ is an “equilibrium term”. The notation in (2.19) means that $\mathbf{G}(t-s)$ is a variable and $\mathbf{C}(t)$ a parameter. The equilibrium term can be considered as the elastic behavior as it supports the contribution of the deformation at the actual time t (immediate contribution).

2. 2. 1 Long term memory effects

The general constitutive law (2.19) requires the history of the tensor \mathbf{C} at all the past times in order to calculate the stress \mathbf{S} . To be consistent with the observation that memories are imperfect, the *principle of fading memory* is introduced: “deformations which occurred in the distant past have a smaller effect on the present forces than have recent deformations” e.g. [Coleman, 1961]. Mathematical interpretation of the fading memory principle asserts that constitutive functionals have continuous Fréchet derivatives relative to a particular norm on a space of histories $\mathbf{G}(t-s)$. This leads to an integral relation between the stress and the strain in a first order theory e.g. APPENDIX A:

$$\mathbf{S} = S_e(\mathbf{C}(t)) + \int_0^\infty \Sigma(\mathbf{G}(t-s), s; \mathbf{C}(t)) ds \quad (2.20)$$

where Σ is a general tensor-valued function with the variables $\mathbf{G}(t-s)$ and s and the parameter \mathbf{C} . Materials with an integral relation between the stress and the strain are called *material of the integral type* e.g. [Truesdell, 1992]. In the particular case where Σ is given by a linear function, we obtain the *finite linear viscoelasticity* e.g. [Coleman, 1961].

2. 2. 2 Short term memory effects

The value of \mathfrak{S} depends only on $\mathbf{C}(t-s)$ for s very close to zero when only a very short part of the history of \mathbf{C} has an influence on the stress. Hence, the material metric tensor $\mathbf{C}(t-s)$ can be approximated, as $s \rightarrow 0$, by its Taylor expansion up to order b . A material for which the stress depends only on a finite number of these time derivatives is called a material of the *differential type* e.g. [Truesdell, 1992]. Here we reduced our description to a first order ($b = 1$), meaning that the viscous stress \mathbf{S}_v depends only on the strain and on the strain rate. According to this differential framework, the constitutive viscoelastic law is expressed by:

$$\mathbf{S} = S_e(\mathbf{C}(t)) + \mathbf{S}_v(\dot{\mathbf{C}}(t); \mathbf{C}(t)) \quad (2.21)$$

2.2.3 General biomechanical constitutive law for soft tissues

It can be assumed that long term memory effects (2.20) and short term memory effects (2.21) act together in the stress response of a viscoelastic material. Rearranging (2.19):

$$S = S_e(C(t)) + \mathfrak{S}_{s=0}^{\delta}\{G(t-s);C(t)\} + \mathfrak{S}_{s=\delta}^{\infty}\{G(t-s);C(t)\} \quad (2.22)$$

where $\delta \sim 0$. Relation (2.22) can be obtained only for linear functional. The second term on the right hand-side of (2.22) can be approximated by a differential type material (2.21):

$$S = S_e(C(t)) + S_v(\dot{C}(t);C(t)) + \mathfrak{S}_{s=\delta}^{\infty}\{G(t-s);C(t)\} \quad (2.23)$$

The functional \mathfrak{S} can be represented by a material of the integral type. We propose then a general viscoelastic description for soft tissue biomechanics:

$$S = S_e(C(t)) + S_v(\dot{C}(t);C(t)) + \int_{\delta}^{\infty} \Sigma(G(t-s), s;C(t)) ds \quad (2.24)$$

where the successive terms of the right-hand side of (2.24) are the immediate (elastic), short term memory and long term memory response of the material, respectively.

This original description decouples the different mechanical behaviours which is an advantage for the identification process, as will be demonstrated in Chapter 4.

2.2.4 Thermodynamical restrictions

Equation (2.24) is a general form for a constitutive law which takes into account elastic, short and long term memory effects. In order to satisfy the general principles of physics (section 2. 1), this law is further restricted by thermodynamical considerations (2.18).

In classical thermodynamics, the specific free energy is a function of deformation e.g. [Coleman, 1964] (in an isothermal process, temperature is a parameter):

$$W_e = W_e(C) \quad (2.25)$$

Equation (2.18) is rewritten as:

$$\left(S - 2\rho_0 \frac{\partial W_e}{\partial C} \right) : \frac{\dot{C}}{2} \geq 0 \quad \forall C, \dot{C} \quad (2.26)$$

If there is no dissipation (elastic process), the thermodynamic process is reversible and (2.26) becomes trivial. Satisfaction of the thermodynamical principles is then reduces to:

$$\mathbf{S}_e = 2\rho_0 \frac{\partial W_e}{\partial \mathbf{C}} \quad (2.27)$$

The elastic materials, whose constitutive law is derived from a potential W_e are called *hyperelastic* materials. The potential W_e is also known as the *strain-energy function* or the stored-energy function.

In case of short term memory effects, a similar framework is applied with the use of a *dissipative potential* $W_v(\dot{\mathbf{C}}; \mathbf{C})$ (or equally called pseudo-potential) from which the viscous stress is derived [Germain, 1973]. It is postulated:

$$\mathbf{S} - 2\rho_0 \frac{\partial W_e}{\partial \mathbf{C}} = 2 \frac{\partial W_v}{\partial \dot{\mathbf{C}}} \quad (2.28)$$

Therefore (2.26) is rewritten as:

$$\frac{\partial W_v}{\partial \dot{\mathbf{C}}} : \dot{\mathbf{C}} \geq 0 \quad \forall \dot{\mathbf{C}} \quad (2.29)$$

This equation holds true when the potential W_v is convex and the value of W_v is zero when the strain rate is equal to zero ($W_v(\dot{\mathbf{C}} = 0) = 0$) e.g. [Coussy, 1995]. Equation (2.29) will be checked for the particular form of W_v chosen during the identification process (Chap. 4).

A comparison between (2.21) and (2.28) yields:

$$\mathbf{S}_e = 2\rho_0 \frac{\partial W_e}{\partial \mathbf{C}} \quad \mathbf{S}_v = 2 \frac{\partial W_v}{\partial \dot{\mathbf{C}}} \quad (2.30)$$

For materials with long term memory effects, thermodynamic variables depend on the history of the strain (temperature is not considered in the present case due to the isothermal process). The specific free energy (2.18) is expressed by e.g. [Coleman, 1964]:

$$W_e = \mathfrak{K}_{s=0}^{\infty} \{ \mathbf{C}(t-s) \} \quad (2.31)$$

where \mathfrak{K} is a functional representing the history of the material strain tensor. An expression for the stress \mathbf{S} can be obtained by defining a differential operator, \mathbf{D}_F which operates on the functional \mathfrak{K} :

$$(\mathbf{S} - 2\rho_0 \mathbf{D}_F \mathfrak{K}_{s=0}^{\infty} \{ \mathbf{C}(t-s) \}) : \frac{\dot{\mathbf{C}}}{2} \geq 0 \quad \forall \mathbf{C}, \dot{\mathbf{C}} \quad (2.32)$$

This representation is a generalisation of the classical thermodynamics inequality (2.26). Therefore (2.26) represents a particular case when the long term memory effects are not considered. A complete derivation of thermodynamics theory applied

to long term memory effects and a precise definition of the differential operator D_F is found in a fundamental paper of Coleman e.g. [Coleman, 1964].

A general thermodynamic formulation for long term memory effects is beyond the scope of the present study. In the particular case where exponential relaxation functions are used, namely

$$\phi(s) = \phi_\infty + a_0 \exp\left(-\frac{s}{\tau_0}\right) \quad \tau > 0 \quad (2.33)$$

where C is held constant, ϕ_∞ , a_0 and τ_0 are parameters, it can be demonstrated that the thermodynamic requirements are satisfied e.g. [Fabrizio, 1985; Rabotnov, 1977].

2. 2. 5 Isotropy and homogeneity

Position variable is written as \mathbf{x} (the material particle) (see equation (2.3)). For convenience, \mathbf{x} was not explicitly written during the theoretical development. In order to get a tractable identification process, the material is considered to be *homogeneous*. In this situation, the mechanical properties are identical for all \mathbf{x} . Therefore, the homogeneity hypothesis implies that there is not an explicit dependence on the position \mathbf{x} .

In this work, we will consider the material to be *isotropic*. This means that the material response to applied loads is identical no matter which direction the load is applied to. The tensorial analysis gives general (irreducible) relations for symmetric tensors in the special cases of symmetry e.g. [Pipkin, 1960].

In case of isotropy, it can be demonstrated that the elastic potential (2.25) could be expressed as function of three invariants of the deformation [Boehler, 1987]:

$$W_e = W_e(I_1, I_2, I_3) \quad (2.34)$$

The variables I_i for $i = 1$ to 3 , are any invariants¹ of the deformation tensor C . The isotropic elastic stress obtained by derivating W_e with regards to C (equation (2.27)) can be expressed by e.g. [Marsden, 1983]:

$$S_e = \frac{\partial W_e}{\partial I_3} I_3 C^{-1} + \left(\frac{\partial W_e}{\partial I_1} + I_1 \frac{\partial W_e}{\partial I_2} \right) I - \frac{\partial W_e}{\partial I_2} C \quad (2.35)$$

Equation (2.35) is a general representation for an isotropic elastic constitutive law.

1. In the present study, the three following invariants were used:

$$I_1 = \text{tr}C \quad I_2 = \frac{1}{2}((\text{tr}C)^2 - \text{tr}C^2) \quad I_3 = \det C$$

The viscous potential depends on two symmetric second order tensors ($\dot{\mathbf{C}}$ and \mathbf{C}). The general isotropic representation of the viscous potential involves eight tensor generators and ten invariants [Boehler, 1987]. Of course, a representation with less invariants can be derived from the identification process.

In case of isotropy, the tensorial representation of function $\Sigma(\mathbf{G}(t-s), s; \mathbf{C}(t))$ can be obtained e.g. [Truesdell, 1992]. As for the viscous potential, particular representation experimentally accessible can be obtained with the identification process. Consequently, the general constitutive law (2.24) expressed in case of isotropy is:

$$\mathbf{S} = \frac{\partial W_e}{\partial I_3} I_3 \mathbf{C}^{-1} + \left(\frac{\partial W_e}{\partial I_1} + I_1 \frac{\partial W_e}{\partial I_2} \right) \mathbf{I} - \frac{\partial W_e}{\partial I_2} \mathbf{C} + \frac{\partial W_v}{\partial \dot{\mathbf{C}}} + \int_{\delta}^{\infty} \Sigma(\mathbf{G}(t-s), s; \mathbf{C}(t)) ds \quad (2.36)$$

The constitutive law (2.36), with satisfaction of inequality (2.29) for W_v and exponential relaxation function, is an *isotropic viscoelastic* description compatible with basic physical requirements.

2.2.6 Incompressibility

The incompressibility is an example of a kinematic constraint. To satisfy this constraint, an arbitrary hydrostatic pressure $-p\mathbf{I}$ must be added to the general constitutive law. This pressure is not defined by a constitutive equation but can be determined by using equations of motion and boundary conditions. Geometrically, the incompressibility assumption implicates conservation of volume during deformation of the body. Mathematically, this constraint is expressed by the relation:

$$I_3 = 1 \quad (2.37)$$

In case of incompressibility, the general constitutive law (2.36) is given by:

$$\mathbf{S} = -p\mathbf{C}^{-1} + \left(\frac{\partial W_e}{\partial I_1} + I_1 \frac{\partial W_e}{\partial I_2} \right) \mathbf{I} - \frac{\partial W_e}{\partial I_2} \mathbf{C} + \frac{\partial W_v}{\partial \dot{\mathbf{C}}} + \int_{\delta}^{\infty} \Sigma(\mathbf{G}(t-s), s; \mathbf{C}(t)) ds \quad (2.38)$$

The constitutive law (2.38), with verification of inequality (2.29) for W_v and exponential relaxation function, is an *isotropic incompressible viscoelastic* description compatible with the basic physical requirements.

CHAPTER 3 *Mechanical tests*

Mechanical tests described in this chapter belong to the second category of Chapter 1 (i.e force and elongation measurements during traction tests). These tests are performed on isolated human cruciate ligaments and on the central part of patellar tendons. Results are reported as the nominal stress as a function of deformation gradient.

Identification of elastic and viscous constitutive laws can be achieved through static and dynamic mechanical tests. From these tests, stress-strain curves at different strain rates and stress relaxation curves are obtained.

This chapter describes the experimental set-up, the different mechanical tests performed and the main experimental results.

3. 1 Material and methods

3. 1. 1 Experimental set-up

The principal objective of the experimental set-up is to measure the forces and displacements directly from the specimens. Measurements can then be interpreted without corrections such as those necessary to account for the component inertia in case of dynamical loading. Direct measurements insure that the viscosity measured during dynamic testing is due to the specimens and not to the supporting structures. A chamber with controlled temperature and humidity was developed to minimize environmental influence. The experimental set-up, schematically depicted in Figure 3.1, can be separated into three groups: the supporting structure, variable measurement and loading control.

3. 1. 1 Supporting structure

The supporting structure was constructed of aluminum and steel. The principal pieces are described in Figure 3.1. A precise screw ball (10) (FAG, Lausanne-

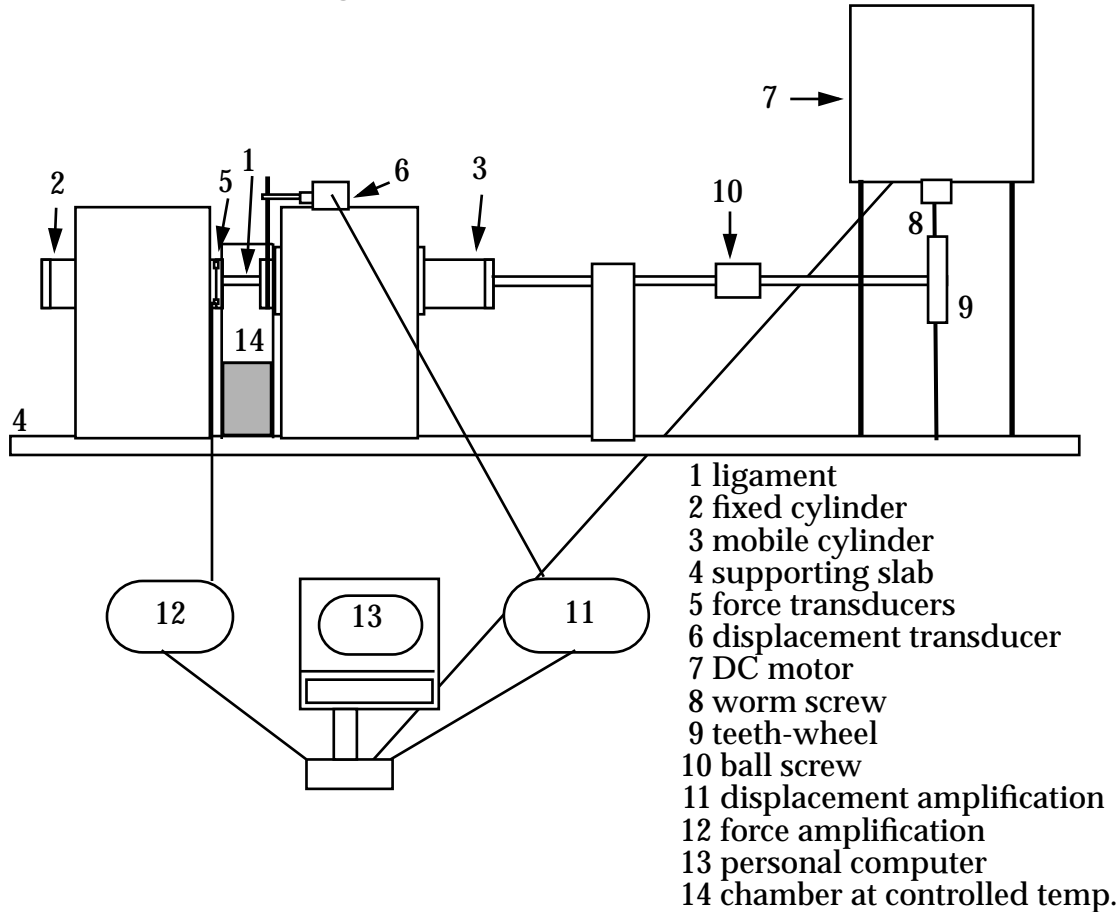


Figure 3.1 General view of the experimental set-up.

Switzerland) was used to transform the circular motion into a linear one. The motor (7) was linked to the ball screw by a worm screw (8 and 9). One revolution of the motor axis corresponds to a linear motion of 0.2mm. Two metallic stems transmitted the displacement of the ball screw to the mobile cylinder (3) holding one end of the ligament (1). The displacement transducer (6) was fixed on the mobile cylinder. Three piezo force transducers (5) were placed at the fixed end of the ligament (fixed cylinder (2)). The displacement and force signal were amplified (11 and 12) and acquired on a personal computer (13). The position of the motor, its axis fixation and the supporting structures were adjustable ensuring an optimal transmission of the load from the motor to the ligament. The worm screw was adjusted to minimize dry friction (preservation of the motor efficacy) and relative motion (preservation of the loading control). The ligament was placed inside a plexiglas chamber (14) that was maintained at 37°C and a humidity of 100% by water circulation.

3. 1. 1. 2 Variables measurement

A computer acquisition card (GW Instruments, Somerville-USA) was used to measure the variables. The analog-to-digital conversion took $12\mu\text{s}$. The corresponding acquisition rate was 40kHz. The card functions as multiplexer mode and the acquisition frequency was reduced to 8kHz with 5 signals (4 inputs and one output in the present case). The scale for the acquisition card was $\pm 10\text{V}$ and the digital resolution was 12 bit. The corresponding analogical resolution was 4.88mV (for input and output). The software for data acquisition was LabView (National Instrument Corporation, Austin-USA).

Force measurement

Three piezo force transducers (Kistler, type 9211, Winthertur-Switzerland) were placed at 120° on the fixed cylinder. The pieces in contact with the transducers had to be perfectly plane to insure an optimal force measurement. Therefore, each transducer was placed between a small polished steel disk and a polished plane steel ring (Figure 3.2).

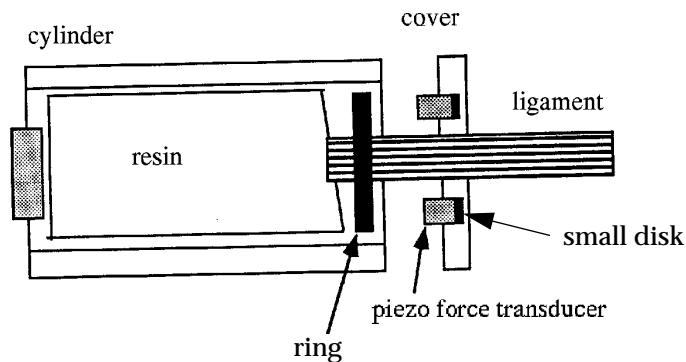


Figure 3.2 Force transmission between the transducers and the ligament

The use of three force transducers placed at 120° and the plane ring insured that the total force was measured if a signal was transmitted through each transducer. The transducer signal (picoCoulomb) was transformed to a proportional tension by charge amplifier (Kistler, type SN5007, Winthertur-Switzerland). Due to the discrete data acquisition, the force resolution was 0.84N.

Displacement measurement

The displacement was measured with an inductive transducer (vibro-meter, type WG173, Fribourg-Switzerland). The transducer signal was proportionally amplified (signal amplification vibro-meter, type ICD108M3, Fribourg-Switzerland). Due to the discrete data acquisition, the displacement resolution was $13\mu\text{m}$.

3. 1. 1. 3 Loading control

The D.C. motor was controlled by a servo-amplification card (Portescap, La Chaux-de-Fonds-Switzerland). The aim of the loading control was to generate controlled constant rates deformation and sinusoidal motions on the tested specimens.

The load (and displacement) was controlled using a PID regulator (proportional, integral, derivative) e.g. [Siarry, 1989]. It had one input (the pursuit error i.e. the order minus the measure) and one output (the order). There are three types of corrections. The proportional corrector is a direct multiplication of the order. The integral corrector rectifies order drift. The derivative corrector diminishes sudden changes by smoothing the correction. The PID algorithm is well adapted to follow sinusoidal signals, but not ramp signals. Hence a basic PID algorithm [Altpeter, 1995] is adapted in a PIID algorithm (proportional, integral, integral double, derivative) and implemented in the present experimental set-up. Modifications of the PID also made it possible to incorporate a low band filter in the algorithm which smoothed the measurements of the force and displacement so that the control was more stable.

3. 1. 1. 4 Environment control

Because the cruciate ligaments are intra-articular but extra-synovial, their *in vivo* environment is more like a humidified tissue than an immersed tissue. The ligaments are at the body temperature (37°C). Mechanical tests were performed with specimens placed in a plexiglas chamber where the temperature and the humidity were controlled. Water kept at a constant temperature circulated in the bottom of the chamber, not in contact with the specimens. A thermometer was placed inside the chamber so that the temperature could be continuously monitored and the water temperature adjusted for a constant chamber air temperature of 37°C. This procedure was stable since the temperature variation was $\pm 0.2^\circ\text{C}$. Due to the water evaporation, the humidity inside the chamber was maintained at 100% with this technique.

3. 1. 1. 5 Tests and validations

The stability of the control motion depended on the values of the PIID parameters. These parameters were previously determined for each selected test. As illustration, control displacement for the 6Hz sinusoidal motion and for the constant 3mm/s elongation rate are presented in Figure 3.3.

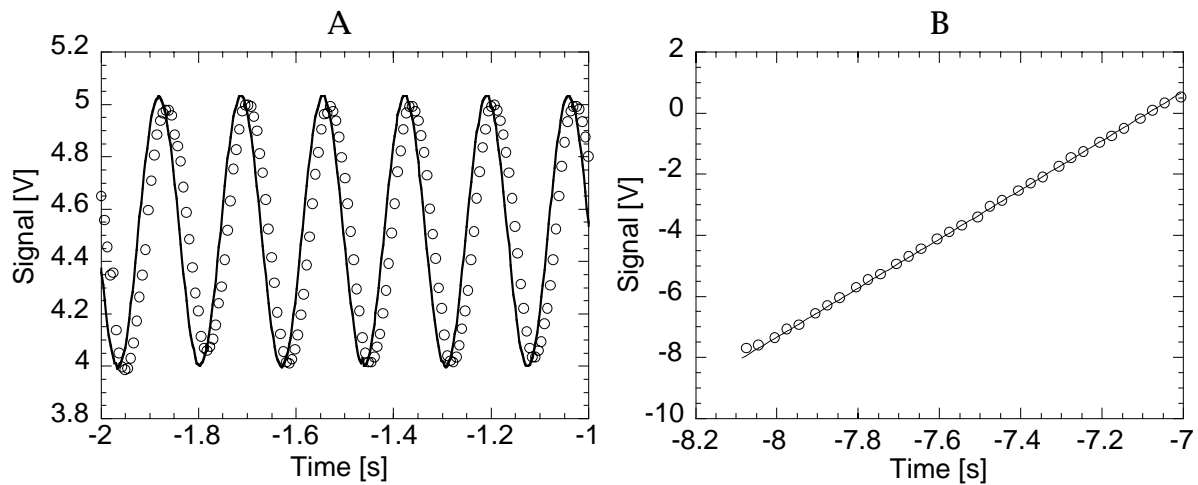


Figure 3.3 Reference signal imposed (plain line) and corresponding displacement signal measured (circle) for the 6 Hz sinusoidal motion (A) and the 3mm/s elongation rate (B).

It was important to verify that stress-strain curves obtained at different elongation rates were not different from each other for a non viscous material. To prove this point, a rope, with identical clamping mode as for the biological specimens, was used. Results in Figure 3.4 show that the measured stress is independent of the elongation rate.

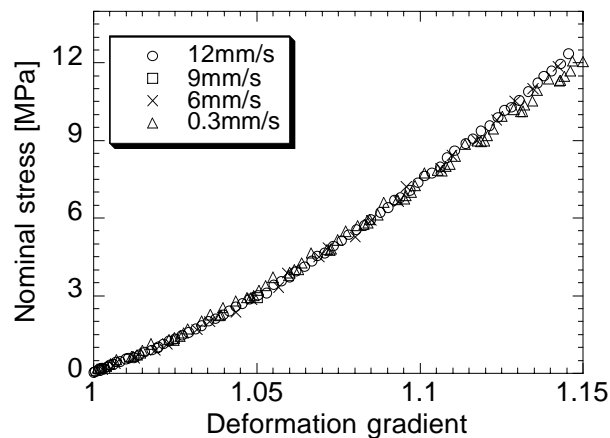


Figure 3.4 Stress-strain curves obtained at 4 different elongation rates for a rope specimen.

The piezo-electric force transducers are appropriate for dynamic force measurements. In case of static stress relaxation tests, the signal drift of the force transducers was estimated. First, measurements were made with a steel piece (not supposed to have a relaxation behavior). This steel piece was charged under different static forces and the force decay was recorded during the following 30 minutes (characteristic time for a stress relaxation test in the present study). In all cases, the force decay was not greater than 1% of the initial force.

3. 1. 2 Specimens

3. 1. 2. 1 Origin and conservation

Calf specimens

The calf knees (age: 4 months; body weight: 100kg) were obtained from an industrial butcher 24 to 48 hours after death. The entire knees were refrigerated at -24°C for no longer than two months. This preservation technique did not influence the mechanical behaviour of the ligaments e.g. [Woo, 1986]. The knees were thawed at room temperature for 8 hours the day of the experiments and the ligaments were tested the same day. Fifty ACL calf knees were used for the different mechanical tests e.g. [Pioletti, 1995; Pioletti, 1996; Pioletti, 1997].

Human specimens

Five fresh frozen caucasian knees (5 males, mean age: 74.8 ± 2.1 years) were obtained from the Anatomical Department, University of Lausanne. Specimens were refrigerated at -30°C for no longer than 6 months. The knees were thawed at room temperature for 8 hours. The two cruciate ligaments (ACL, PCL) and the 10mm width central part of the patellar tendon (PT) were collected with their proximal and distal bone attachments and frozen again at -24°C until the day of the tests.

3. 1. 2. 2 Specimen preparation

From the dissection until the experiments, an identical protocol was followed for all specimens. The bone insertions of isolated ligaments and tendons were potted in a synthetic resin (Beracryl-Pulver). The solidification process took place in a freezer to minimize the heat effects. The specimens were then fixed upon the supporting structure of the experimental set-up with maximal fibers aligned in the load direction. The entire preparation took approximately one hour. The specimens stayed in the chamber at 37°C and 100% humidity for 30 minutes to obtain a thermal equilibrium. They were then preconditioned with a 0.3mm/s elongation rate until a force of 300 newton was reached. The first test began 30 minutes after preconditioning. There was a 30 minutes interval between each test in order that the specimens were in an identical mechanical situation for each test.

3. 1. 2. 3 Specimen dimensions

The length and cross-sectional area of the specimens were used for the strain and stress calculations. The reference configuration under which these two values were obtained is not relevant for the Lagrangian description adopted for the theoretical description. For consistency, the reference length and the reference cross-sectional area were measured when a 2 newton force was applied to the specimens.

Reference length

The reference length of the specimens was measured with a caliper square. It was defined as the mean of 4 successive measurements performed between four different attachment sites. The length resolution was 0.5mm.

For the calf ACL (50 specimens), the mean length was 31.89 ± 0.73 mm [\pm SE].

For the human ACL, PCL and PT (5 specimens each), the mean lengths were:

Human specimens	Mean length \pm SE [mm]
ACL	23.31 ± 1.05
PCL	25.00 ± 2.79
PT	51.26 ± 1.41

Reference cross-sectional area

The reference cross-sectional area of the specimens was assumed to have an elliptical shape. The two corresponding principal diameters were measured at three different positions along the specimens. The mean of these three measurements defined the reference cross-sectional area. The principal diameters were measured with an optical (non contact) method (Figure 3.5) based on the shadow cast principle [Marcuse, 1981].

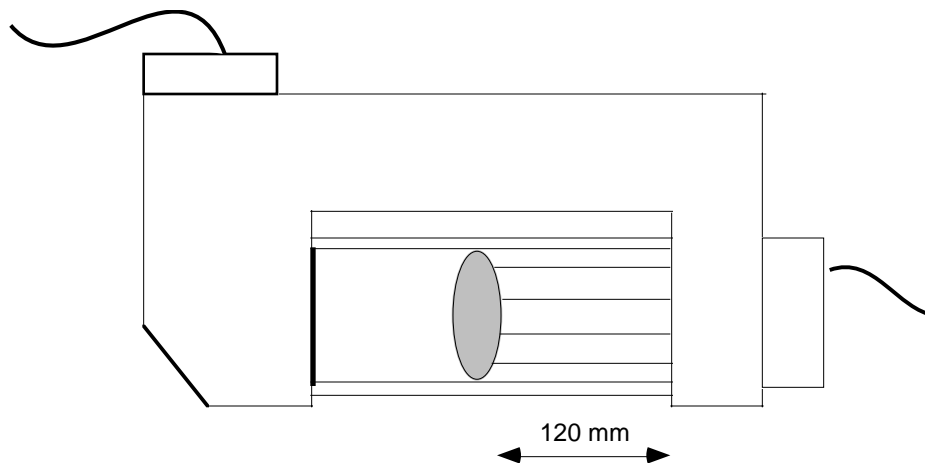


Figure 3.5 View of the optical device (Zimmer UDM 5000-20) used to measure the two principal diameters of the specimens.

The diameter resolution was $4\mu\text{m}$.

For the calf ACL (50 specimens), the mean cross-sectional area was 89.92 ± 3.45 mm² [\pm SE].

For the human ACL, PCL and PT (5 specimens each), the mean cross-sectional area were:

Human specimens	Mean cross-sectional area ± SE [mm ²]
ACL	72.68 ± 15.38
PCL	132.65 ± 8.68
PT	99.09 ± 5.71

3. 1. 3 Tests performed

The first mechanical tests were performed on calf ligaments in order to establish a precise experimental protocol which was then strictly followed. Constant elongation rate and stress relaxation tests were performed¹.

3. 1. 3. 1 Constant strain rate tests

In this study, constant elongation rate corresponds closely to constant strain rate. These two terms are used synonymously hereafter. Specimens were loaded to a maximum 300N with four different constant elongation rates: 0.3, 6, 9 and 12mm/s. As example, these elongation rates corresponded for the mean ACL length to strain rate values of 1.2, 25, 38 and 50%/s respectively. At the end of the tests, the specimens were loaded again with the 0.3mm/s elongation rate to assess reproducibility of the tests.

3. 1. 3. 2 Stress relaxation tests

The ligaments were loaded with a constant elongation rate (0.3mm/s) at different initial strains. Then, the stress relaxation was measured for 1800s because the long term memory effects vanish after this period. At the end of the trials, the specimens were loaded again with the first initial strain to assess reproducibility.

3. 1. 4 Results variables

The definitions of the variables used in the results section are summarized here.

The deformation gradient (or equivalently strain) is defined as:

1. The sinusoidal tests are only performed with the ACL calf specimens e.g. [Pioletti, 1996]. The corresponding results are not presented in this chapter, but will be analyzed in the discussion section.

$$\frac{l}{l_0}$$

with l the actual length and l_0 the reference length. The deformation gradient is dimensionless.

The nominal stress is defined as:

$$\frac{f}{S_0}$$

with f the actual force and S_0 the reference cross-sectional area. The nominal stress is given in MPa.

The normalized stress corresponding to the initial strain x is given the ratio:

$$\frac{\text{stress relaxation obtained with initial strain } x}{\text{stress relaxation obtained with the highest initial strain}}$$

The relative stress relaxation after 1800 seconds is given by the ratio:

$$\frac{\text{stress at } t = 1800 \text{ seconds}}{\text{stress at } t = 0 \text{ second}}$$

and was reported for the tests performed with the highest initial strain.

3. 2 Experimental results

Results for the human specimens ACLH, PCLH and PTH (H for human) are presented for the two types of tests performed. The specimen one was used to test the set-up and therefore the first result reported is experiment number 2. Identical behaviors were observed for the 50 calf ACL specimens.

3. 2. 1 Constant strain rate tests

3. 2. 1. 1 ACL

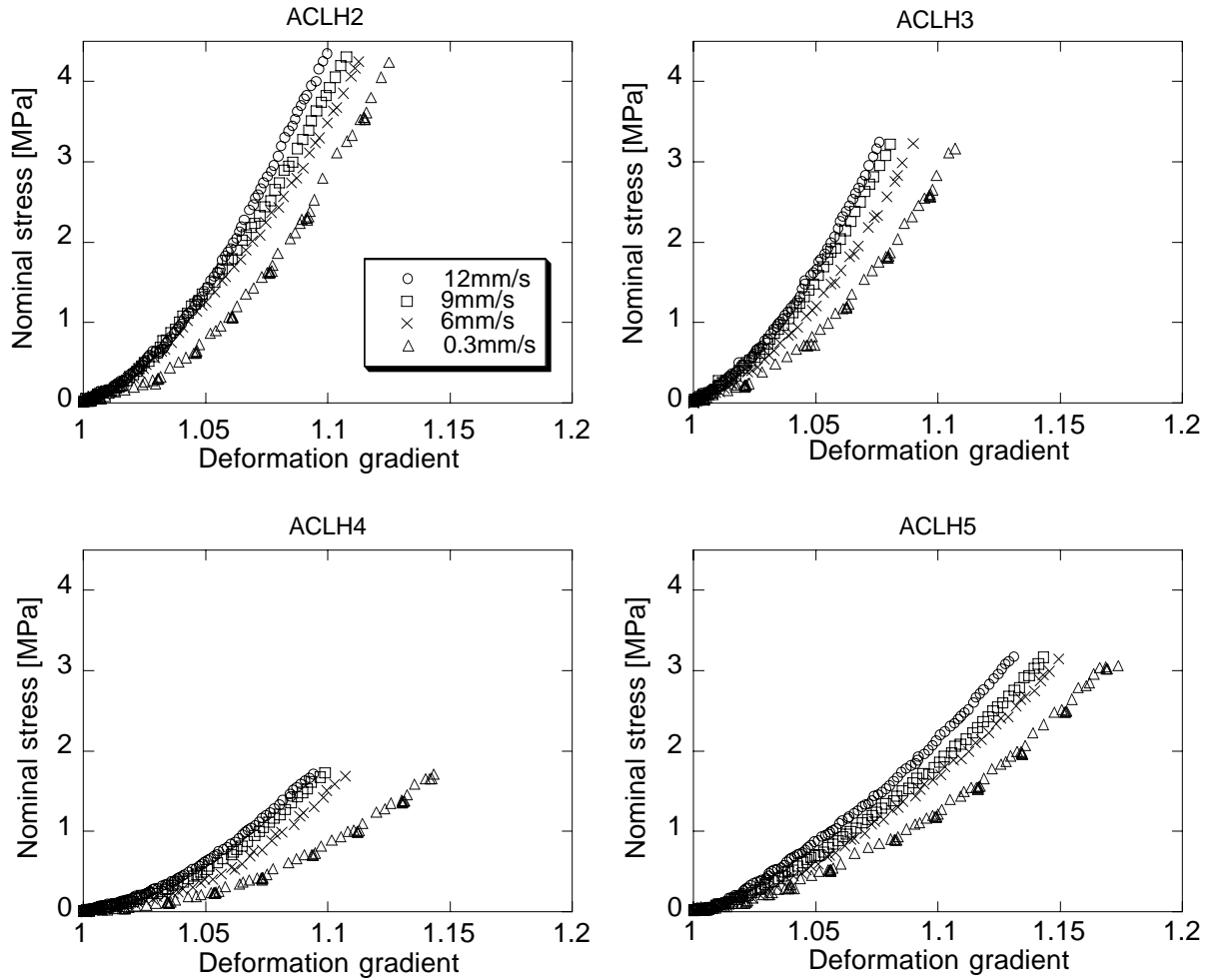


Figure 3.6 Stress-strain curves at 4 different elongation rates for 4 human ACL specimens. The graphics highlight the different mechanical behavior between the ACL specimens. At 10% of strain (deformation gradient equal to 1.1), the corresponding stress can vary from 1 to 4 MPa between the specimens. However, the effects of strain rate are visible for all the specimens. These effects are especially apparent among the lowest rate and the other three.

3. 2. 1. 2 PCL

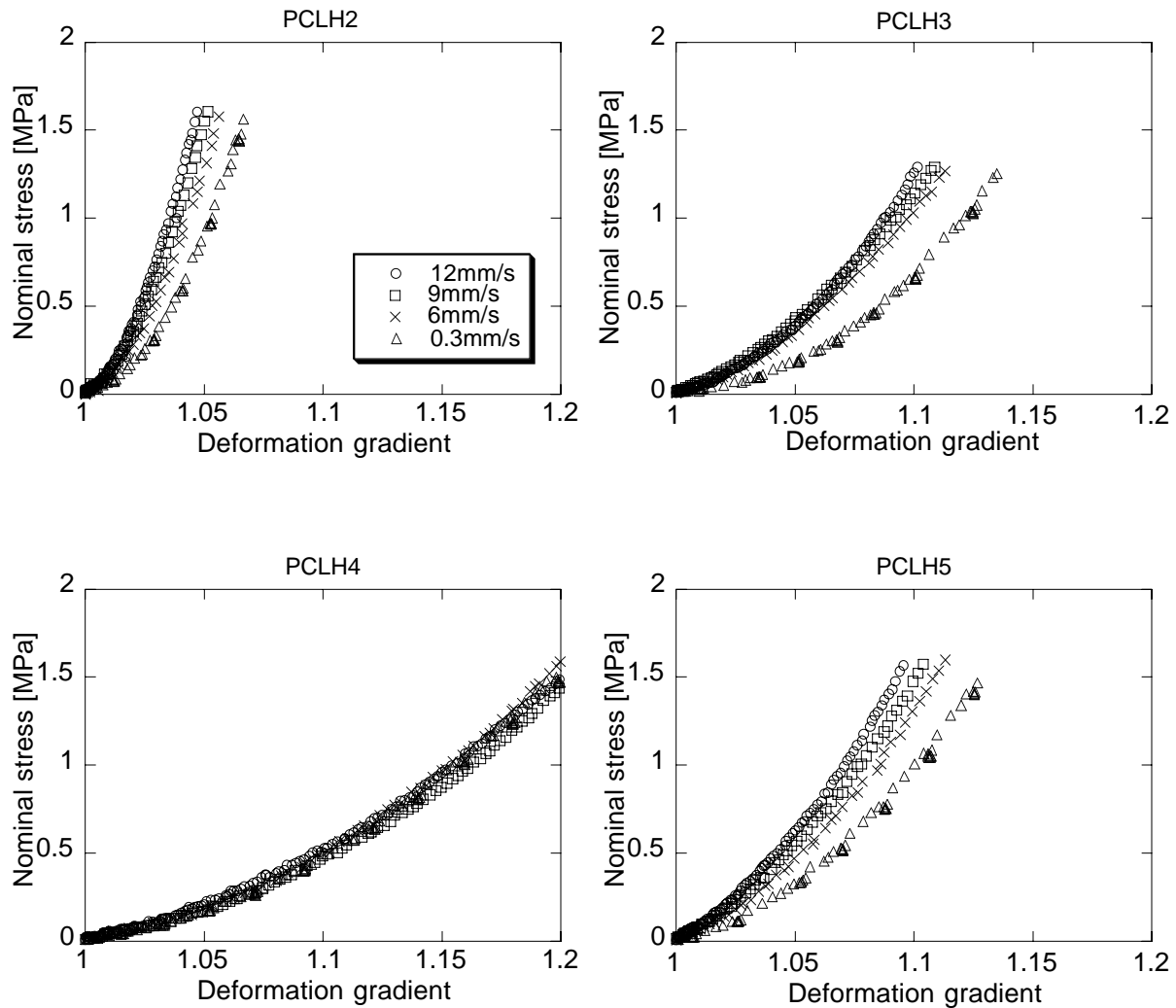


Figure 3.7 Stress-strain curves at 4 different elongation rates for 4 human PCL specimens. The PCL specimens have different mechanical behavior. Despite the fact that the final stress value is almost the same among specimens, the corresponding strain is different. The mechanical behavior of the PCLH4 specimen has no strain rate dependence. Omitting this specimen, trends similar to those of the ACL specimens were found.

3.2.1.3 PT

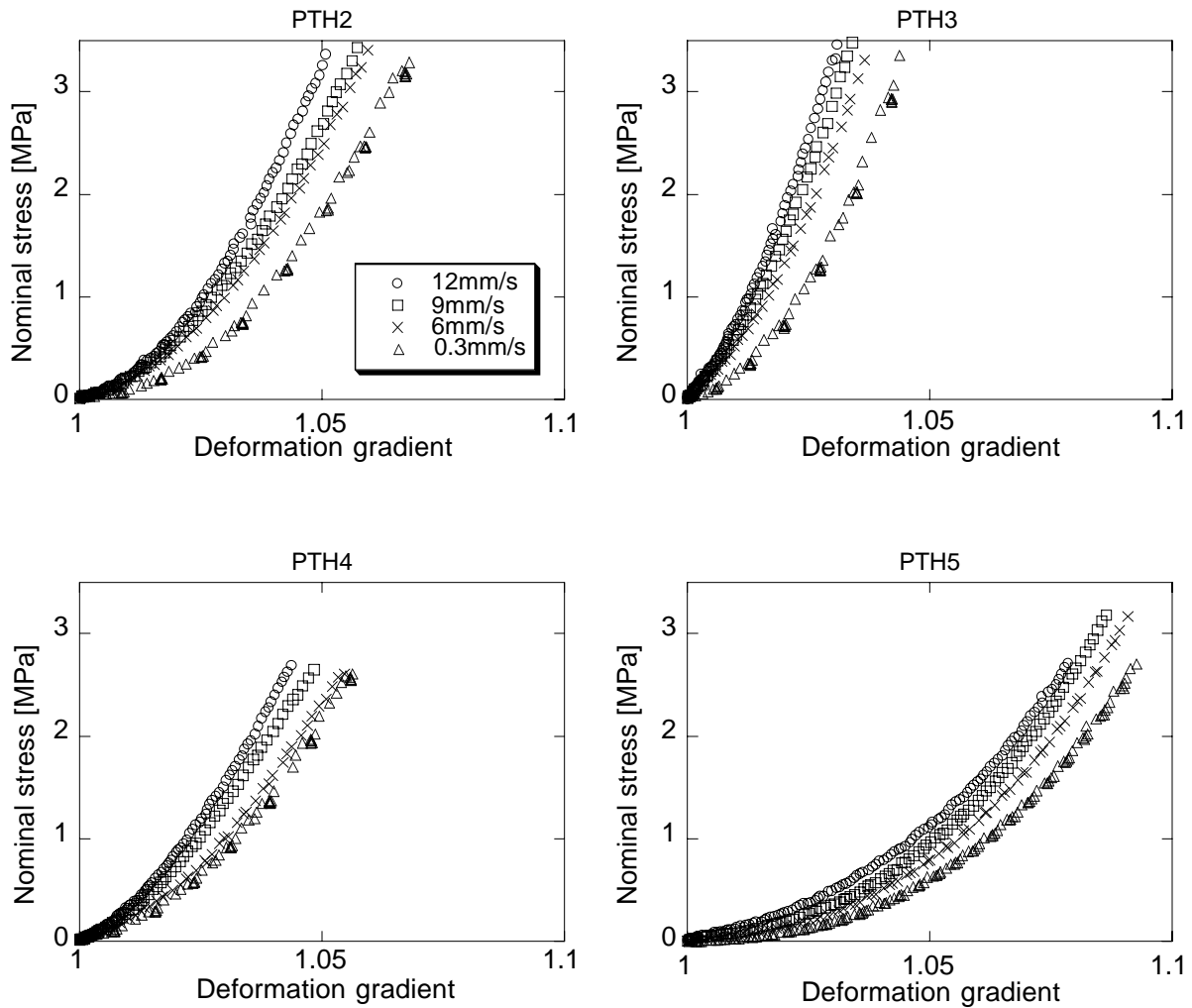


Figure 3.8 Stress-strain curves at 4 different elongation rates for 4 human PT specimens. The PT specimens exhibit a constant mechanical behavior. Without regard to specimen 5, the stress-strain curves are similar in shape and values among specimens. Here again, the strain rate effects are most important among the lowest value and the other three. The toe region of the PTH5 specimen is more important than for the other specimens.

For all specimens, the stress-strain curves are non-linear and the strain rate effects are noticeable. Differences between stress-strain curves for different strain rates are mainly observed in the beginning of the curves (toe region). The second part of the curves, which is almost linear, is not affected much by the increase of strain rate. From a qualitative point of view, the shape of the stress-strain curves appears similar among the specimens from the same knee. The stress-strain curves almost resemble each other when comparing ACLH2 and PCLH2 specimens and when comparing ACLH3 and PCLH3. However, this is not verified for the PT specimens.

3. 2. 2 Stress relaxation tests

3. 2. 2. 1 ACL

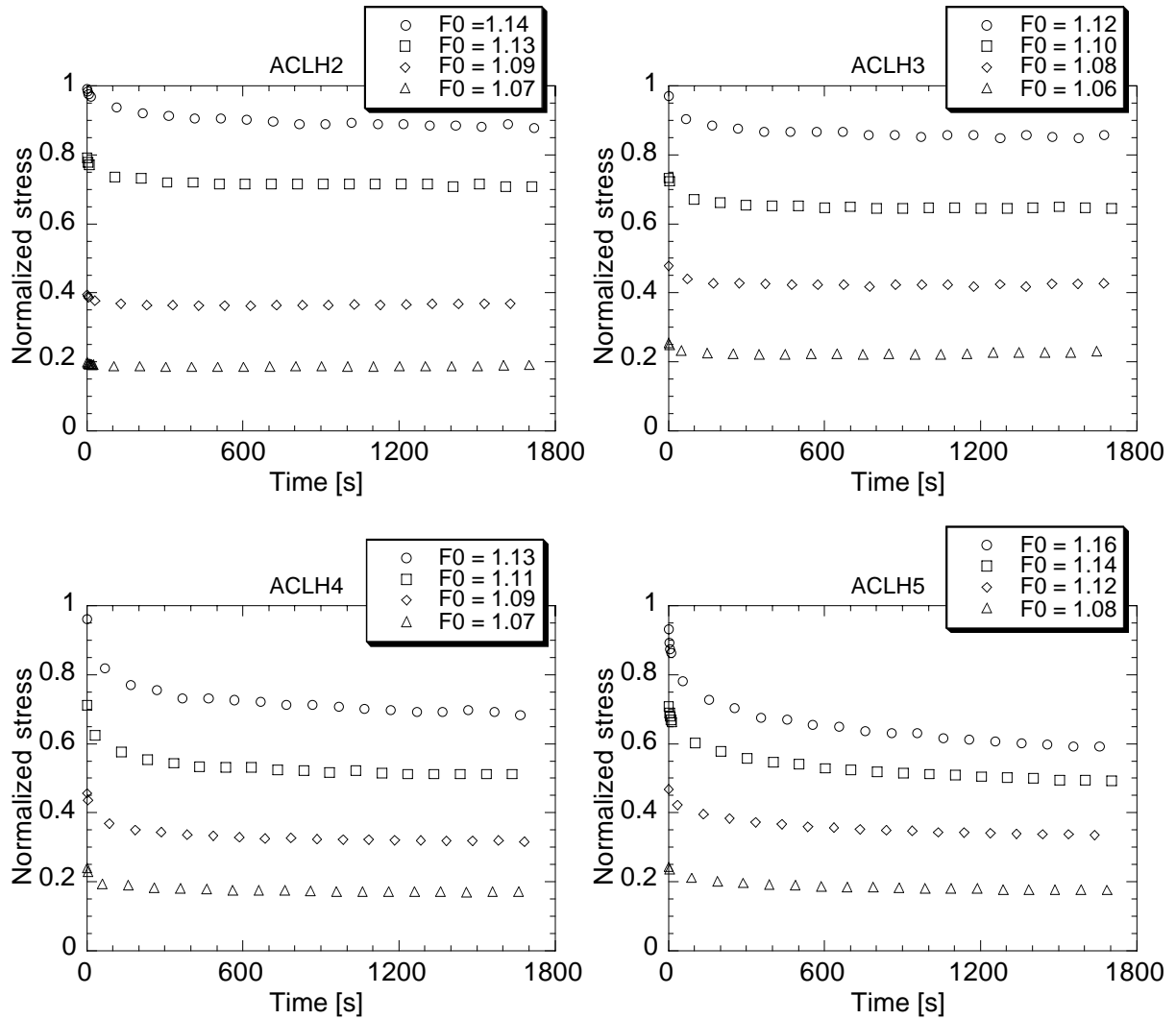


Figure 3.9 Normalized stress relaxation curves at 4 different initial strains (F_0) for 4 human ACL specimens. It is observed that the stress relaxation is important during the first seconds of the tests, then is moderated during the following minutes and finally reaches a quasi-static state after 30 minutes. An identical trend is found for all the specimens. Some differences appeared in the beginning of the relaxation between specimens.

specimen #	ACLH2	ACLH3	ACLH4	ACLH5
relative stress relaxation [%]	0.86	0.85	0.68	0.58

3. 2. 2. 2 PCL

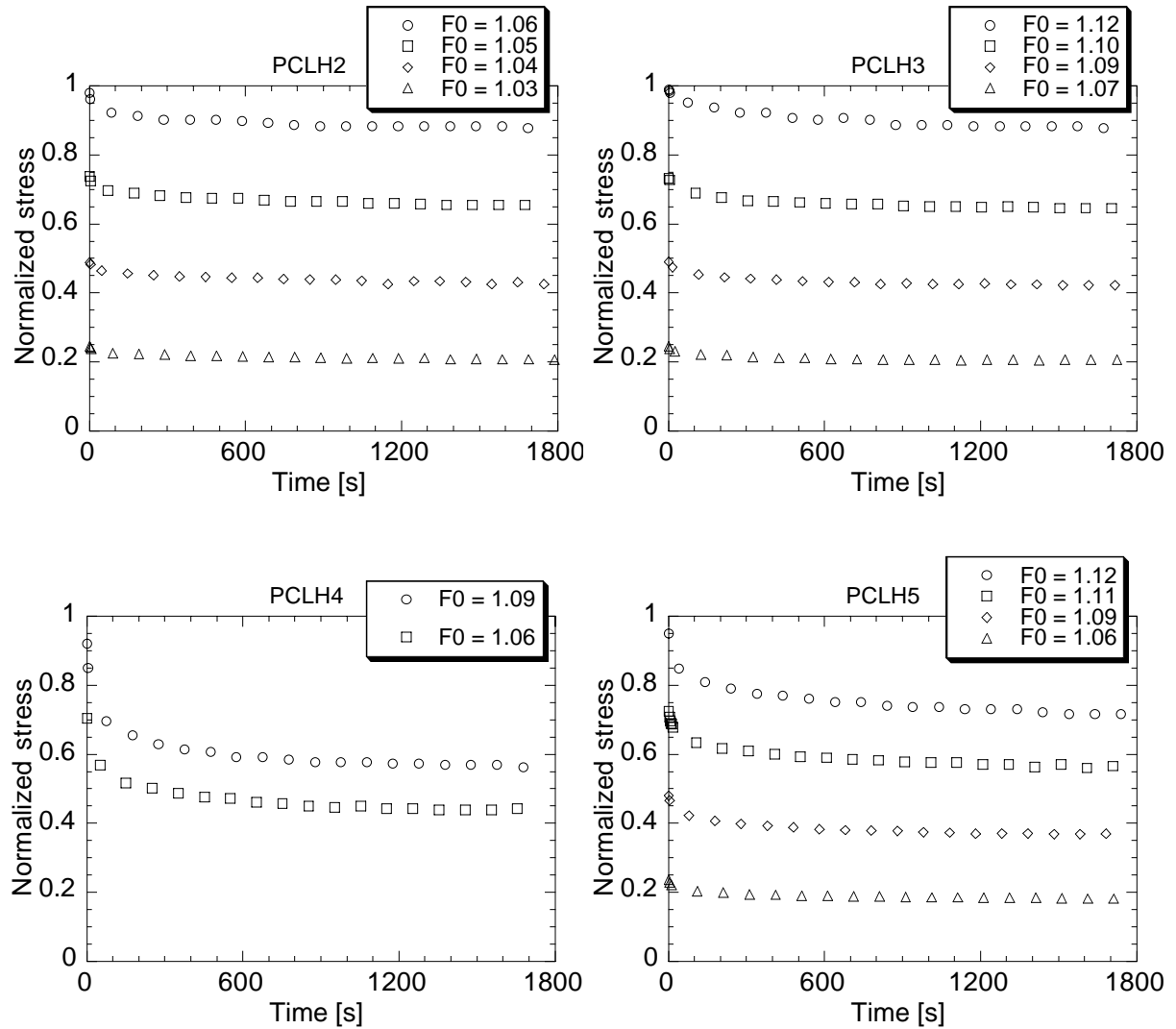


Figure 3.10 Normalized stress relaxation curves at 4 different initial strains (F_0) for 4 human PCL specimens. Specimen 4 has been tested for only two initial strains because a rupture occurred during the third test. The stress relaxation behavior is similar for all the specimens.

specimen #	PCLH2	PCLH3	PCLH4	PCLH5
relative stress relaxation [%]	0.86	0.85	0.58	0.74

3. 2. 2. 3 PT

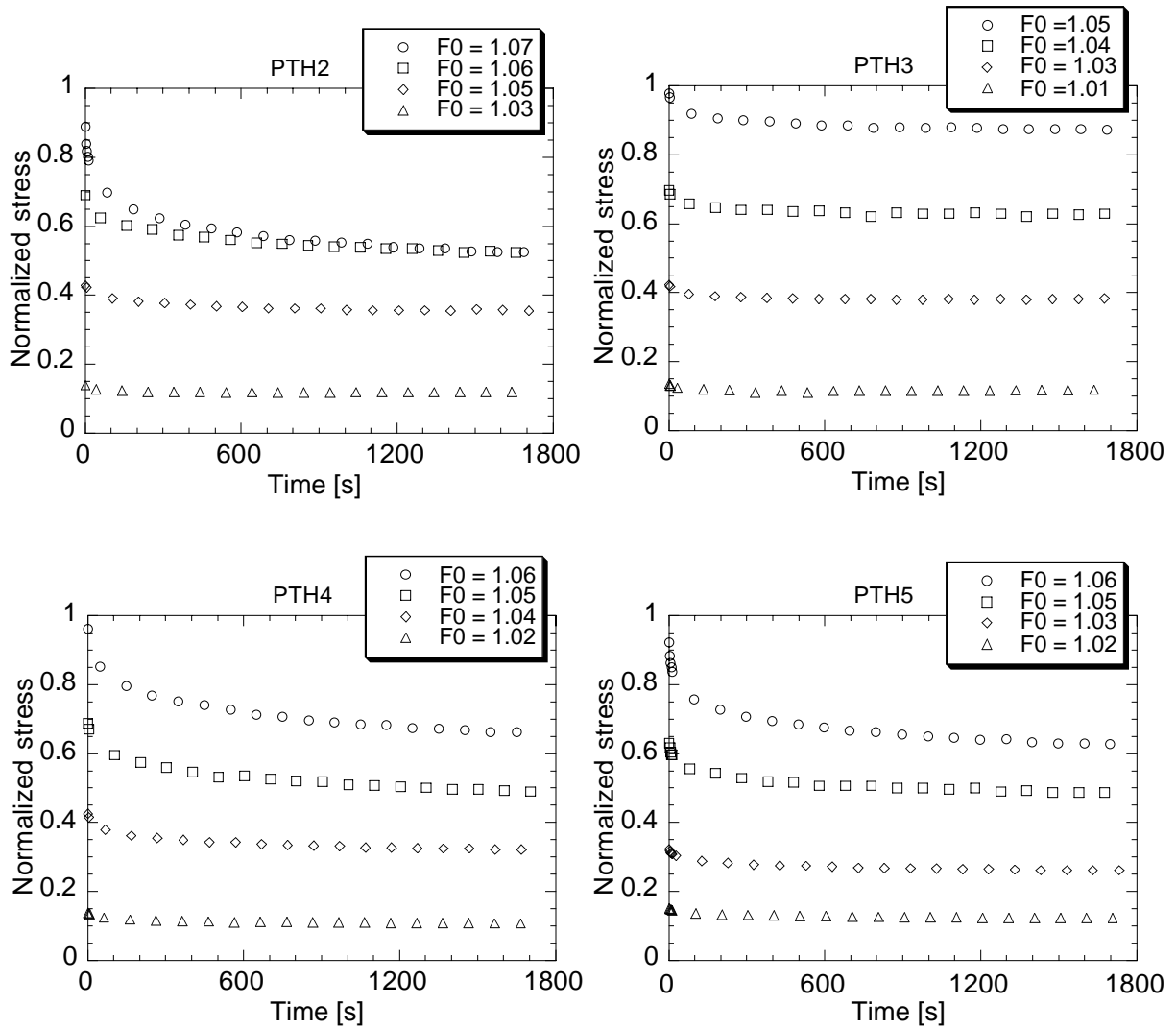


Figure 3.11 Normalized stress relaxation curves at 4 different initial strains (F_0) for 4 human PT specimens. Specimen 2 presents a slightly different trend for the highest initial strain. With the omission of this test, all the specimens have a similar relaxation behavior.

specimen #	PTH2	PTH3	PTH4	PTH5
relative stress relaxation [%]	0.52	0.86	0.66	0.62

3. 3 Discussion

The mechanical testing performed on soft tissues is a delicate process. The response of a same specimen to identical tests can differ if some important variables are not carefully addressed. The preconditioning of the biological specimens is certainly one of the most important parameters in obtaining reproducible data. The natural alignment of the fibers is lost if the specimen is in a stress free state. It is generally accepted that the preconditioning realigned the fibers along the load direction. When the fibers are realigned, consistent results can be obtained from repeated mechanical tests.

Temperature and hydration of the specimens are also two important variables e.g. [Lauper, 1996]. The chamber with constant temperature at 37°C and 100% humidity creates an *in vitro* environment which approaches *in vivo* conditions. The specimens were not in contact with the bath. Otherwise the effects of water content of different solutions should have been considered when examining viscoelastic properties [Chimich, 1992; Haut, 1990]. Mechanical dependence of specimen orientation also needed to be evaluated. Surprisingly, this parameter was not relevant in the present study. However, it was demonstrated that ligament orientation is important for the tensile mechanical tests e.g. [Woo, 1987]. This apparent contradiction can be explained by the fact that the present tests are performed at relatively low stress to preserve the integrity of the specimens between the tests. In the range of the stress applied, the orientation of the fibers is apparently not consequential but would presumably play a non-negligible role with the application of higher stress.

The mechanical properties of ligaments have been found to depend on the age of the specimens [Woo, 1993]. Ultimate failure and the slope of linear part of the stress-strain curves decrease with age for the human ACL [Noyes, 1976]. This is not the case for the human patellar tendon [Blevins, 1994; Flahiff, 1994; Noyes, 1976], even in case of stress relaxation tests [Johnson, 1994]. Therefore, results for the present specimens, which are relatively old (mean age: 74.8), should take age into account when considering the cruciate ligament specimens, but not for the patellar tendon.

The behavior of specimen PCLH4 is different from the others. Surprisingly, this specimen exhibits no strain rate dependence. Rupture occurs at the third relaxation test. In Chapter 1, it was noted that ruptures can occur without macroscopic evidence. Accordingly, it can be hypothesized that this specimen sustains a rupture during the strain rate tests. Its results should be uniquely considered.

The soft tissues remember their previous stress states. Preliminary tests allowed us to discern that 30 minutes was the characteristic time necessary for the specimen to forget its previous stress states. This time scale corresponds to what is found in the literature e.g. [Hubbard, 1988]. Note that an extended rest is not advisable since this may induce a loss of fibers orientation rendering the preconditioning process useless. Reproducibility of the experiments was checked by repeating the entire mechanical tests on several calf specimens. Comparisons between the two sets of data did not

show significant differences for neither the strain rate tests nor the relaxation stress tests. It can be assumed then that by following the protocol, reproducible mechanical answers is obtained with identical tests. Therefore, it is possible to quantitatively compare results from different specimens.

The ACL and PCL cross-sectional areas vary along their length [Fu, 1993]. The mean of three measurements made near the tibial insertion, the femoral insertion and in the middle of the specimen results in a more appropriate value when the measurement is only performed in the middle of the specimen. The assumption that the shape of the cross-sectional area is elliptical is a good approximation. This is especially true for the patellar tendon, but questionable for the cruciate ligaments. Upon comparison of the cross-sectional area measurements based on the elliptical hypothesis with a precise method of cross-sectional measurements, results were found to be acceptable [Woo, 1990]. The non-contact measurement method, as used in this study, is even more precise than the area micrometer generally used e.g [Butler, 1986].

The results from the mechanical tests demonstrated that the behavior of the specimens depends on the time scale of the experiments. First, it is observed that the specimens respond immediately to the load and secondly that the specimens are also sensitive, with a short term delay, to variation of the load (strain rate dependence). Thirdly, the specimens remember the previous loads until reaching the end of a characteristic relaxation time. The contribution of these different phenomenon is shown with the different tests.

Cyclic tests performed on calf specimens gave important qualitative results. They revealed a marked non-linear stress-strain behaviour. With these tests, the importance of viscosity was demonstrated via hysteresis curves. Nevertheless, cyclic tests did not provide quantitative results describing these phenomenons. The effects of strain rate (frequency dependence) and stress relaxation (relaxation of the static stress) appear to be coupled. To quantify these phenomenons separately, constant strain rate and stress relaxation tests must be performed.

The effect of the strain rate is important. An increase of the strain rate generates a supplementary stress in the specimens. With an elongation rate of 12mm/s, 60 to 70 percent of the stress is due to the strain rate. The shape of the stress-strain curves is not altered by various strain rates, except for the toe region which appears at lower strain. This observation is similar to observations reported in the literature e.g. [Haut, 1969]. The linear part of the stress-strain curves does not show significant differences between tests performed at different strain rates. Hence, it can not be concluded that there is no strain rate effect on the stress-strain curves in regards to the linear part of these curves, as was proposed e.g. [Blevins, 1994]. The effects of the strain rate on the failure mode is not clearly known. In a study, e.g [Noyes, 1974] it was reported that in bone-ligament-bone preparations the ligament failed at a fast velocity but the bone insertion area was the weakest component at a slow velocity. Another study, e.g. [Danto, 1993] showed that the strain rate has no effect on the failure mode for neither the ACL nor the PT. Nevertheless, a biomechanical description of the ligaments and

tendons should include the strain rate as a variable since it clearly increases the stress in the specimens

The stress relaxation seems to be governed by 3 characteristic times: a fast relaxation immediately after the deformation followed by a moderate relaxation until 500 to 1000 seconds and finally an almost inexistent relaxation till the equilibrium state (1800 seconds). The mean of the relative stress relaxation is similar among the 3 groups (ACL, PCL and PT) with an average value of almost 0.70. This value is comparable with what can be found in the literature e.g. [Lyon, 1988]. For the ACL, stress relaxation stabilizes at 0.8 of the initial stress [Fu, 1993]. It is interesting to note that value of the relative stress relaxation is approximately identical for the ACL, PCL and PT of the same knee.

Some stress relaxation curves show unexpected behavior. After 500 to 1000 seconds, the stress stops relaxing and begins to increase. This phenomenon was observed for 5 specimens (3 PT and 2 ACL). In all the cases, a low initial strain was imposed. To the best of our knowledge, this contraction phenomenon for human cruciate ligaments and patellar tendon has not been reported in the literature. This phenomenon was reported for the human lumbodorsal fascia e.g. [Yahia, 1993]. Theories taking into account modifications in environmental factors such as temperature, pH and ionic content were proposed, but with a set-up similar to this study, the influence of these factors was found to be irrelevant. The only explanation could be the presence of muscle fibers in the specimens [Yahia, 1993]. Further studies need to be performed in this area before a definitive answer can be given.

CHAPTER 4 *Identification of the constitutive laws*

The identification process consists of determining the theoretical parameters from the experimental data. A general framework was proposed in Chapter 2 to describe the contributions of the elasticity, the viscosity, short term and long term memory effects. The identification process follows the same approach. The elastic identification process will be described first, followed by the contribution of the short term memory effects and finally by the long term memory effects. Only the human specimens are considered in this chapter.

4.1 Elastic identification

The elastic constitutive law is given by a partial derivative of the elastic potential with respect to strain to satisfy the basic thermodynamic relations (equation (2.27)). In addition, five others conditions must be satisfied to obtain an admissible constitutive law:

- a) $S(\mathbf{I}) = \mathbf{0}$
- b) $S_{22} = 0$
- c) $C_{11} > 1 \Rightarrow C_{22} < 1$
- d) correct stress-strain curve fit
- e) convexity of the elastic potential W_e

Point a) reflects the fact that the reference geometry is stress free. Point b) means that the experimental traction tests were performed in the absence of lateral forces on the specimens. Point c) is an obvious requirement for a normal material, but could not be verified by a particular constitutive law. Point d) is a qualitative requirement. Finally, point e) is fundamental for the existence and uniqueness of the solution in a boundary-value problem e.g. [Chen, 1988; Curnier, 1994]. Uniqueness of the solution is essential in numerical simulations where analytical solutions do not always exist. It is the only way to have confidence in the numerical results.

The experimental stress-strain curves obtained in Chapter 3 clearly show the stress dependence on strain rate. Consequently, the elastic stress-strain curve was

arbitrarily defined as the curve obtained at the lowest rate of elongation (0.3mm/s), where strain rate effects are minimal.

4.1.1 Compressible elastic law

The determination of an elastic law begins with the choice of an elastic potential. From the shape of the experimental stress-strain curves, an exponential form has been proposed e.g. [Fung, 1981]. In this study, we adopted an exponential-based potential. The five conditions were then checked.

For example, the identification process is detailed for the following potential (which correspond to limited development of the potential proposed by Veronda [Veronda, 1970]):

$$W_e = \alpha \left\{ \left(1 + \beta(I_1 - 3) + \frac{\beta^2}{2}(I_1 - 3)^2 + \frac{\beta^3}{6}(I_1 - 3)^3 \right) - 1 \right\} + c_1(I_2 - 3) \quad (4.1)$$

where α , β and c_1 are three material parameters. $I_1 = \text{tr}C$ and $I_2 = (1/2)((\text{tr}C)^2 - \text{tr}C^2)$ are two strain invariants. The polynomial $(I_1 - 3)$ represents the third order development of the exponential $(I_1 - 3)$. Partial derivation of this potential with regard to C results in the material constitutive law:

$$S(C) = 2\rho_0 \frac{\partial W_e}{\partial C} = 2 \left\{ \alpha \left(\beta I + \beta^2(I_1 - 3)I + \frac{\beta^3}{2}(I_1 - 3)^2 I \right) + c_1(I_1 I - C) \right\} \quad (4.2)$$

Condition a)

$$c_1 = -\frac{\alpha\beta}{2} \quad (4.3)$$

Condition b)

$$S_{22} = 1 + \beta(C_{11} + 2C_{22} - 3) + \frac{\beta^2}{2}(C_{11} + 2C_{22} - 3)^2 - \frac{1}{2}(C_{11} + C_{22}) = 0 \quad (4.4)$$

$$\Rightarrow C_{22} = C_{22}(C_{11}) \quad (4.5)$$

provided the isotropy hypothesis, $C_{33} = C_{22}$.

Condition c) is checked with relation (4.5).

Converted in nominal formulation, the elastic stress-stress law (4.2) combined with (4.3) and (4.5) becomes:

$$P_{11} = P_{11}(F_{11}) = 2\alpha F_{11} \left\{ \beta + \beta^2(F_{11} + 2C_{22} - 3) + \frac{\beta^3}{2}(F_{11} + 2C_{22} - 3)^2 - \beta C_{22} \right\} \quad (4.6)$$

Condition d)

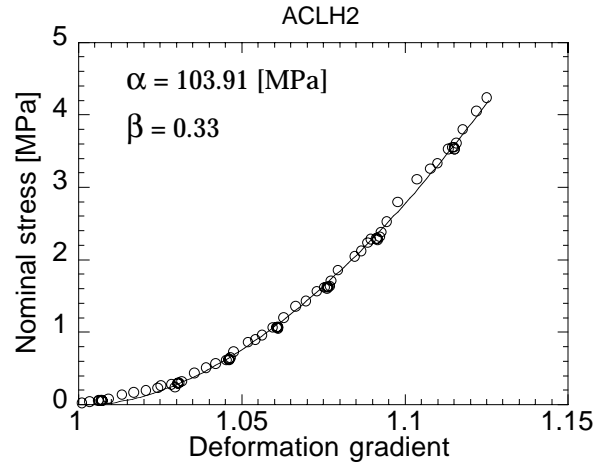


Figure 4.1 Identification of the parameters α and β using a least square fit (plain line) of the experimental stress-strain points (dot points).

Condition e)

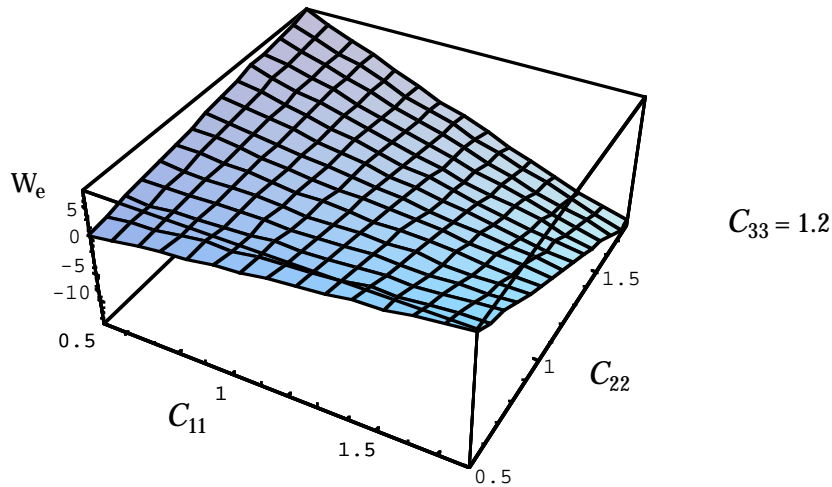


Figure 4.2 Convexity of the elastic potential W_e (4.1) in function of C_{11} and C_{22} ($C_{33} = 1.2$ in this example).

The elastic potential (4.1) with constant $\alpha = 103.91$ and $\beta = 0.33$ is not convex (Figure 4.2.). The elastic potential, therefore must be rejected. This entire procedure was repeated with different potentials. In APPENDIX B, we present the tested potentials with the conditions satisfied and not satisfied. None of these different potentials satisfied the five necessary conditions. Hence, it seems, despite the fact that some potentials result in very nice curve fits, that the shape of the stress-strain curve renders the simultaneous fulfillment of the five conditions impossible.

In order to get an admissible potential, a supplementary hypothesis was formulated and incompressibility of the specimens was assumed. The physical motivation behind this assumption was that the ligaments and tendons are mainly composed of water which is known to be nearly incompressible.

4. 1. 2 Incompressible elastic law

The assumption of incompressibility presupposes that the volume of the body does not change when it deforms (c.f. section 2. 2. 6). Mathematically, incompressibility is expressed as:

$$I_3 = 1 \quad (4.7)$$

with $I_3 = \det \mathbf{C}$. The incompressibility identification is slightly different than the compressible one and is detailed for the following elastic potential proposed by Veronda [Veronda, 1970]:

$$W_e = \alpha \exp[\beta(I_1 - 3)] + c_1(I_2 - 3) \quad (4.8)$$

where α , β and c_1 are three parameters.

Partial derivation of potential (4.8) in regards to \mathbf{C} gives the material constitutive law:

$$\mathbf{S} = -p\mathbf{C}^{-1} + \alpha\beta(2 \exp[\beta(I_1 - 3)])\mathbf{I} + 2c_1(I_1\mathbf{I} - \mathbf{C}) \quad (4.9)$$

where p is an undetermined hydrostatic pressure.

Condition a)

$$c_1 = -\frac{\alpha\beta}{2} \quad (4.10)$$

Condition b)

$$S_{22} = -pC_{22}^{-1} + \alpha\beta(2 \exp[\beta(I_1 - 3)] - I_1) + \alpha\beta C_{22} = 0 \quad (4.11)$$

$$\Rightarrow p = \alpha\beta(2 \exp[\beta(I_1 - 3)] - I_1 + C_{22})C_{22} \quad (4.12)$$

In case of principal strains, (4.7) gives a relation between C_{22} and C_{11} (provided the isotropy hypothesis, $C_{33} = C_{22}$).

Condition c) is satisfied with (4.7).

Converted in nominal formulation, the elastic stress-stress law (4.9) combined with (4.7) and (4.10) becomes:

$$P_{11} = P_{11}(F_{11}) = \alpha\beta \left\{ \left(-2 \exp \left[\beta \left(F_{11}^2 + \frac{2}{F_{11}} - 3 \right) \right] + F_{11}^2 + \frac{1}{F_{11}} \right) \frac{1}{F_{11}^3} + 2 \exp \left[\beta \left(F_{11}^2 + \frac{2}{F_{11}} - 3 \right) \right] - \frac{2}{F_{11}} \right\} F_{11} \quad (4.13)$$

Condition d)

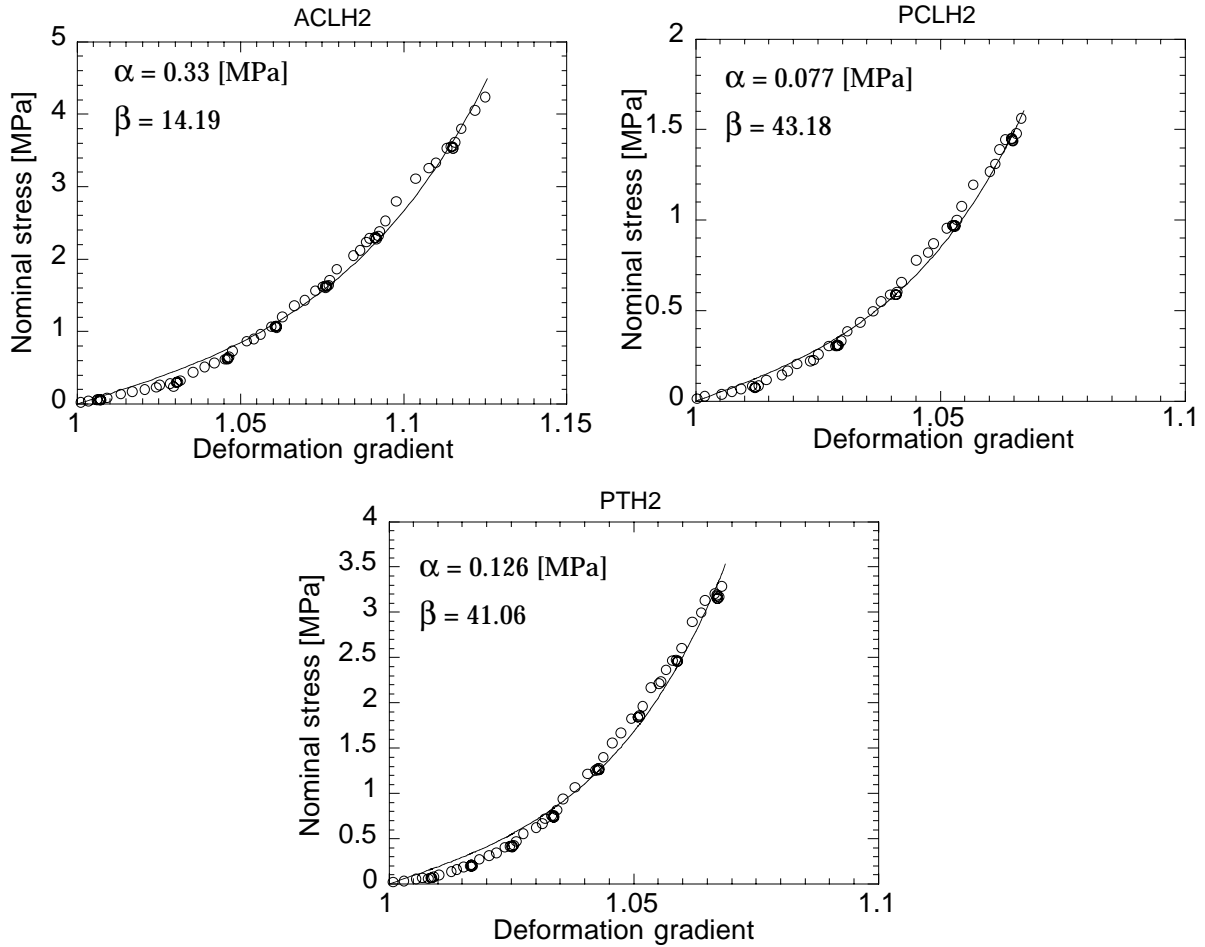


Figure 4.3 Identification of the parameters α and β using a least square fit (plain line) of the experimental stress-strain points (dot points) (incompressible assumption).

Condition e)

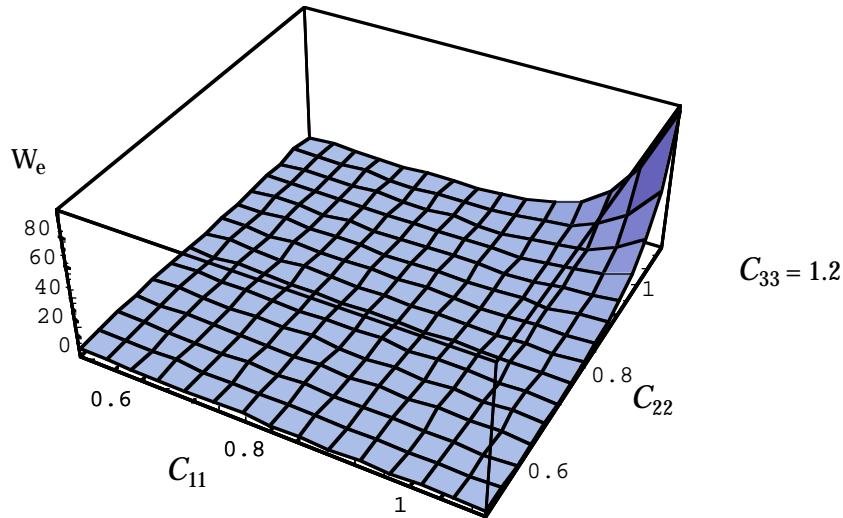


Figure 4.4 Convexity of the elastic incompressible potential W_e (4.8) in function of C_{11} and C_{22} ($C_{33} = 1.2$ in this example).

Now, the convexity condition is fulfilled (c.f. Figure 4.4) and the elastic potential (4.8) is hence admissible.

The elastic potential (4.8) is then used for the elastic identification process and the results are given in APPENDIX C for all human specimens.

Mean values and standard error of the α and β parameters for the elastic potential (4.8) are given in TABLE 4.1 for the human ACL, PCL and PT specimens.

TABLE 4.1

Mean values and standard error of the parameters α and β appearing in the elastic potential (4.8) for the human ACL, PCL and PT specimens.

	α [MPa]	β
ACL	0.30 ± 0.08	12.20 ± 2.18
PCL	0.18 ± 0.05	17.35 ± 8.82
PT	0.09 ± 0.02	66.96 ± 12.99

Student t-tests reveal no statistical difference between the mean values of the ACL, PCL and PT for the parameter α (p values varied between 0.2 and 0.4). However, for the mean value of β , statistical differences exist between the CL (cruciate ligaments) and the PT ($0.06 < p < 0.09$) but not between the CL themselves ($p = 0.7$).

4. 2 Viscous identification

4. 2. 1 Short term memory effects

A framework similar to the elastic identification was used for the viscous constitutive law. Hereafter, the incompressibility hypothesis was imposed. The verification of the entropy inequality (2.29) can be directly checked:

$$\frac{\partial W_v}{\partial \dot{C}} : \dot{C} \geq 0 \quad (4.14)$$

Condition a) is modified and becomes:

$$S(\dot{C} = 0; C = I) = 0$$

Other conditions (b, c, d) remain identical.

A viscoelastic incompressible constitutive law for the case of short term memory effects can be expressed by (c.f. (2.38)):

$$S = -pC^{-1} + 2\rho_0 \frac{\partial W_e}{\partial C} + 2 \frac{\partial W_v}{\partial \dot{C}}$$

W_e is the elastic potential (4.8). In Chapter 2, the viscous potential was said to be convex in \dot{C} and equal to zero when $\dot{C} = 0$ to be thermodynamically acceptable. Hence, we proposed the following original viscous potential to satisfy these two requirements:

$$W_v = \frac{\eta'}{4} \text{tr}(\dot{C})^2 (I_1 - 3) \quad (4.15)$$

where η' is a viscous parameter. Equation (4.14) combined with viscous potential (4.15) becomes:

$$2\eta'(I_1 - 3)\dot{C} : \dot{C} \geq 0$$

Since the scalar product of 2 tensors is positive, this inequality reduces to:

$$\eta'(I_1 - 3) \geq 0$$

In case of incompressibility, $(I_1 - 3)$ is always greater or equal to zero. Therefore, viscous potential (4.15) is thermodynamically admissible if:

$$\eta' \geq 0 \quad (4.16)$$

Inequality (4.16) is checked *a posteriori*.

The constitutive viscoelastic law, derived from the elastic potential (4.8) and viscous potential (4.15), is expressed by:

$$\mathbf{S} = -p\mathbf{C}^{-1} + \alpha\beta(2 \exp[\beta(I_1 - 3)] - I_1)\mathbf{I} + \alpha\beta\mathbf{C} + \eta'(I_1 - 3)\dot{\mathbf{C}} \quad (4.17)$$

Condition a) is satisfied with the constitutive law (4.17).

Condition b)

$$\begin{aligned} S_{22} &= -pC_{22}^{-1} + \alpha\beta(2 \exp[\beta(I_1 - 3)] - I_1) + \alpha\beta C_{22} + \eta'(I_1 - 3)\dot{C}_{22} = 0 \\ \Rightarrow p &= \{ \alpha\beta(2 \exp[\beta(I_1 - 3)] - I_1 + C_{22}) + \eta'(I_1 - 3)\dot{C}_{22} \} C_{22} \end{aligned}$$

Here again, in case of principal strains, (4.7) provides a relation between C_{22} and C_{11} (due to the isotropy hypothesis, $C_{33} = C_{22}$):

Condition c) is satisfied with (4.7).

Equation (4.7) also provides a relation between \dot{C}_{11} and \dot{C}_{22} :

$$\dot{C}_{22} = -\frac{\dot{C}_{11}}{2C_{11}\sqrt{C_{11}}} \quad (4.18)$$

(due to the isotropy hypothesis, $\dot{C}_{33} = \dot{C}_{22}$)

In nominal formulation, the viscoelastic stress-strain law (4.17) combined with (4.7) and (4.18) becomes:

$$\begin{aligned} P_{11} = P_{11}(\dot{F}_{11}; F_{11}) &= \alpha\beta \left\{ \left(-2 \exp \left[\beta \left(F_{11}^2 + \frac{2}{F_{11}} - 3 \right) \right] + F_{11}^2 + \frac{1}{F_{11}} \right) \frac{1}{F_{11}^3} \right. \\ &\quad \left. + 2 \exp \left[\beta \left(F_{11}^2 + \frac{2}{F_{11}} - 3 \right) \right] - \frac{2}{F_{11}} \right\} F_{11} \\ &\quad + \eta' \dot{F}_{11} \left(F_{11}^2 + \frac{2}{F_{11}} - 3 \right) \left(2F_{11}^2 + \frac{1}{F_{11}^4} \right) \end{aligned} \quad (4.19)$$

The two elastic parameters α and β were previously determined with the elastic identification.

Condition d)

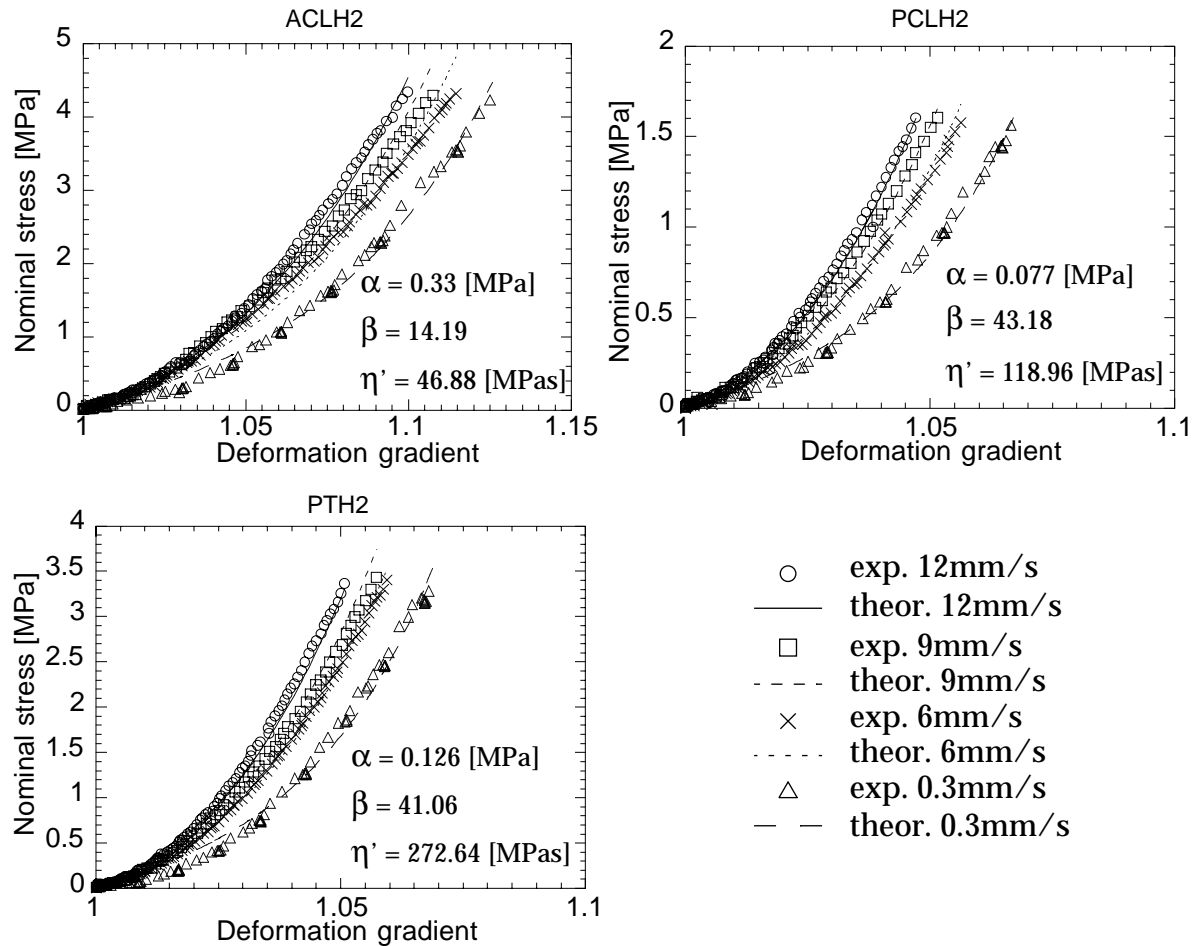


Figure 4.5 Identification of the parameter η' using a least square fit of the experimental stress-strain curves (incompressible assumption).

Since the viscous parameter η' is positive, thermodynamics requirements (4.16) are satisfied. The viscous potential (4.15) is then used for the short term memory effects identification process and the results for all human specimens are given in APPENDIX C Mean value and standard error of the parameter η' for the human ACL, PCL and PT are in TABLE 4.2. Student t-tests reveal no difference between mean values of the ACL, PCL and PT for the parameter η' (p values varied between 0.3 and 0.8).

TABLE 4.2

Mean value and standard error of the parameter η' for the human ACL, PCL and PT specimens.

	η' [MPa s]
ACL	39.29 ± 10.98
PCL	48.67 ± 35.20
PT	438.13 ± 232.20

4.2.2 Long term memory effects

A general formulation of the long term memory effects is given by (2.24):

$$\int_{\delta}^{\infty} \Sigma(\mathbf{G}(t-s), s; \mathbf{C}(t)) ds \quad (4.20)$$

The tensor-valued function Σ is a function of time and strain. In the present case, identification is performed with relaxation tests. In a relaxation process, the deformation is applied at $s = t$ and maintained at constant value \mathbf{C}_0 thereafter. The deformation history \mathbf{G} becomes a constant independent of time, called \mathbf{G}_0 e.g. [Lianis, 1963]. Equation (4.20) is then expressed:

$$\int_{\delta}^t \Sigma(\mathbf{G}_0, s; \mathbf{C}_0) ds \quad (4.21)$$

It is difficult to perform an identification with a function of two variables. Consequently, we assume that the function Σ can be expressed by (variables separation):

$$\Sigma(\mathbf{G}(t-s), s; \mathbf{C}(t)) = \kappa(\mathbf{G}(t-s); \mathbf{C}(t)) \phi(s) \quad (4.22)$$

With a relaxation test, (4.22) means that the temporal behavior of the relaxation function should not be influenced by the strain at which this test is performed. The hypothesis of variables separation in long term memory effects has been widely used in soft tissues biomechanics e.g. [Fung, 1981; Johnson, 1994; Sauren, 1983; Woo, 1981]. However, only a few studies have been concerned with its validity. Relaxation modes were found to be qualitatively different at different strain levels [Lanir, 1980]. The experimental protocol for this study was unclear. In an other study e.g. [Soden, 1974], the relaxation modes showed only slight strain dependences for soft tissues. To the best of our knowledge, experimental verification of the variables separation for the human ACL, PCL and PT specimens is missing. Therefore, we propose a quantitative experimental assessment of the hypothesis of variables separation. In order to identify a one dimensional relaxation test performed at different constant initial strain F_0 , (2.24) is given in nominal description:

$$P(t) = P_e(F_0) + \tilde{\kappa}(\mathbf{G}_0; \mathbf{C}_0) \int_{\delta}^t \phi(s) ds \quad (4.23)$$

where $\tilde{\kappa}$ is the corresponding nominal description of κ . The short term memory effects vanishes during stress relaxation test (strain rate equal to zero). The relaxation function $M(s)$ is defined by:

$$M(s) = \int_{\delta}^t \phi(s) ds \quad (4.24)$$

Determination of the relaxation function is then obtained by:

$$\frac{P(t) - P_e(F_0)}{\kappa(\mathbf{G}_0; \mathbf{C}_0)} = \int_{\delta}^t \phi(s) ds \quad (4.25)$$

We define the relative relaxation function $R(t)$ as the ratio:

$$R(t) = \frac{M(s)}{M(1800)} = \frac{P(t) - P_e(F_0)}{P(1800) - P_e(F_0)} \quad (4.26)$$

If the hypothesis of variables separation (4.22) is justified, the temporal behavior of the relative relaxation function R should be independent of the initial strain F_0 . It means that for tests made with different initial strains F_0 , the value of the relaxation function (4.25) should be the same for the same time. The results for the ACL, PCL and PT of one knee are presented in Figure 4.6. The results for all the specimens are given in APPENDIX C

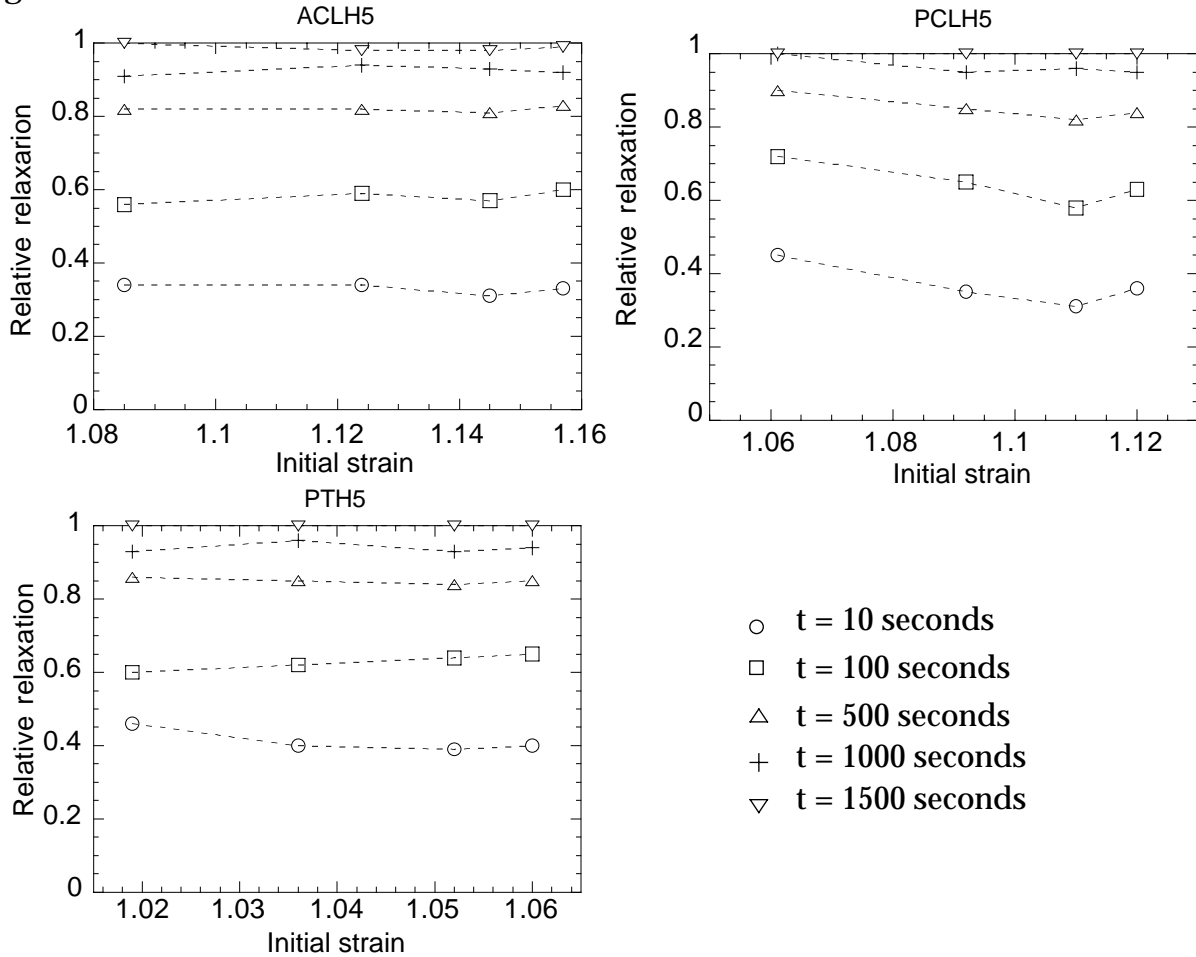


Figure 4.6 Relative relaxation function $R(t)$ at different times in function of the initial strain F_0 .

Figure 4.6 reveals that time behavior of the relative relaxation function is not influenced by the initial strain. Therefore, it can be concluded that the strain does not influence the relaxation function. The hypothesis of variables separation (4.22) is justified, therefore, for the human ACL, PCL and PT in the range of strains used.

Next, identification of the relaxation function $M(s)$ was performed. In Chapter 2, exponential were mentioned as a possible function for the time relaxation identification. Moreover this kind of function satisfies the thermodynamical requirements. Hence, a normalized exponential Prony series was used. It was demonstrated that three exponentials are sufficient to correctly describe the time relaxation behavior e.g. [Lauper, 1996]. $M(s)$ has then the form:

$$M(s) = \frac{\sum_{k=1}^3 a_k \exp\left(-\frac{s}{\tau_k}\right)}{\sum_{k=1}^3 a_k} \quad (4.27)$$

Since it was demonstrated that the initial strain does not to influence the time behavior of the relaxation, identification with the equation (4.27) can be performed on a normalized stress relaxation. We present the results for one knee specimen. All the results are given in the APPENDIX C

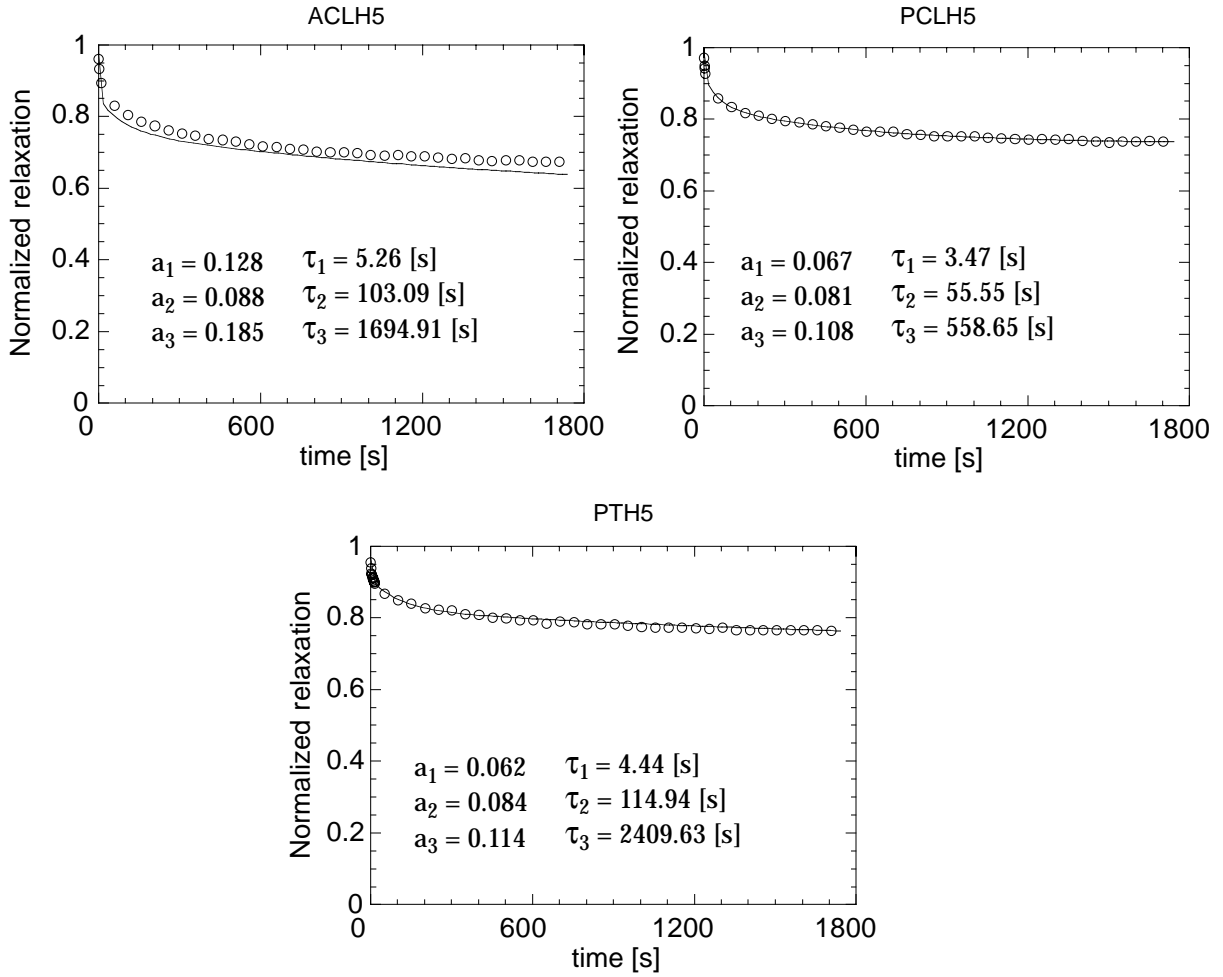


Figure 4.7 Experimental (dot) and Prony series (plain line) of the normalized relaxation in function of time.

In order to take into account the non-linear relationship between the strain and the stress, some investigators have proposed using elastic stress in (4.22) e.g. [Findley, 1976; Fung, 1981; Lockett, 1972]:

$$\kappa(\mathbf{G}(t-s); \mathbf{C}(t)) = \mathbf{S}_e(\mathbf{C}(t-s)) \quad (4.28)$$

This makes it possible to handle non-linear problem in a same framework. Equation (4.20) takes then form:

$$\int_{\delta}^t \mathbf{S}_e(\mathbf{C}(t-s)) \dot{\mathbf{M}}(s) ds \quad (4.29)$$

4.3 Viscoelastic constitutive law

In summary, the general constitutive law (2.24)

$$S = S_e(C) + S_v(\dot{C}; C) + \int_{\delta}^{\infty} \Sigma(G(t-s), s; C(t)) ds$$

takes the following form after the identification process:

$$S_e = -pC^{-1} + \alpha\beta(2 \exp[\beta(I_1 - 3)] - I_1)I + \alpha\beta C$$

$$S_v = \eta'(I_1 - 3)\dot{C}$$

$$\int_{\delta}^{\infty} \Sigma(G(t-s), s; C(t)) ds = \int_{\delta}^t S_e(C(t-s)) \dot{M}(s) ds$$

where $M(s)$ is given by (4.27).

The originality of the present description is given by the fact that the elasticity, the viscosity, short and long term memory effects are described in one framework which satisfies all of the basic physical requirements. Therefore, it is possible to consider only one behavior (for example elasticity) independently of the others. This makes the identification process very convenient and facilitates the interpretation of the different mechanical behaviors.

4.4 Discussion

The presented identification process made it possible to completely characterize the mechanical behavior of the specimens tested. It was shown that the identification process can not only be reduced to a curve fitting of the experimental data. The five conditions required to obtain a correct identification process reduce the mathematical form of the admissible constitutive laws. The resulting constitutive laws satisfy the basic physical laws of conservation.

Traction tests performed with the lowest elongation rate (0.3mm/s) was defined as the elastic response. On one hand, a stress relaxation would probably occur if a too low elongation rate was applied but, on the other hand, the ligament response took into account part of the viscosity (strain rate dependence) if the elongation rate used was too high. Previous comparisons between different elongation rates (0.03mm/s, 1.5mm/s, 3mm/s) performed with some calf and human specimens showed no significant differences. Hence, the 0.3mm/s elongation rate was chosen.

In this work, compressible identification gives unsatisfactory results. Some elastic potentials satisfied four conditions but were not convex. These potentials were numerically implemented anyway but gave no physical results. Therefore, the

incompressible hypothesis had to be considered. This hypothesis has been widely used in soft tissue biomechanics e.g. [DeHoff, 1966; Demiray, 1972; Veronda, 1970; Weiss, 1994]. The physical motivation behind this assumption was that the ligaments and tendons are mainly composed of water which is known to be nearly incompressible. The experimental curve fitting of the incompressible law overestimates the stress in the toe region for almost all the specimens. In this sense, the compressible law gives better results. Further work should be done to determine if it is the shape of the stress-strain curve which does not allow a correct identification e.g. [Davet, 1985]. Incompressibility has the advantage of having automatically satisfied the point b) (i.e. lateral contraction during a traction test) and mathematically facilitating the verification of the point c) (transverse stress equal to zero). The incompressibility hypothesis facilitates the identification process.

In order to be in agreement with the infinitesimal linear elastic description where only two parameters are used, the general form of the elastic constitutive laws was restricted to only two parameters. Physical interpretation of these two parameters is difficult. It has been suggested e.g. [Fung, 1981] that a correlation could exist between the parameters appearing in an exponential strain energy function and the number of collagen fibers stretched. However, this hypothesis was not based on experimental data and should be considered with caution. Linearization of the elastic constitutive law (4.9) furnishes a relation between the elastic parameters (α and β) and Young's modulus ε . It is found that: $\alpha\beta = \varepsilon/3$ which is valid around the origin $F_{11} = 1$. The comparisons between mean values of ε show that a statistical difference only exists between PCL and PT specimens ($p = 0.047$). There was no difference between ACL and PT specimens ($p = 0.11$).

The simplest admissible elastic potential in case of incompressibility is only dependent on the strain invariant I_1 (first term of the right-hand side (4.8)) e.g. [Demiray, 1972; Fung, 1981; Veronda, 1970]. This elastic potential has been used to describe ligaments and tendons biomechanics e.g. [Woo, 1986]. The corresponding constitutive law is only proportional to the identity tensor. This is an important limitation, because shear behavior can not be described. This limitation promoted the choice of an elastic potential which is a function of the first and second strain invariant (I_1, I_2) such that shear behavior could be described.

The description used in this study assumes mechanical isotropy of the specimens. It would have been more appropriate to consider a transverse isotropic situation, but for this case, traction tests in the transverse direction should be performed. In view of the specimen dimensions, transverse traction tests would be difficult to achieve experimentally without the presence of severe artifacts. It was proposed to perform longitudinal and transverse traction tests on fascia specimens whose dimensions are more appropriate to such tests. Then, transverse isotropic constitutive law was identified and proposed to model the mechanical behavior of tendons and ligaments [Weiss, 1994]. Unfortunately, it was shown e.g. [Butler, 1984], that the mechanical properties are significantly different between tendons and fascia. It is therefore

difficult to make generalizations about the constitutive identified law and apply it to different type of specimens.

The short term memory effects are often implicitly characterized by considering the dependence of mechanical properties on the strain rate [Blevins, 1994; Chiba, 1993; Danto, 1993; Haut, 1969]. In these studies, the parameters of an elastic model are given as a function of the strain rate in order to extend elastic model to viscoelastic model. By applying the same implicit description in the present study, the parameters α and β would become functions of the strain rates \dot{F} : $\alpha = \alpha(\dot{F})$ and $\beta = \beta(\dot{F})$. Tested on some specimens, this kind of identification gives inconstant results making it difficult to determine a mathematical form for the two functions $\alpha(\dot{F})$ and $\beta(\dot{F})$. The interpretation of the viscosity behavior by these parameters greatly depends on the adopted mathematical function for the elastic stress-strain law. In the present study this is no longer the case. The strain rate is considered as an explicit variable and characterization of short term memory effects is achieved with an independent parameter, η' . Since the value of η' is positive, thermodynamical requirements are satisfied.

The constitutive identified short term memory effects law exhibits a linear strain rate behavior. This trend has already been noted in previous works e.g. [Abrahams, 1967; Sanjeevi, 1982]. The contribution of the present work is to formulate the viscous law in a formal framework which satisfies the basic physical requirements. Moreover, the application of the obtained constitutive viscous law to large deformation theory extends the range of application of the identified viscous law. The appearance of the first strain invariant in the viscous law (coupling between elasticity and viscosity) is the result of this extension. Elastic and viscous coupling in large deformation theory has already been noted e.g. [Pioletti, 1996].

There is no statistical difference between the viscous parameters η' for the three type of specimens. The mechanical tests were performed on only four different specimens within each group. Increasing the number of specimens could reveal a difference in the viscous parameter between specimens. However, the scattering of the parameter values is an indication that the interpretation of mean values should be considered carefully. Mechanical characterization of soft tissues is an attempt to classify between different types of specimens. Nevertheless, it appears that each specimen has its own behavior. This is not surprising because living tissues are known to adapt to their mechanical environment. Each specimen experiences *in vivo* a different mechanical history which causes their mechanical responses to be quantitatively different.

The short term memory effects were well described with the proposed viscous potential W_v (4.15). It is observed, however, that the corresponding constitutive law gives better curve fitting at the end of the traction curve than at the beginning. In the toe region (F varying between 1.0 and 1.02), the comparison between experimental and calculated stress was acceptable and a slight overestimation of the calculated stress was obtained. Since the stress is the sum of the elastic and viscous stress, this

incorrect estimation is due to the elastic identification which presented the overestimation (see above).

Attempts were made to use the quasi-linear viscoelastic theory of Fung in short term memory effects for tendon [Haut, 1972] and ligament [Woo, 1981] specimens. For the tendon specimens tested with relatively low strain rates (0.06 to 0.75%/s), the calculated stress were close to the experimental curves. In the second study, the ligament specimens were tested at higher strain rates (till 10%/s) and the results show that the calculated stress was within the range of the experimental curves. However, careful reading of these curves reveals that the effects of strain rate were not precisely described and therefore can not be quantitatively described by the quasi-linear viscoelastic theory.

The long term memory effects are usually modeled, in soft tissue mechanics, with the quasi-linear viscoelastic theory e.g. [Dortmans, 1984; Johnson, 1994; Woo, 1981]. This theory was obtained by directly assuming some hypotheses. First the variables separation of the relaxation function was assumed *a priori*. Then the superposition principle, valid in infinitesimal theory, was applied regardless of the strain values. The present approach is different. It starts from a general description and gradually reduces the constitutive law to describe long term memory effects. From the general viscoelastic description, an integral type description was obtained and constituted the starting point for describing the long term memory effects. The general constitutive framework suggested this approach.

The variables separation of the relaxation function was checked. The results in Figure 4.6 show that this hypothesis is justified for human ACL, PCL and PT until a strain of 15%. To the best of our knowledge, these results for human specimens have not been previously reported in the literature. Use of a Prony series of three exponentials accurately described the time behavior of the relaxation in accordance with what was mentioned in Chapter 3. It was observed that the relaxation process is governed by three characteristic times. No matter how precise the fit is, the parameters of the exponential series are not unique. Therefore, interpretation of the exponential parameters should be carefully performed. Identification of exponential functions for the relaxation function is in agreement with the principle of fading memory c.f. APPENDIX A Moreover, the relaxation function of the exponential type is compatible with the second law of thermodynamics.

Using a different approach, the addition of elastic, short term memory and long term memory effects has already been proposed for one dimensional situation. The relaxation function was expressed as the sum of delta distribution as a function of time e.g. [Mandel, 1978]. However, in addition to the elastic response, short term memory effects and long term memory effects, this development generates higher order time derivatives of strain. Conceptually, it is difficult to physically interpret time strain derivative higher than the first order.

The present identification results in a complete three dimensional viscoelastic description. This constitutive law can be used for soft tissue biomechanics regardless

of the strain and rotation values. Therefore, the obtained constitutive law can be incorporated into a finite element code. For example, numerical tests calculating stress in a ligament during a flexion of the knee can be performed at large flexion angles or large strains.

CHAPTER 5 *Numerical simulations of the ligament stress field*

Now, the problem is completely and rigorously defined. Basic mechanical laws of conservation are satisfied when equation (2.11) is verified. Thermodynamical requirements are satisfied with the framework imposed on the determination of the constitutive laws. Resolution of particular boundary problems can be obtained because the existence of a unique solution is insured by the convexity of the potential. Due to geometric and material non-linearities, no analytical solution exists. Therefore, when complex geometries and boundary conditions are imposed, numerical simulations is necessary to obtain a solution of the mechanical problem. Based on three different numerical methods (finite element, finite difference and linear iteration), a powerful algorithm is available to satisfy equation (2.11). In this chapter, some applications of numerical methods to soft tissues biomechanics are presented:

determination of the stress in an ACL during a neutral, external and internal knee flexion

determination of the stress in an ACL during an anterior tibial drawer test with the knee in neutral, internal and external position

5. 1 Numerical model

Numerical simulations can be performed under the following conditions: 1) the geometry of the specimens are provided; 2) specimens' mechanical behaviors are given; 3) the existence of an adequate spatial discretization (meshing); 4) the existence of appropriate boundary conditions. These conditions are described in this section and tests for their validity are given.

A geometrical model and mesh design (pre-processing) were created using the software package program PATRAN 1.4.3 (The MacNeal-Schwender Corporation, Los Angeles-USA). The data analysis (post-processing) was performed with the same software.

The numerical resolutions (solver) are achieved with the software package program ABAQUS 5.4 (Hibbitt, Karlsson, & Sorensen Inc., Newpark-USA).

5.1.1 Geometrical model

The insertion zones of the ACL, obtained from a different study e.g. [Heegaard, 1993], were delimited by 5 pellets in both the femur and tibia (see section 5.1.4.2 below for details). An interpolation method based on an isoparametrisation was developed to reconstruct the insertion zones e.g. [Pioletti, 1995]. The external contours of the ACL at the tibial and femoral insertion sites were determined. These external contours took into account the fiber orientation of the ligament. Since, the exact three dimensional shape of the ligament was not available, a solid that joins the two reconstructed insertion zones was created. This solid was based on the fiber orientation. The bone insertions around the ligament was constructed. These bone insertions were separated into two distinct zones corresponding to the cortical (3mm of depth) and spongy bones (12mm depth).

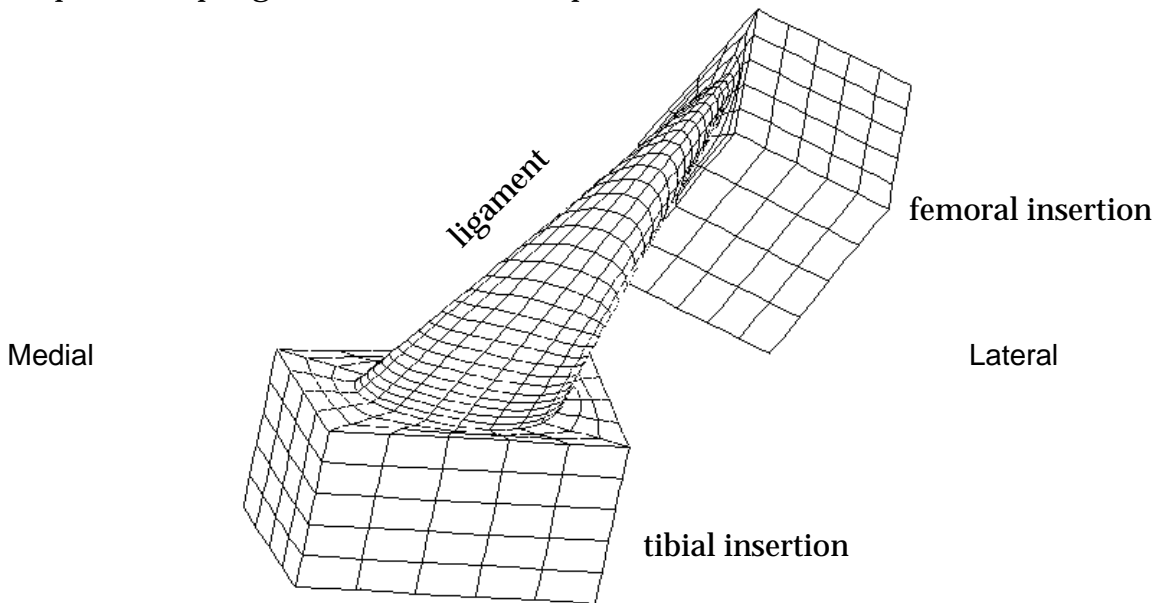


Figure 5.1 Antero-posterior view of the geometrical model and corresponding meshing of the ligament with its two bony insertions.

5.1.2 Material properties

The constitutive law used for the ligament is restricted to the elastic case and corresponds then to the identified potential W_e (4.8):

$$W_e = \alpha \exp[\beta(I_1 - 3)] - \frac{\alpha\beta}{2}(I_2 - 1)$$

The α and β values correspond to the ACLH2 specimen in the present numerical simulations. An isotropic linear constitutive law was used to model the cortical and spongy bony insertions. The values of the Young's modulus and Poisson's ratio for

cortical bone are 17000 [MPa] and 0.36, respectively and for the spongy bone they are 14000 [MPa] and 0.40, respectively e.g. [Cowin, 1989].

5.1.3 Meshing

The ligament was discretized with 600 isoparametric quadratic elements (3350 nodes) which support large deformations (element name C3D20H). A hybrid pressure-displacement formulation was used to account for the incompressible constitutive laws. The displacement field is augmented with an hydrostatic stress field. The hydrostatic stress plays the role of a Lagrange multiplier field enforcing the incompressibility constraint. Interpolation was performed over each element, so that the constraint was satisfied in an integrated (average) sense. The mesh was refined near the insertion zones to take into account high stress gradients.

Both cortical and spongy bony insertions were discretized with 130 isoparametric quadratic elements (727 nodes) and 240 elements (1996 nodes), respectively which support large deformations (element name C3D20).

5.1.4 Boundary conditions

5.1.4.1 Initial stress

The ACL has no stress free state. At all the flexions, a stress is present in the ligament e.g. [Duerselen, 1992]. The precise experimental distribution of this stress field is not known. However, some experimental works have furnished the resulting force of the ACL as a function of the knee flexion. In this study, a resulting force of 100N along the ligament axis at full extension was adopted. This value represents a mean value between different studies e.g. [Roberts, 1994; Wascher, 1993].

5.1.4.2 Three dimensional kinematics

The three dimensional experimental kinematics were obtained from a different study e.g. [Heegaard, 1993]. Briefly, two intact fresh frozen postmortem knees (mean age: 69) were mounted in a device which allowed knee flexion angles. Three flexions were performed for each knee: a neutral one with no torque applied about the tibial axis, an external one with a -3Nm torque applied about the tibial axis and an internal one with a +3Nm torque. Six radio opaque markers were inserted in both the femur and the tibia. A Roentgen Stereophotogrammetric Analysis system [Selvik, 1974] was used to reconstruct the 3D positions of these artificial landmarks with an accuracy of 0.01 mm. The knees were rotated from full extension to 150 degrees of knee flexion in 15 degrees increments. The knees were then dissected in order to reach the insertion sites of the ACL. Five fibers were identified and then marked at their femoral and tibial insertions with additional radio opaque markers. An additional

Roentgenogram provided the relative position of these new markers with respect to the previous markers in the femur and the tibia.

In the present work, an algorithm was developed to get the rotational matrix and translation vector between a set of points at 2 different positions. Hence, the kinematics of the ACL insertions zones were determined e.g. [Pioletti, 1995]. These kinematics were used as boundary conditions for the numerical model. Three kinds of kinematics can be applied: neutral, internal or external corresponding to a normal flexion, a flexion with an internal rotational torque or a flexion with an external rotational torque, respectively. In order to diminish the numerical artifacts of an imposed rigid body motion in the ligament, the kinematics were imposed on the cortical surface bone nodes.

5. 1. 4. 3 Tibial drawer test

The tibial drawer test allows the clinician to determine the antero-posterior laxity of a knee when the patient is supine and his knee is at 20° of flexion. The clinician applies an anterior load perpendicular to tibial axis and evaluates the corresponding laxity. This test was numerically simulated in the following way. Next the initial stress and the kinematics corresponding to the knee flexion of 20° were applied, an anterior 4mm displacement was imposed on the tibial bony insertion. Four millimeter tibial drawer tests represent a mean value of what can be found during clinical tests with an intact ACL [Benvenuti, 1997].

5. 1. 5 Validations

To obtain some confidence in the numerical simulations, several tests need to be performed and each step of the model must be checked.

The precise ACL geometry inside the knee was not available in this study and therefore, the geometry was based on its bony insertion sites. The influence of the ligament geometry on the stress distribution was tested. Different ACL geometries were generated using identical insertion sites. Minor stress differences were found between the geometries. In the limit of an “acceptable” geometry (i.e. with some ACL resemblances), the general stress trends were similar regardless of the geometry.

Experimental traction tests were simulated with two different boundary conditions. First, the ligament was represented by a cylinder. This cylinder was free to deform in the transverse plane, even at its extremities. This particular problem has an analytical

solution which is compared to the numerical one at different strains (Figure 5.2). Verification of the computed constitutive law was achieved in this way.

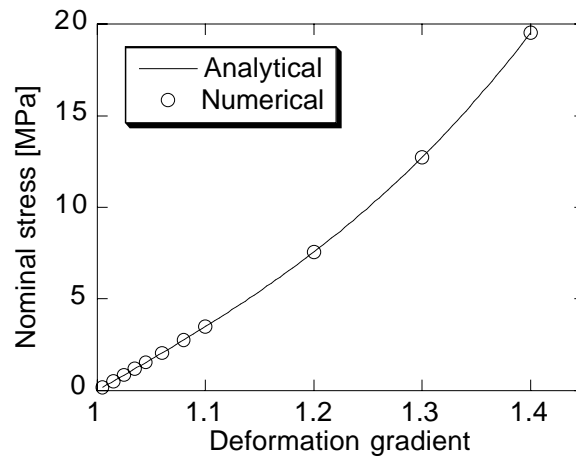


Figure 5.2 Comparison between analytical and numerical solutions in case of traction tests performed on a cylinder.

Secondly, the reconstructed ligament geometry was used. Loads similar to the experimental values were applied and the ligament extremities were not allowed to deform in the transverse plane. This situation corresponds to the experimental case. Here, no analytical solutions exist and therefore numerical solutions (in the middle of the reconstructed ligament) were compared to the present experimental results to check the meshing refinement. Obviously, the precision of the numerical solution increases with the mesh refinement. A compromise must be found between the number of elements used (computational time consuming) and the desired precision of the solution. This precision was judged acceptable (Figure 5.3) when cubic elements were used and higher element density was applied near the insertion zones.

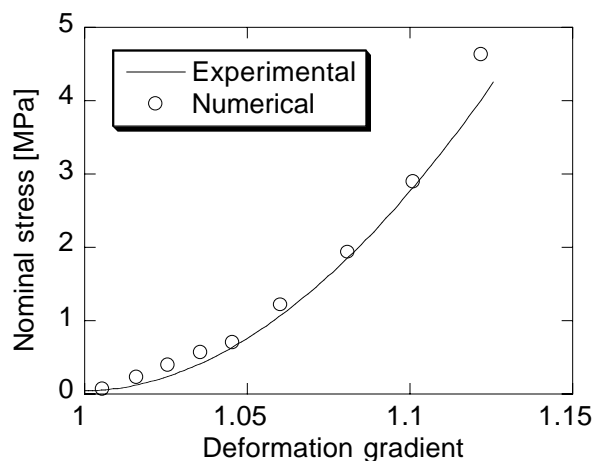


Figure 5.3 Comparison between experimental and numerical stress in case of traction tests.

5. 2 Numerical results

Numerical simulations furnish large amount of data that must be post-processed. Two stress invariants results (hydrostatic stress and Von Mises stress) are presented.

The hydrostatic stress p is defined by:

$$p = -\frac{1}{3J}tr(\mathbf{F}\mathbf{S}\mathbf{F}^T)$$

where $J = det\mathbf{F} = 1$ in the incompressible case and tr represents the trace of a tensor.

If we define the deviatoric stress \mathbf{T} by:

$$\mathbf{T} = \mathbf{F}\mathbf{S}\mathbf{F}^T + p\mathbf{I}$$

the Von Mises stress q is given by:

$$q = \sqrt{\frac{3}{2}(\mathbf{T}:\mathbf{T})}$$

where “:” represents the scalar product between two tensors.

The stress invariants fields in the ACL are presented under an antero-posterior view of the knee and are reported in the initial position of the knee (full extension) in order to compare the results. The results are displayed in the form of fringe plots where the red and white color represents the largest and the smallest values, respectively of hydrostatic stress and Von Mises stress.

5. 2. 1 Flexion of the knee

We present the results from full extension (0°) until 55° of flexion for the neutral case (Figure 5.4 to Figure 5.6). The results for the internal and external cases are displayed at the third step of flexion (~20°) (Figure 5.7).

During knee flexion, an increase in both the Von Mises stress and hydrostatic stress are found near the anterior femoral insertion of the ligament. The region around the tibial insertion is not affected much by the knee flexion.

The stress in the ligament is increased with the knee in internal rotation.

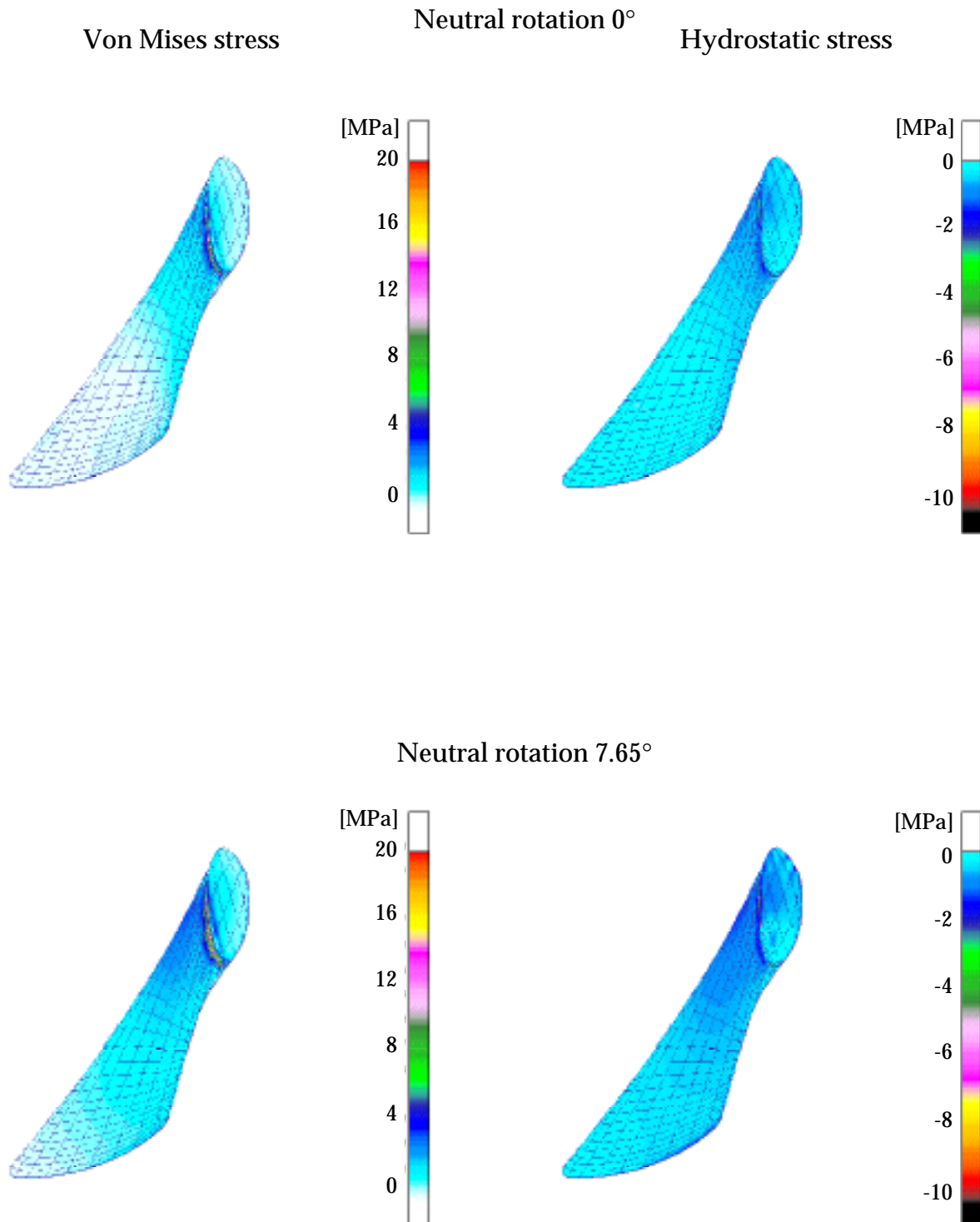


Figure 5.4 Von Mises and hydrostatic stress in the ligament for the first and second step of flexion for the neutral case.

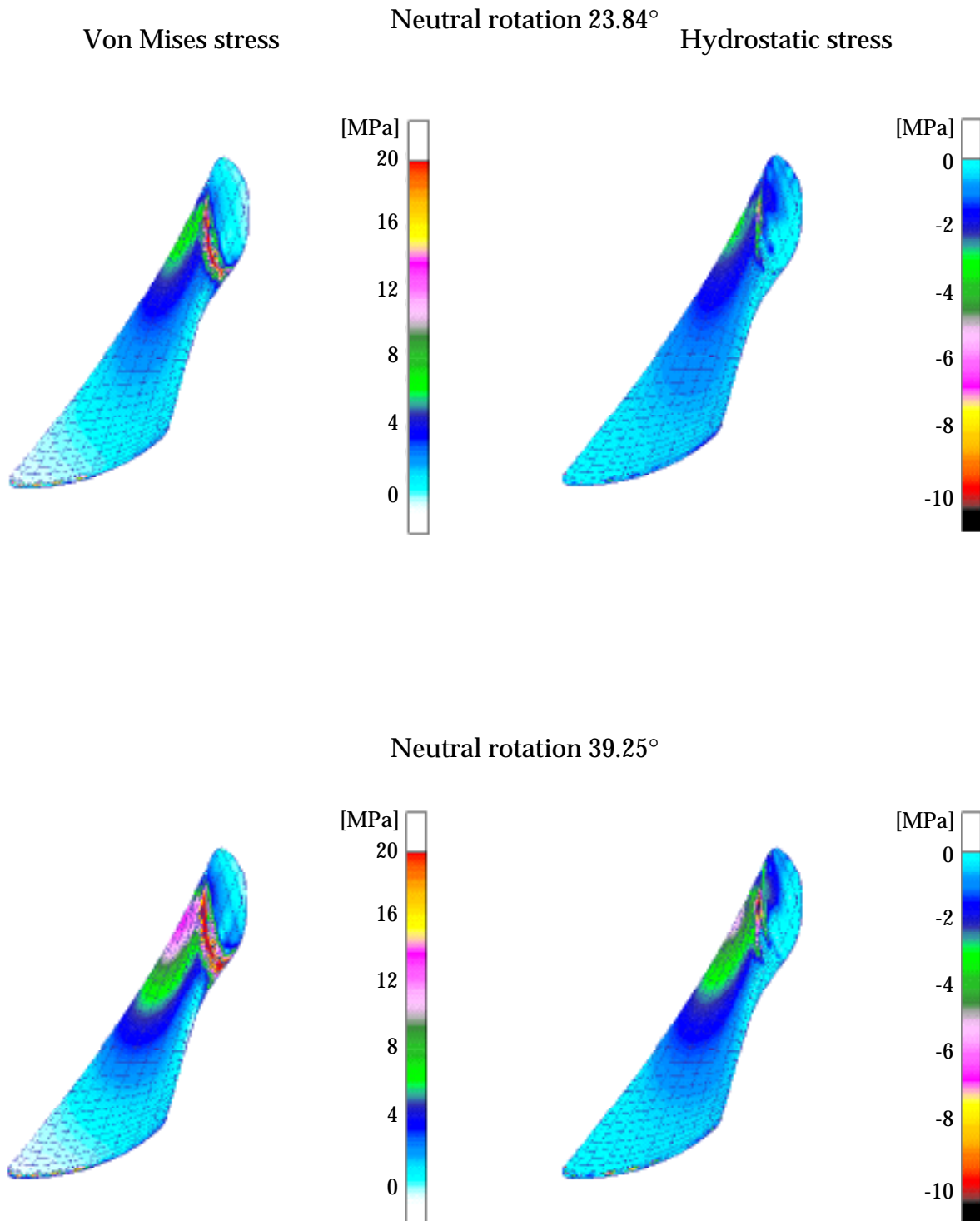


Figure 5.5 Von Mises and hydrostatic stress in the ligament for the third and fourth step of flexion for the neutral case.

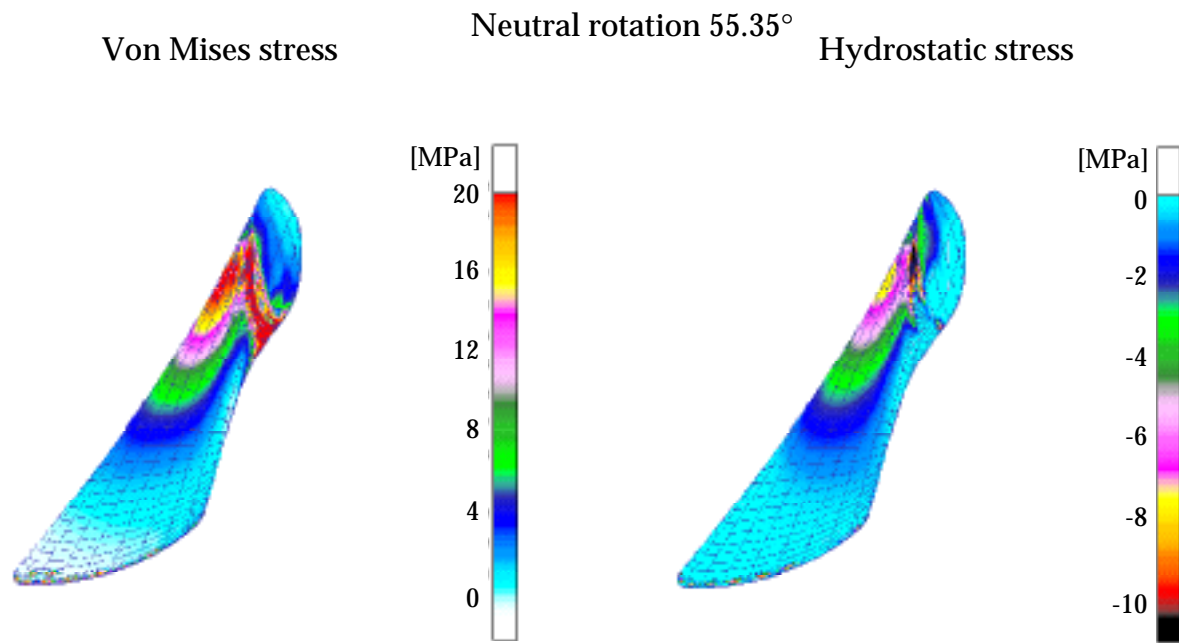


Figure 5.6 Von Mises and hydrostatic stress in the ligament for the fifth step of flexion for the neutral case.

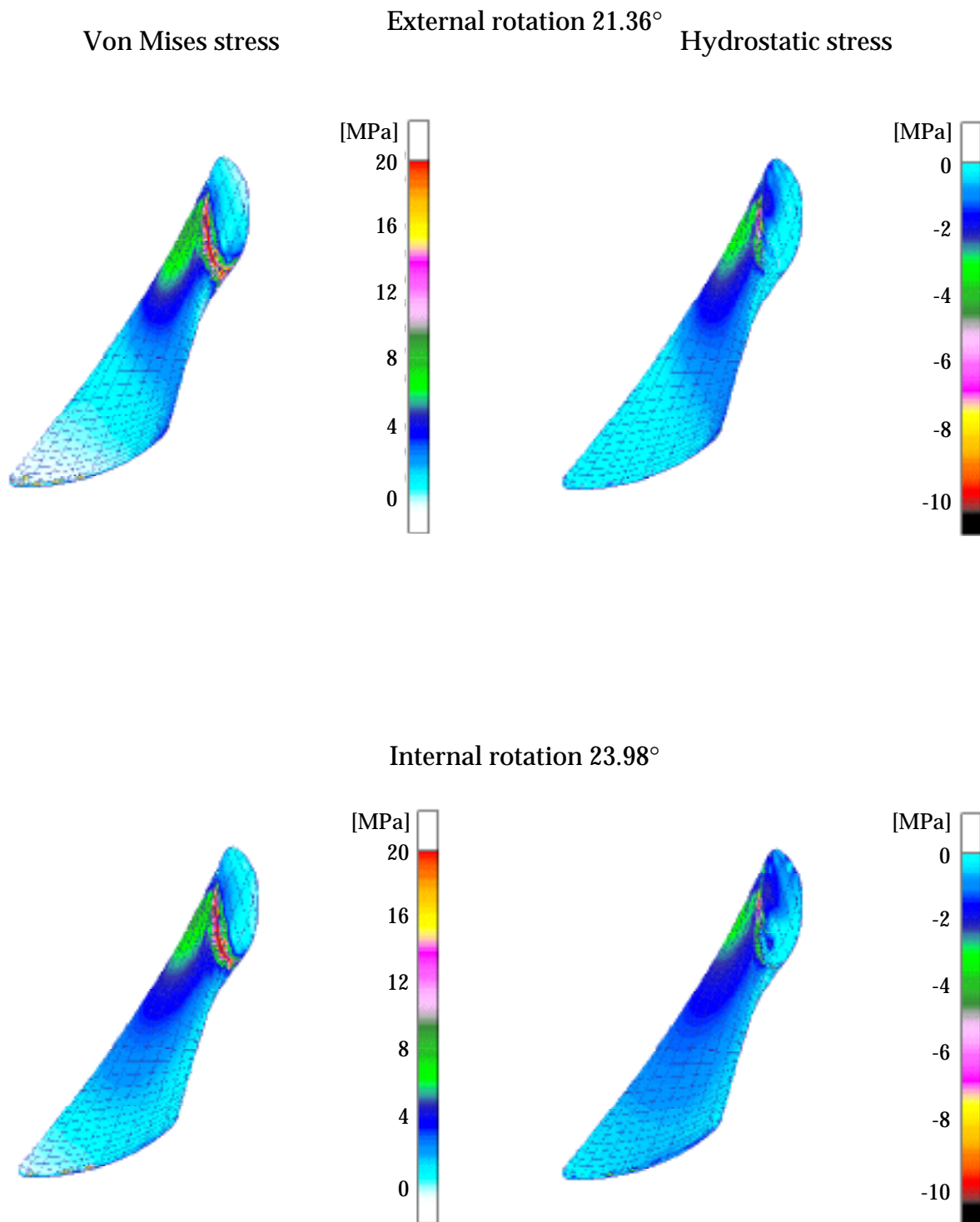


Figure 5.7 Von Mises and hydrostatic stress in the ligament for the third step of flexion (~20°) for the external and internal case.

5. 2. 2 Tibial drawer test

Numerical tibial drawer tests are presented for the neutral case with a 4 mm anterior displacement and a 4mm posterior displacement to check the reliability of this test (Figure 5.8).

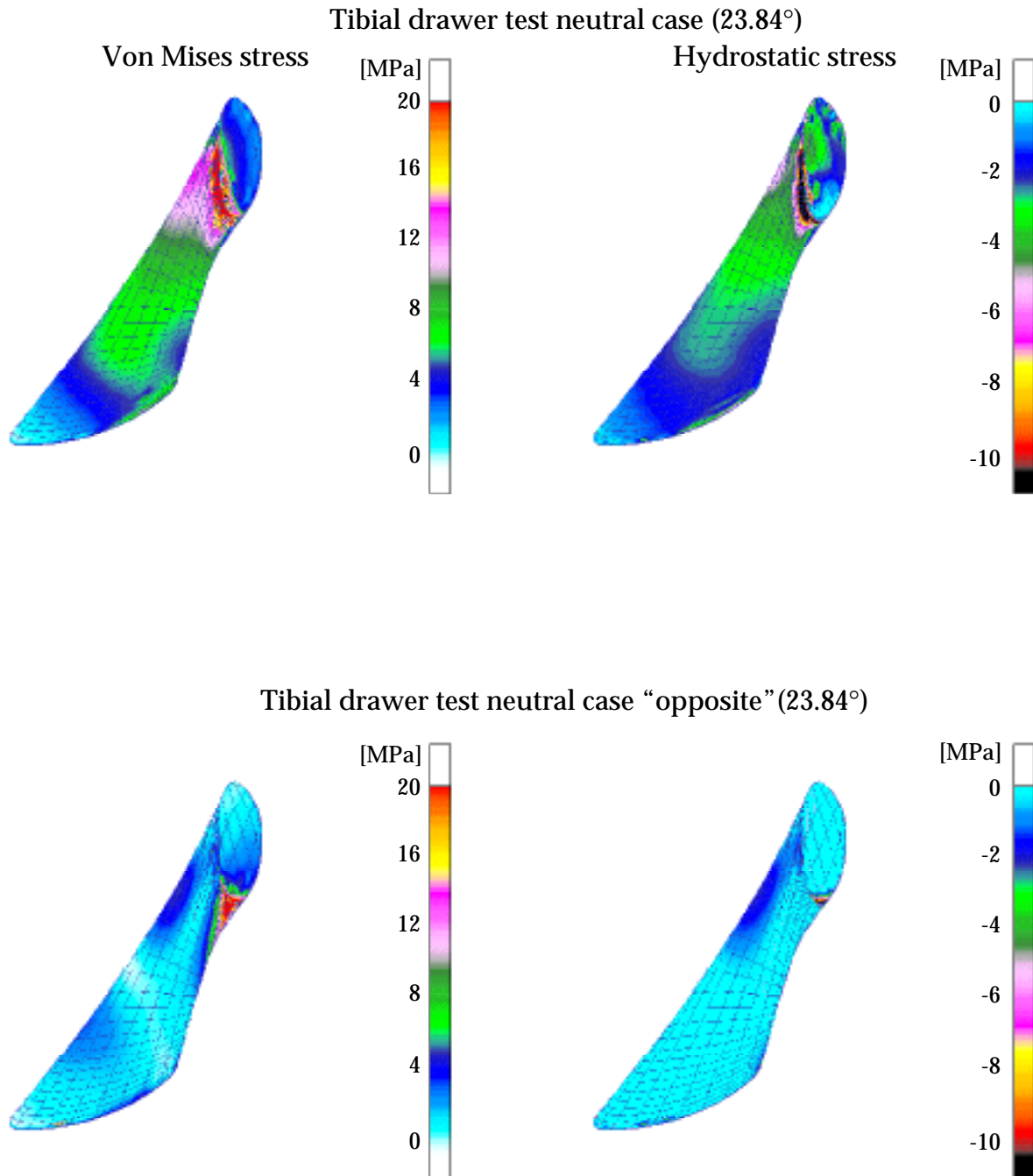
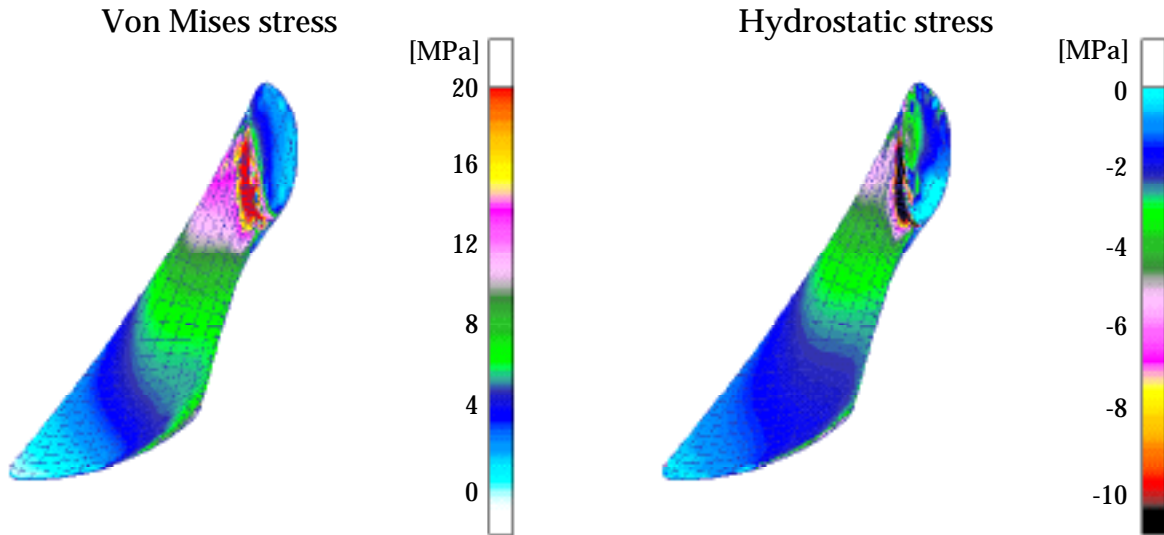


Figure 5.8 Tibial drawer test (antero-postero and postero-antero) for the neutral case.

Tibial drawer tests for the external and internal cases are displayed in Figure 5.9.

Tibial drawer test external case (21.36°)



Tibial drawer test internal case (23.98°)

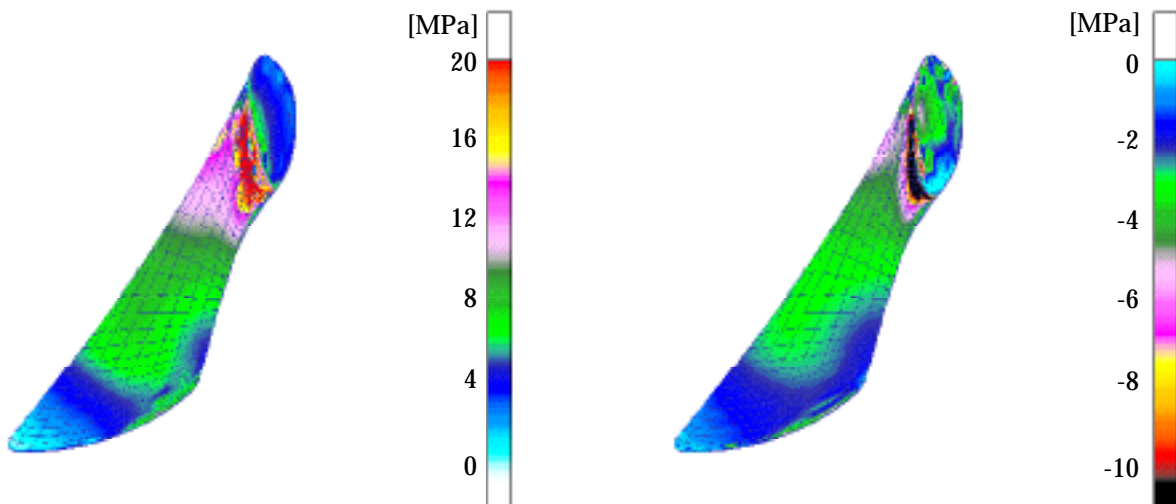


Figure 5.9 Tibial drawer test for the external and internal cases.

The tibial drawer tests clearly increase the stress in the ligament. The posterior tibial drawer tests allows one to verify that the ACL is a major restraint to antero-posterior motions but not to postero-anterior ones. This increase of the ligament stress was found for all three different cases. However, external case was found to slightly decrease the stress in regards to the neutral case, while the internal case increases the ligament stress.

5.3 Discussion

The numerical results were compared to experimental studies of knee flexion and tibial drawer tests. In the present study, the calculated stress field was inhomogeneous in the ACL during flexion and tibial drawer tests. The highest calculated stress was located in the anteriomedial portion of the ligament near the femoral insertion. Clinical study has shown that ruptures of the ACL mainly occur in the intrasubstance of the ligament e.g. [Duncan, 1995]. Moreover, partial ruptures of the anteriomedial ACL bundle have been described as the consequence of stress increase during knee flexion e.g. [Fruensgaard, 1989]. It was concluded that the highest stress is located in the anteriomedial intrasubstance of the ligament which confirms the present numerical results. The simulated tibial drawer test clearly highlighted that the anteriomedial fibers of the ACL are an important restraint to anterior displacement of the tibia. This result is also confirmed by *in vitro* studies e.g. [Blomstrom, 1993; Duerselen, 1992; Hollis, 1988; Livesay, 1995]. Internal rotation of the knee increased the calculated stress in the ACL for the flexion and tibial drawer test. Effects of this internal rotation on the ACL was experimentally investigated with either knee flexion e.g. [Berns, 1992; Duerselen, 1992; Markolf, 1990] or tibial drawer tests e.g. [Ahmed, 1992]. Results showed that internal rotation increases the stress in the ACL and they are, therefore, in accordance with the present numerical study.

Despite good correlation were found between the present numerical study and experimental studies, several limitations of the numerical model should be noted. First, the present study considers the ligament as a single bundle. The ACL is in fact composed of two principal bundles: an anteriomedial and a posteriorlateral bundles. A geometry with two bundles would increase the difficulty of the numerical modeling because interaction between the two parts of the ligament would have to be numerically described. Moreover, *in vitro* studies demonstrated that the anteriomedial bundle of the ACL is mainly stressed during knee flexions or antero-posterior motions e.g. [Blomstrom, 1993; Fruensgaard, 1989; Hollis, 1988]. Addition of the posteriorlateral bundle would certainly increase the reliability of the numerical model when the knee is at full extension as it was shown that the posteriorlateral bundle contributes to the stability of the knee at that position e.g. [Fruensgaard, 1989]. During knee flexion, the posteriorlateral bundle plays a secondary role for the knee stability. Secondly, the cruciate ligaments wrap around each other during knee flexion, especially with internal rotation of the knee e.g. [Hefzy, 1983]. The

consequence of this wrapping could be an increase of the stress value in the ACL. Thirdly, the imposed kinematics were obtained from a passive knee flexion. It was shown that muscular activity increases the stress in the ACL e.g. [Beynnon, 1995; Dürselen, 1996]. Finally, the effects of viscosity were not incorporated into the numerical study. It can be evaluated from the experimental work performed in this study that the stress in the ACL will be increased during dynamic motions. In view of the three latter limitations, the stress calculated in the present study is certainly an underestimation.

Despite the above limitations, the present numerical study gives results that are in accordance with experimental studies. Therefore, the numerical simulations furnished reliable results for comparing the effects of different tests.

A comparison with other numerical studies is difficult because, to the best of our knowledge, no finite model elements for cruciate ligaments are available in the literature. Until now, numerical studies involving flexion of the knee considered the cruciate ligaments as linear or non-linear springs e.g. [Andriacchi, 1983; Loch, 1992; Moeinzadeh, 1983; Mommersteeg, 1996; Wismans, 1980]. The results of these studies can at best give the resultant force of the ligament but not the stress field.

The present numerical study gives complementary results to the experimental studies. It was shown that the resultant force decreases in the ligament as the knee flexion increases e.g. [Roberts, 1994; Wascher, 1993]. Similar results are obtained in the present numerical study if only the posterior part of the ligament near the tibial insertion is considered. This is not the case if anteriomedial part of the ligament is considered. In the present numerical study, anteriomedial fibers clearly showed a stress increase when the flexion increased, a situation also observed in a study concerned with only anteriomedial fibers e.g. [Takai, 1993]. Hence, differences in stress distribution can be important and may be missed with experimental studies. The inhomogeneity of the stress could be measured at some discrete positions with the use of strain gage placed at different locations on the ligament e.g. [Beynnon, 1993]. *In vitro* studies, which furnish the resultant force in the ACL, can only describe partially the mechanical behavior of the ligament during a flexion or a tibial drawer test. Therefore, the present numerical simulations, which gives the stress field, provide a model that is complementary to experimental results.

CHAPTER 6 *Conclusions and perspectives*

6.1 Conclusions

6.1.1 Biomechanical conclusions

The present work, devoted to the study of the biomechanical properties of soft tissues is based on a continuum approach and developed a general framework to test different constitutive laws. The basic mechanical and thermodynamical requirements are satisfied *a priori* in this framework. Five conditions that a constitutive law must fulfill to obtain a rigorous identification process were highlighted. The proposed general constitutive law, taking simultaneously into account elastic, short term memory and long term memory contributions, was completely defined for a three dimensional situation. Moreover, the proposed constitutive law had the advantage to be meaningful in large deformations. Experimental identification of the constitutive law with cruciate ligaments and patellar tendons specimens revealed important differences between different types of soft tissues (cruciate ligaments and patellar tendons) and between knee specimens. Hence, it was difficult to characterize a type of tissue by the use of mean values only. In fact, ligaments and tendons of each knee specimen had particular mechanical properties due to their specific remodelling processes, depending on the mechanical history of the specimen.

Numerical simulations were performed to determine the stress within the ligament during a knee flexion. The stress field was found to be inhomogeneous in the ligament with the highest stress in the antero-medial portion of the ligament. Tibial drawer tests, which were numerically simulated, revealed that the antero-medial portion of the ACL was stressed mainly during antero-postero displacement of the tibia. Internal rotation of the knee was found to increase the stress in the ligament for all simulated motions. Numerical simulations yielded complementary results to the experimental data, based on experiments which measured only resultant or partial forces.

6.1.2 Clinical relevance

Several clinical relevance of the present biomechanical can be noted. Diagnosis of an ACL rupture is generally determined by a contralateral comparison of antero-postero

knee laxity (tibial drawer test), which is measured under a quasi-static load. The ligament was demonstrated to be viscoelastic. Therefore, comparison between knees would be more precise if the load was dynamically applied to the knee: a knee with a rupture ACL would not show any effect, whereas a knee with an intact ACL would become stiffer with increasing the strain rate. This viscoelastic behavior could also be exploited for preconditioning: experimental results show that the ligament becomes stiffer when it is preconditioned. Consequently, flexing of a patient's knee several times prior to a tibial drawer test would increase the difference in measured laxities between a healthy knee and one suffering an ACL rupture.

In view of the diversity of ligament's and tendon's mechanical behaviors, ACL surgery should ideally be personalized to each patient, by the use of ACL grafts with the same mechanical behavior (elastic and viscous) as the patient's injured ACL. Up to date, no such material has been developed.

During rehabilitation programs following an ACL suture or replacement, knee flexion in an internal position should be avoided because numerical simulations showed that knee flexions with internal position of the knee lead to an increase of the resulting stress of the ligament.

6.2 Perspectives

Numerical simulations were performed with an ACL geometry based on its insertion zones. A refinement of this geometry would certainly increase the precision of the numerical simulations. Precise ligament or tendon geometries could be obtained with modern methods of image acquisition such as magnetic resonance imaging (MRI). It would also be appropriate to consider the ACL geometry made of two bundles. Initial stress could have different values in the two bundles, which would correspond to a more realistic *in vivo* situation. With some geometrical improvements of the present numerical study, surgical replacement of the ACL could be simulated. Parameters such as tensioning of the graft, orientation of the bone tunnels could then be evaluated in the ACL replacement procedure. The short term memory effects could be directly implemented in a finite element code if a constitutive law with an explicit strain rate dependence could be used in the code. Therefore, flexion of the knee at different rates could be simulated. This kind of test would result in further insight into ACL rupture, since ACL rupture generally occurs in dynamic situations. Scattering of the mechanical parameters rendered the use of mean values difficult for the characterization of a group of specimens (ACL, PCL, PT). An interesting perspective could be to determine correlations between mechanical parameters used in this study and biological or structural properties of the ligaments and tendons as done in bone mechanics, where the bone density is correlated to its elastic behavior.

In this study, a constitutive law, taking into account different mechanical behaviors of ligaments and tendons, was determined. This law provided a new method to

describe the stress within soft tissues, such as ligaments and tendons. However, like most living tissues, ligaments and tendons are known to gradually adapt to imposed mechanical stimuli, a process called “remodelling”. The next step for a more complete description of ligament and tendon biomechanics would therefore be the incorporation of the present mechanical description into a remodelling model of ligaments and tendons.

Bibliography

- [1] Abrahams M. (1967). Mechanical behavior of tendon in vitro. *Med Biol Engng.* 5: 433-443.
- [2] Aglietti P., Buzzzi R., D'Andria S. and Zaccherotti G. (1992). Long-term study of anterior cruciate ligament reconstruction for chronic instability and using the central one-third patellar tendon and a lateral extraarticular tenodesis. *Am J Sports Med.* 20(1): 38-45.
- [3] Aglietti P., Buzzzi R., Zaccherotti G. and De Biase P. (1994). Patellar tendon versus doubled semitendinosus and gracilis tendons for anterior cruciate ligament reconstruction. *Am J Sports Med.* 22(2): 211-218.
- [4] Ahmed A. M., Burke D. L., Duncan N. A. and Chan K. H. (1992). Ligament tension pattern in the flexed knee in combined passive anterior translation and axial rotation. *J Orthop Res.* 10(6): 854-867.
- [5] Altpeter F., Salzmann C., Gillet D. and Longchamp R. (1995). A general instrument for real time control and data acquisition. IFAC Workshop.
- [6] Amendola A. and Fowler P. (1992). Allograft anterior cruciate ligament reconstruction in a sheep model. The effect of synthetic augmentation. *Am J Sports Med.* 20(3): 336- 346.
- [7] Amis A. A. (1989). Anterior cruciate ligament replacement. Knee stability and the effects of implants. *J. Bone Joint Surg.* 71-B(5): 819-824.
- [8] Amis A. A. and Scammell B. E. (1993). Biomechanics of intra-articular and extra-articular reconstruction of the anterior cruciate ligament. *J Bone Joint Surg.* 75-B(5): 812-817.
- [9] Amis A. A., Kempson S. A. and Hukkanen M. (1994). Polyester fiber ACL implants - will they form new ligaments in-vivo? 40th ORS.
- [10] Amis A. A. and Zavras T. D. (1995). Review: Isometricity and graft placement during anterior cruciate ligament reconstruction. *The Knee.* 2(1): 5-17.
- [11] Andersen H. N., Bruun C. and Sondergard-Petersen P. E. (1992). Reconstruction of chronic insufficient anterior cruciate ligament in the knee using a synthetic Dacron prosthesis. A prospective study of 57 cases. *Am J Sports Med.* 20(1): 20-23.
- [12] Anderson K., Wojtys E. M., Loubert P. V. and Miller R. E. (1992). A

- biomechanical evaluation of taping and bracing in reducing knee translation and rotation. *Am J Sports Med.* 20(4): 416-421.
- [13] Andriacchi T. P., Mikosz R. P., Hampton S. J. and Galante J. O. (1983). Model studies of the stiffness characteristics of the human knee joint. *J Biomech.* 16(1): 23-29.
- [14] Ault H. K. and Hoffman A. H. (1992). A composite micromechanical model for connective tissues: part I-theory (part II-application to rat tail tendon and joint capsule). *J Biomech Engng.* 114: 137-146.
- [15] Barrett G. R., Line L. L., Shelton W. R., Manning J. O. and Phelps R. (1993). The Dacron ligament prosthesis in anterior cruciate ligament reconstruction. A four-year review. *Am J Sports Med.* 21(3): 367-373.
- [16] Barry D. and Ahmed A. M. (1986). Design and performance of a modified buckle transducer for the measurement of ligament tension. *J Biomech Engng.* 108: 149-152.
- [17] Benvenuti J. F., Vallotton J. A., Meystre J. L. and Leyvraz P. F. (1997). Objective assessment of the anterior tibial translation in Lachman test position: comparison between three types of measurement. submitted to *Knee Surg Sports Trauma Arthro.*
- [18] Berns G. S., Hull M. L. and Patterson H. A. (1992). Strain in the anteromedial bundle of the anterior cruciate ligament under combination loading. *J Orthop Res.* 10: 167-176.
- [19] Beynnon B. D., Fleming B. C., Pope M. H. and Johnson R. J. (1993). The measurements of anterior cruciate ligament strain *in vivo*. In: The anterior cruciate ligament: current and future concepts. Ed. Jackson DW. Raven Press. New York. : 101-111.
- [20] Beynnon B. D., Johnson R. J. and Fleming B. C. (1993). The mechanics of anterior cruciate ligament reconstruction. In: The anterior cruciate ligament: current and future concepts. Ed. Jackson DW. Raven Press. New York. : 259-272.
- [21] Beynnon B. D., Flemming B. C., Johnson R. J., Nichols C. E., Renström P. A. and Pope H. M. (1995). Anterior cruciate ligament strain behavior during rehabilitation exercises *in vivo*. *Am J Sports Med.* 23(1): 24-34.
- [22] Blankevoort L., Huiskes R. and de Lange A. (1991). Recruitment of knee-joint ligaments. *J Biomech. Engng.* 113: 94-103.
- [23] Blevins F. T., Hecker A. T., Bigler G. T., Boland A. L. and Hayes W. C. (1994). The effects of donor age and strain rate on the biomechanical properties of bone-patellar tendon-bone allografts. *Am J Sport Med.* 22(3): 328-333.
- [24] Blomstrom G. L., Livesay G. A., Fujie H., Smith B. A., Kashiwaguchi S. and Woo S. L. Y. (1993). Distribution of in-situ forces within the human anterior cruciate ligament. ASME Bioengineering Conference.
- [25] Boehler J. P. (1987). Applications of tensor functions in solid mechanics.

- Springer-Verlag.
- [26] Bosch U. and Kasperczyk W. J. (1992). Healing of the patellar tendon autograft after posterior cruciate ligament reconstruction-a process of ligamentization? An experimental study in a sheep model. *Am J Sports Med.* 20(5): 558-566.
- [27] Brand R. A. (1986). Knee ligaments : a new view. *J Biomech Engng.* 108: 106-110.
- [28] Bray R. C. and Daudy D. J. (1989). Meniscal lesions and chronic anterior cruciate ligament deficiency. *J. Bone Joint Surg.* 71-B(1): 128-130.
- [29] Brown C. H., Hecker A. T., Hipp J. A., Myer E. R. and Hayes W. C. (1993). The biomechanics of interference screw fixation of patellar tendon anterior cruciate ligament grafts. *Am J Sports Med.* 21(6): 880-886.
- [30] Butler D. L., Grood E. S., Noyes F. R., Zernickes R. F. and Brackett K. (1984). Effects of structures and strain measurement technique on the material properties of young human tendons and fascia. *J Biomech.* 17(8): 579-596.
- [31] Butler D. L., Kay M. D. and Stouffer D. C. (1986). Comparison of material properties in fascicle-bone units from human patellar tendon and knee ligaments. *J Biomech.* 19(6): 425-432.
- [32] Butler D. L., Guan Y., Kay M., Cummings J., Feder S. and Levy M. (1992). Location-dependent variations in the material properties of the anterior cruciate ligament. *J Biomech.* 25(5): 511-518.
- [33] Campbell W. (1939). Reconstruction of the ligaments of the knees. *Am J Surg.* 43: 473-480.
- [34] Chen W. F. and Han D. J. (1988). Plasticity for structural engineers. Springer-Verlag.
- [35] Chiba M. and Komatsu K. (1993). Mechanical responses of the periodontal ligament in the transverse section of the rat mandibular incisor at various velocities of loading in vitro. *J. Biomech.* 26(4/5): 561-570.
- [36] Chimich D., Shrive N., Frank C., Marchuk L. and Bray R. (1992). Water content alters viscoelastic behaviour of the normal adolescent rabbit medial collateral ligament. *J Biomech.* 25(8): 831-837.
- [37] Coleman B. D. and Noll W. (1961). Foundations of linear viscoelasticity. *Review of modern physics.* 3(2): 239-249.
- [38] Coleman B. D. (1964). Thermodynamics of materials with memory. *Arch Rational Mech Anal.* 17: 1-46.
- [39] Coussy O. (1995). Mechanics of porous continua. Wiley.
- [40] Cowin S. C. (1989). Bone mechanics. CRC Press.
- [41] Crowninshield R. D. and Pope M. H. (1976). The strength and failure characteristics of rat medial collateral ligament. *J Trauma.* 16: 99-105.
- [42] Curnier A. (1994). Computational methods in solid mechanics. Kluwer Academic Publishers.

- [43] Daniel D. M. (1993). Selecting patients for ACL surgery. In: The anterior cruciate ligament: current and future concepts. Ed. Jackson DW. Raven Press. New York. : 251-258.
- [44] Danto M. I. and Woo S. L. Y. (1993). The mechanical properties of skeletally mature rabbit anterior cruciate ligament and patellar tendon over a range of strain rates. *J Orthop Res.* 11: 58-67.
- [45] Davet J. L. (1985). Sur les densités d'énergie en élasticité non linéaire: confrontation des modèles et de travaux expérimentaux. *Annales Ponts et Chaussées.* (4): 2-33.
- [46] Decraemer W. F., Maes M. A., Vanhuysse V. J. and Vanpeperstraete P. (1980). A non-linear viscoelastic constitutive equation for soft biological tissues, based upon a structural model. *J Biomech.* 13(7): 559-564.
- [47] DeHoff P. H., Lianis G. and Goldberg W. (1966). An experimental program for finite linear viscoelasticity. *Trans Soc Rheol.* 10: 385-398.
- [48] Demiray H. (1972). A note on the elasticity of soft biological tissues. *J Biomech.* 5: 309-311.
- [49] Demmer P., Fowler M. and Marino A. A. (1991). Use of carbon fibers in the reconstruction of the knee ligaments. *Clin Ortho.* 271(10): 225-232.
- [50] Djian P., Christel P., Roger B. and Witvoet J. (1994). Evaluation radiologique et IRM des ligamentoplasties intra-articulaires utilisant le tendon rotulien. *Rev Chirg Orthop.* 80: 403-412.
- [51] Dorlot J. M., Ait Ba Sidi M., Tremblay G. M. and Drouin G. (1980). Load elongation behaviour of the canine anterior cruciate ligament. *J Biomech Eng.* 102: 190-193.
- [52] Dortmans L. J. M., Sauren A. A. H. J. and Rousseau E. P. M. (1984). Parameter estimation using the quasi-linear viscoelastic model proposed by Fung. *J biomech Engng.* 106: 198-203.
- [53] Duerselen L., Paessler H., Treugut-Roesch B. and Claes L. (1992). Biomechanical effects of pretensioning of augmented PT-ligament replacement. VII ESB. Rome.
- [54] Duncan J. B., Hunter R., Purnell M. and Freeman J. (1995). Meniscal injuries associated with acute anterior cruciate ligament tears in alpine skiers. *Am J Sports Med.* 23(2): 170-172.
- [55] Dunn M. G., Tria A. J., Kato Y. P., Bechler J. R., Ochner R. S., Zawadsky J. P. and Silver F. H. (1992). Anterior cruciate ligament reconstruction using a composite collagenous prosthesis. A biomechanical and histological study in rabbits. *Am J Sports Med.* 20(5): 507-515.
- [56] Dürselen L., Claes L. and Kiefer H. (1996). The influence of muscle forces and external loads on cruciate ligament strain. *Am J Sports Med.* 23(1): 129-136.
- [57] Fabrizio M. and Morro A. (1985). Thermodynamic restriction on relaxation

- functions in linear viscoelasticity. *Mech Res Comm.* 12(2): 101-105.
- [58] Ferreti A., Papandrea P., Conteduca F. and Mariani P. P. (1992). Knee ligament injuries in volleyball players. *Am J Sports Med.* 20(2): 203-207.
- [59] Fetto J. E. and Marshall J. L. (1980). The natural history and diagnosis of anterior cruciate ligament insufficiency. *Clin Orthop.* 147: 29-38.
- [60] Findley W. N., Lai J. S. and Onaran K. (1976). Creep and relaxation of nonlinear viscoelastic materials. Dover Publication.
- [61] Flahiff C. M., Brooks A. T., Hollis J. M., Vander Schilden J. L. and Nicholas R. W. (1994). Biomechanical properties of patellar tendons from donors of various age groups. 40th ORS. New Orleans.
- [62] Fridén T., Zätterström R., Lindstrand A. and Moritz U. (1991). Anterior-cruciate-insufficient knees treated with physiotherapy. *Clin Ortho.* 263(2): 190-199.
- [63] Fruensgaard S. and Johannsen H. V. (1989). Incomplete ruptures of the anterior cruciate ligament. *J. Bone Joint Surg.* 71-B(3): 526-530.
- [64] Fu F. H., Harner C. D., Johnson D. L., Miller M. D. and Woo S. L. Y. (1993). Biomechanics of knee ligaments. *J Bone Joint Surg.* 75-A(11): 1716-1727.
- [65] Fu F. H. and Schulte K. R. (1996). Anterior cruciate ligament surgery 1996. State of the art? *Clin Orthop Rel Res.* 325: 19-24.
- [66] Fujie H., Livesay G. A., Woo S. L. Y., Kashiwaguchi S. and Blomstrom G. (1995). The use of a universal force-moment sensor to determine in-situ forces in ligaments: a new methodology. *J biomech Engng.* 117: 1-7.
- [67] Fung Y. C. (1973). Biorheology of soft tissues. *Biorheology.* 10: 139-155.
- [68] Fung Y. C. (1981). Biomechanics : mechanical properties of living tissues. Springer-Verlag.
- [69] Germain P. (1973). Cours de mécanique des milieux continus. Masson & Cie.
- [70] Germain P. (1986). Mécanique-Tome I et II. Ellipses.
- [71] Goldstein S. A., Armstrong T. J., Chaffin D. B. and Matthews L. S. (1987). Analysis of cumulative strain in tendons and tendon sheaths. *J Biomech.* 20(1): 1-6.
- [72] Graf B. K. and Vanderby R. (1993). Autograft reconstruction of the anterior cruciate ligament: placement, tensioning and preconditioning. In: The anterior cruciate ligament: current and future concepts. Ed. Jackson DW. Raven Press. New York. : 281-289.
- [73] Gurtin M. E. (1981). An introduction to continuum mechanics. Academic Press.
- [74] Harper K. A. and Grood E. S. (1993). A three dimensional finite element model of an ACL reconstruction. ASME Bioengineering Conference.
- [75] Haut R. C. and Little R. W. (1969). Rheological properties of canine anterior cruciate ligaments. *J Biomech.* 2: 289-298.

Bibliography

- [76] Haut R. C. and Little R. W. (1972). A constitutive equation for collagen fibers. *J Biomech.* 5: 423-430.
- [77] Haut R. C. (1983). Age-dependent influence of strain rate on the tensile failure of rat-tail tendon. *J Biomech Engng.* 105: 296-299.
- [78] Haut R. C. and Powlison A. C. (1990). The effects of test environment and cyclic stretching on the failure properties of human patellar tendon. *J Orthop Res.* 8: 532-540.
- [79] Hayashi K. (1996). Personal Communication.
- [80] Hayashi K., Kamiya A. and Ono K. (1996). Remodeling of tendon autograft in ligament reconstruction. In: *Biomechanics-Functional adaptation and remodeling.* Springer-Verlag. Tokyo. : 213-250.
- [81] Heegaard J. H. (1993). Large slip contact in biomechanics: kinematics and stress analysis of the patello-femoral joint. *Thesis.* EPFL.
- [82] Hefzy M. S. and Grood E. S. (1983). An analytical technique for modeling knee joint stiffness-part II : Ligamentous geometric nonlinearities. *J Biomech Engng.* 105(May): 145-153.
- [83] Hefzy M. S. (1986). Sensitivity of insertion locations on length patterns of anterior cruciate ligament fibers. *J Biomech Engng.* (108): 73-82.
- [84] Holden J. P., Grood E. S., Korvick D. L., Cummings J. F., Butler D. L. and Bylski-Austrow D. I. (1994). In vivo forces in the anterior cruciate ligament: direct measurements during walking and trotting in a quadruped. *J Biomech.* 27(5): 517-526.
- [85] Hollis J. M., Marcin J. P., Horibe S. and Woo S. L. Y. (1988). Load determination in ACL fiber bundles under knee loading. 13th ORS.
- [86] Hollis J. M. and Woo S. L. Y. (1993). The estimation of anterior cruciate ligament loads *in situ*: indirect methods. In: *The anterior cruciate ligament: current and future concepts.* Ed. Jackson DW. Raven Press. New York. : 85-93.
- [87] Hubbard R. P. and Chun K. J. (1988). Mechanical responses of tendons to repeated extensions and wait periods. *J Biomech Engng.* 110: 11-19.
- [88] Jackson W. D. and Lemos M. J. (1993). Autograft reconstruction of the anterior cruciate ligament. Bone-patellar tendon-bone. In: *The anterior cruciate ligament: current and future concepts.* Ed. Jackson DW. Raven Press. New York. : 291-303.
- [89] Jamison C. E., Marangoni R. D. and Glaser A. A. (1968). Viscoelastic properties of soft tissue by discrete model characterization. *J Biomech.* 1: 33-46.
- [90] Johnson G. A., Tramaglini D. M., Levine R. E., Ohno K., Choi N. Y. and Woo S. L. Y. (1994). Tensile and viscoelastic properties of human patellar tendon. *J Orthop Res.* 12: 796-803.
- [91] Kannus P., Järvinen M., Johnson R., Renström P., Pope M., Beynon B., Nichols C. and Kaplan M. (1992). Function of the quadriceps and hamstrings muscles

- in knees with chronic partial deficiency of the anterior cruciate ligament. Isometric and isokinetic evaluation. *Am J Sports Med.* 20(2): 162-168.
- [92] Kennedy J. C., Weinberg H. W. and Wilson A. S. (1974). The anatomy and function of the anterior cruciate ligament. *J. Bone Joint Surg.* 56-A(2): 223-235.
- [93] Kennedy J. C., Hawkins R. J., Willis R. B. and Danylchuk K. D. (1976). Tensions studies of human knee ligaments. *J Bone Joint Surg.* 58-A: 350-355.
- [94] Kerboull L., Christel P. and Meunier A. (1993). Influence de la technique et du materiel de suture sur le comportement mécanique du transplant de Mac Intosh renforcé. *Revue de Chirurgie Orthopédique.* 79: 185-193.
- [95] Lam T. C., Thomas C. G., Shrive N. G., Frank C. B. and Sabiston C. P. (1990). The effects of temperature on the viscoelastic properties of the rabbit medial collateral ligament. *J Biomech Engng.* 112(May): 147-152.
- [96] Lanir Y. (1979). A structural theory for the homogeneous biaxial stress-strain relationship in flat collagenous tissues. *J Biomech.* 12: 423-436.
- [97] Lanir Y. (1980). A microstructure model for the rheology of mammalian tendon. *J biomech Engng.* 102: 332-339.
- [98] Lauper F. (1996). Mesures et modélisation des effets de la viscosité à mémoire longue du ligament croisé antérieur, Diplôme d'ingénieur physicien, EPFL.
- [99] Lewis J. L., Lew W. D. and Schmidt J. (1982). A note on the application and evaluation of the buckle transducer for knee ligament force measurement. *J Biomed Engng.* 104: 125-128.
- [100] Lewis J. L., Lew W. D., Hill J. A., Hanley P., Ohland K., Kirstukas S. and Hunter R. E. (1989). Knee joint motion and ligament forces before and after ACL reconstruction. *J Biomech Engng.* 111: 97-106.
- [101] Lianis G. (1963). Small deformation superposed on an initial large deformation in viscoelastic bodies. Fourth international congress on rheology.
- [102] Lindenfeld T. N., Schmitt D. J., Hendy M. P., Mangine R. E. and Noyes F. R. (1994). Incidence of injury in indoor soccer. *Am J Sports Med.* 22(3): 364-371.
- [103] Livesay G. A., Fujie H., Kashiwaguchi S., Morrow D. A., Fu F. H. and Woo S. L. Y. (1995). Determination of the *In Situ* forces and force distribution within the human anterior cruciate ligament. *Annals Biomed Eng.* 23: 467-474.
- [104] Loch D. A., Luo Z., Lewis J. L. and Stewart N. J. (1992). A theoretical model of the knee and ACL : theory and experimental verification. *J Biomech.* 25(1): 81-90.
- [105] Lockett F. J. (1972). Nonlinear viscoelastic solids. Academic Press Inc.
- [106] Lyon R. M., Lin H. C., Kwan M. K., Hollis J. M., Akeson W. H. and Woo S. L. Y. (1988). Stress relaxation of the anterior cruciate ligament (ACL) and the patellar tendon (PT). 34th ORS.
- [107] Madey S. M., Cole K. J. and Brand R. A. (1993). The sensory role of the anterior

- cruciate ligament. In: The anterior cruciate ligament: current and future concepts. Ed. Jackson DW. Raven Press. New York. : 23-33.
- [108] Maeda A., Inoue M., Shino K., Nakata K., Nakamura H., Tanaka M., Seguchi Y. and Ono K. (1993). Effects of solvent preservation with or without gamma irradiation on the material properties of canine tendon allografts. *J Orthop Res.* 11: 181-189.
- [109] Mandel J. (1978). Propriétés mécaniques des matériaux. Editions Eyrolles.
- [110] Marcuse D. (1981). Principles of optical fiber measurements. Academic press.
- [111] Markolf K. L., Gorek J. F., Kabo J. M. and Shapiro M. S. (1990). Direct measurement of resultant forces in the anterior cruciate ligament. *J. Bone Joint Surg.* 72-A(4): 557-567.
- [112] Marsden J. E. and Hughes T. J. R. (1983). Mathematical foundation of elasticity. Prentice Hall.
- [113] McDaniel W. J. and Dameron T. B. (1980). Untreated ruptures of the anterior cruciate ligament. *J. Bone Joint Surg.* 62-A(5): 696-704.
- [114] Moeinzadeh M. H., Engin A. E. and Akkas N. (1983). Two-dimensional dynamic modelling of human knee joint. *J Biomech.* 16(4): 253-264.
- [115] Mommersteeg T. J. A., Blankevoort L., Huiskes R., Kooloos J. G. M. and Kauer J. M. G. (1996). Characterization of the mechanical behavior of human knee ligaments: a numerical-experimental approach. *J Biomech.* 29(2): 151-160.
- [116] Nagineni C. N., Amiel D., Green M. H., Berchuck M. and Akeson W. H. (1992). Characterization of the intrinsic properties of the anterior cruciate and medial collateral ligament cells: an in vitro cell study. *J Orthop Res.* 10(4): 465-475.
- [117] Noll W. (1958). A mathematical theory of the mechanical of continuous media. *Arch Rational Mech Anal.* 2: 199-226.
- [118] Nowalk M. D. and Logan S. E. (1991). Distinguishing biomechanical properties of intrinsic and extrinsic human wrist ligaments. *J Biomech Engng.* 113: 85-93.
- [119] Noyes F. R., Delucas J. L. and Torvik P. J. (1974). Biomechanics of anterior cruciate ligament failure. an analysis of strain-rate sensitivity and mechanisms of failure in primates. *J Bone Joint Surg.* 56-A: 236-253.
- [120] Noyes F. R. and Grood E. S. (1976). The strength of the anterior cruciate ligament in humans and rhesus monkeys. *J Bone Joint Surg.* 58-A: 1074-1082.
- [121] O'Brien S. J., Warren R. F., Pavlov H., Panariello R. and Wickiewicz T. L. (1991). Reconstruction of the chronically insufficient anterior cruciate ligament with the central third of the patellar ligament. *J Bone Joint Surg.* 73-A(2): 278-286.
- [122] O'Connor J. J. and Zavatsky A. (1993). Anterior cruciate ligament forces in activity. In: The anterior cruciate ligament: current and future concepts. Ed. Jackson DW. Raven Press. New York. : 131-140.
- [123] Oakes B. W. (1993). Collagen ultrastructure in the normal ACL and in ACL

- graft. In: The anterior cruciate ligament: current and future concepts. Ed. Jackson DW. Raven Press. New York. : 209-217.
- [124] Paulos L. E., Rosenberg T. D., Grewe S. R., Tearse D. S. and Beck C. L. (1992). The GORE-TEX anterior cruciate ligament prosthesis. A long-term followup. *AM J Sports Med.* 20(3): 246-252.
- [125] Pioletti D. P., Heegaard J. H., Rakotomanana R. L., Leyvraz P. F. and Blankevoort L. (1995). Experimental and mathematical methods for representing relative surface elongation of the ACL. *J Biomech.* 28(9): 1123-1126.
- [126] Pioletti D. P., Rakotomanana R. L. and Leyvraz P. F. (1995). Non linear viscoelastic model and experimental identification of the ACL. ASME Bioengineering Conference.
- [127] Pioletti D. P., Rakotomanana L., Gilliéron C., Leyvraz P. F. and Benvenuti J. F. (1996). Nonlinear viscoelasticity of the ACL: Experiments and theory. In *Computer Methods in Biomechanics and Biomedical Engineering*. Ed. J. Middletown. Gordon & Breach. : 271-280.
- [128] Pioletti D. P., Rakotomanana R. L., Leyvraz P. F. and Benvenuti J. F. (1997). Experimental measurement of static and dynamic tangent moduli of the ACL. *J Bone Joint Surg.* 79-B(Supplement I): 4.
- [129] Pipkin A. C. and Rivlin R. S. (1960). The formulation of constitutive equations in continuum physics. *Arch Rational Mech Anal.* 4: 129-144.
- [130] Rabotnov Y. N. (1977). Elements of hereditary solid mechanics. Mir Publisher.
- [131] Race A. and Amis A. A. (1994). The mechanical properties of the two bundles of the human posterior cruciate ligament. *J Biomech.* 27(1): 13-24.
- [132] Roberts C. S., Cummings J. F., Grood E. S. and Noyes F. R. (1994). In-vivo measurement of human anterior cruciate ligament forces during knee extension exercises. 40th ORS.
- [133] Robson M. A. (1903). Ruptured crucial ligaments and their repair by operation. *Ann Surg.* 37: 716-718.
- [134] Romano V. M., Graf B. K., Keene J. S. and Lange R. H. (1993). Anterior cruciate ligament reconstruction. The effect of tibial tunnel placement on range of motion. *Am J Sports Med.* 21(3): 415-418.
- [135] Sanjeevi R. (1982). A viscoelastic model for the mechanical properties of biological materials. *J Biomech.* 15(2): 107-109.
- [136] Sauren A. A. H. J. and Rousseau E. P. M. (1983). A concise sensitivity analysis of the quasi-linear viscoelastic model proposed by Fung. *J biomech Engng.* 105: 92-95.
- [137] Selvik G. (1974). Roentgen stereophotogrammatry. A method for the study of the kinematics of the skeletal system. *Thesis*. University of Lund.
- [138] Siarry P. (1989). Automatique de base. ellipse.

- [139] Sidles J. A., Larson R., Garbini J., Downey D. J. and Matsen F. A. (1988). Ligament length relationships in the moving knee. *J Orthop Res.* 6: 593-610.
- [140] Soden P. D. and Kershaw I. (1974). Tensile testing of connective tissues. *Med Biol Eng.* : 510-518.
- [141] Sommerlath K., Odensten M. and Lysholm J. (1992). The late course of acute partial anterior cruciate ligament tears. (A nine to 15-year follow-up evaluation). *Clin Ortho.* 281(8): 152-158.
- [142] Speer K. P., Warren R. F., Wickiewicz T. L., Horowitz L. and Henderson L. (1995). Observation on the injury mechanism of anterior cruciate ligament tears in skiers. *Am J Sports Med.* 23(1): 77-81.
- [143] Stouffer D. C., Butler D. L. and Kim H. (1983). Tension-torsion characteristics of the canine anterior cruciate ligament-part I: theoretical framework. *J Biomech Engng.* 105: 154-159.
- [144] Takai S., Woo S. L. Y., Livesay G. A., Adams D. J. and Fu F. H. (1993). Determination of the in situ loads on the human anterior cruciate ligament. *J Ortho Res.* 11: 686-695.
- [145] Truesdell C. and Noll W. (1992). The non-linear field theories of mechanics-second edition. Springer-Verlag.
- [146] Veronda D. R. and Westmann R. A. (1970). Mechanical characterization of skin-finite deformation. *J Biomech.* 3: 111-124.
- [147] Wascher D. C., Markolf K. T., Shapiro M. S. and Finerman G. A. (1993). Direct in vitro measurement of forces in the cruciate ligaments. Part I: the effect of multiplane loading in the intact knee. *J. Bone Joint Surg.* 75-A(3): 377-386.
- [148] Weiss J. A. (1994). A constitutive model and finite element representation for transversely isotropic soft tissues. *Thesis.* University of Utah.
- [149] Wismans J., Veldpaus F., Janssen J., Huson A. and Struben P. (1980). A three-dimensional mathematical model of the knee-joint. *J Biomech.* 13(8): 677-685.
- [150] Woo S. L. Y., Gomez M. A. and Akeson W. H. (1981). The time and history-dependent viscoelastic properties of the canine medial collateral ligaments. *J Biomech Engng.* 103: 293-298.
- [151] Woo S. L. Y. (1986). Biomechanics of tendons and ligaments. Ed. G.W. Schmid-Schönbein, Springer-Verlag. : 180-195.
- [152] Woo S. L. Y., Orlando C. A., Camp J. F. and Akeson W. H. (1986). Effects of postmortem storage by freezing on ligament tensile behavior. *J Biomech.* 19(5): 399-404.
- [153] Woo S. L. Y., Hollis J. M., Roux R. D., Gomez M. A., Inoue M., Kleiner J. B. and Akeson W. H. (1987). Effects of knee flexion on the structural properties of the rabbit femur-anterior cruciate ligament-tibia complex (FATC). *J Biomech.* 20(6): 557-563.
- [154] Woo S. L. Y., Danto M. I., Ohland K. J., Lee T. Q. and Newton P. Q. (1990). The

- use of a laser micrometer system to determine the cross-sectional shape and area of ligaments: a comparative study with two existing methods. *J Biomech Engng.* 112: 425-430.
- [155] Woo S. L. Y. and Blomstrom G. L. (1993). The tensile properties of the anterior cruciate ligament as a function of age. In: *The anterior cruciate ligament: current and future concepts*. Ed. Jackson DW. Raven Press. New York. : 53-61.
- [156] Yahia L. H., Pigeon P. and DesRosiers E. A. (1993). Viscoelastic properties of the human lumbodorsal fascia. *J Biomed Eng.* 15: 425-429.
- [157] Yamamoto N. and Hayashi K. (1996). Mechanical properties of rabbit patellar tendon at high strain rates.

APPENDIX A *Mathematical background of the long term memory effects*

The following theory was mainly obtained from the work of Truesdell and Noll e.g. [Truesdell, 1992].

A. 1 Three general principles

In a strict mechanical point of view (thermal, chemical and electrical effects neglected), the stress \mathbf{S} in a body is given by the history of the motion χ of that body (*principle of determinism*):

$$\mathbf{S}(t) = \mathfrak{S}'_{s=0}^{\infty}\{\chi(t-s)\} \quad (\text{A.1})$$

\mathfrak{S}' is a functional representing the history of the motion. Equation (A.1) is a general constitutive equation without any internal constraint.

The *principle of local action* could be expressed by the following: in determining the stress at a given particle \mathbf{x} , the motion outside an arbitrary neighborhood of \mathbf{x} may be disregarded. Consequently, this principle enables to approximate χ by its directional derivative and (A.1) can be expressed by:

$$\mathbf{S}(t) = \wp_{s=0}^{\infty}\{\mathbf{F}(t-s)\} \quad (\text{A.2})$$

\wp is a functional representing the history of the deformation gradient \mathbf{F} . A material where the stress depends only on the deformation gradient is called a simple material.

The *principle of material frame-indifference* (or equivalently called the objectivity of the constitutive law) is necessary especially in case of large deformations. This requirement is automatically satisfied if the constitutive law is express in term of objective tensors. Postulating constitutive law between the stress \mathbf{S} and the deformation \mathbf{C} enables the fulfillment of the objectivity requirement.

Consequently, the three general principles governing the mechanical behaviour of a material are satisfied when postulating constitutive law of the kind:

$$S(t) = \mathfrak{S}_{s=0}^{\infty}\{C(t-s)\} \quad (\text{A.3})$$

where \mathfrak{S} is a functional representing the history of the material strain tensor.

Equation (A.3) can be rewritten as:

$$S(t) = S_e(C(t)) + \mathfrak{S}_{s=0}^{\infty}\{G(t-s);C(t)\} \quad (\text{A.4})$$

where $G(t-s) = C(t-s) - C(t)$ describes a deformation history and $S_e(C(t))$ represents an “equilibrium term”. In fact this term can be considered as the *elastic* response as it supports the contribution of the deformation at the actual time t (immediate contribution). Notation in (A.4) means that $G(t-s)$ is a variable and $C(t)$ is a parameter.

A. 2 Mathematical interpretation of the fading memory principle

The principle of fading memory can be interpreted as a requirement of smoothness for the functional response \mathfrak{S} . To make precise the notion of smoothness, a topology must be introduced in the space functions characterizing the history of the deformation, i.e. it is necessary to have a way of knowing when two histories are close to each other. This is achieved by defining a norm. Before, the function $h(s)$ called an *influence function* is defined. $h(s)$ characterizes the rate at which the memory fades. This function has to verify:

$$1) h(0) = 1 \text{ (normalization)} \quad (\text{A.5})$$

$$2) \lim_{s \rightarrow \infty} s^r h(s) = 0 \quad (\text{A.6})$$

As example, $h(s) = e^{-\beta s}$ with $\beta > 0$ is an influence function.

The norm of the deformation history $G(s)$ is defined by:

$$\|G(s)\|^2 = \int_0^{\infty} |G(s)|^2 h^2(s) ds \quad (\text{A.7})$$

with

$$|G(s)| = \sqrt{\text{tr}|G(s)|^2} \quad (\text{A.8})$$

The concept of fading memory is automatically satisfied with this norm definition. The principle of fading memory can hence be defined as the following: there exists an influence function $h(s)$ of order r (c.f. (A.6)) such that the response functional

$\mathfrak{S}\{G(s)\}$ is defined and π times Fréchet-differentiable in a neighborhood of the zero history of the space function. The collection of all the histories with finite norm given by (A.7) forms an Hilbert space H .

When $\pi = 1$, the response functional \mathfrak{S} reduces to a single term. Consequently, \mathfrak{S} is one time Fréchet-differentiable if there is a continuous linear function $\delta\mathfrak{S}$ such that (variable t removed for clarity):

$$\mathfrak{S}_{s=0}^{\infty}\{G(s);C\} = \delta\mathfrak{S}_{s=0}^{\infty}\{G(s);C\} + \mathfrak{R}_{s=0}^{\infty}\{G(s);C\} \quad (\text{A.9})$$

with

$$\lim_{\|G(s)\|^2 \rightarrow 0} \|G(s)\|^{-1} \mathfrak{R}_{s=0}^{\infty}\{G(s)\} = 0$$

$\delta\mathfrak{S}$ is called the first variation or Fréchet differential of \mathfrak{S} . It is a continuous linear functional.

In the general case, the first variation is expressed by:

$$\delta\mathfrak{S}_{s=0}^{\infty}\{G(s);C\} = \int_0^{\infty} \Sigma(G(s), s;C) ds \quad (\text{A.10})$$

where Σ is a tensor-valued function with the variables G and s and the parameter C . Equation (A.4) can be rewritten as:

$$S = S_e(C) + \int_0^{\infty} \Sigma(G(s), s;C) ds \quad (\text{A.11})$$

In the particular case where the tensor-valued function Σ is linear, the theorem of the theory of Hilbert spaces states that every continuous linear functional may be written as an inner product:

$$\delta\mathfrak{S}_{s=0}^{\infty}\{G(s);C\} = \int_0^{\infty} \Gamma(C;s)[G(s)] ds \quad (\text{A.12})$$

where $\Gamma(C;s)[\dots]$ for each choice of $s \geq 0$ and C , is a linear functional of one tensor variable. Equation (A.4) can be rewritten in the linear case as:

$$S = S_e(C) + \int_0^{\infty} \Gamma(C;s)[G(s)] ds \quad (\text{A.13})$$

Equation (A.13) is called the finite linear viscoelasticity.

APPENDIX B *Elastic potentials tested in the compressible case*

The elastic identification is performed first by postulating an elastic potential. Five conditions must then be verified to get an admissible constitutive law:

- a) $S(\mathbf{I}) = \mathbf{0}$
- b) $S_{22} = 0$
- c) $C_{11} > 1 \Rightarrow C_{22} < 1$
- d) correct stress-strain curve fit
- e) convexity of the potential

In the following Table, we present the tested potentials with the conditions satisfied and not satisfied. The notation \tilde{Exp} means that the exponential function is replaced by its third order limited development (LD).

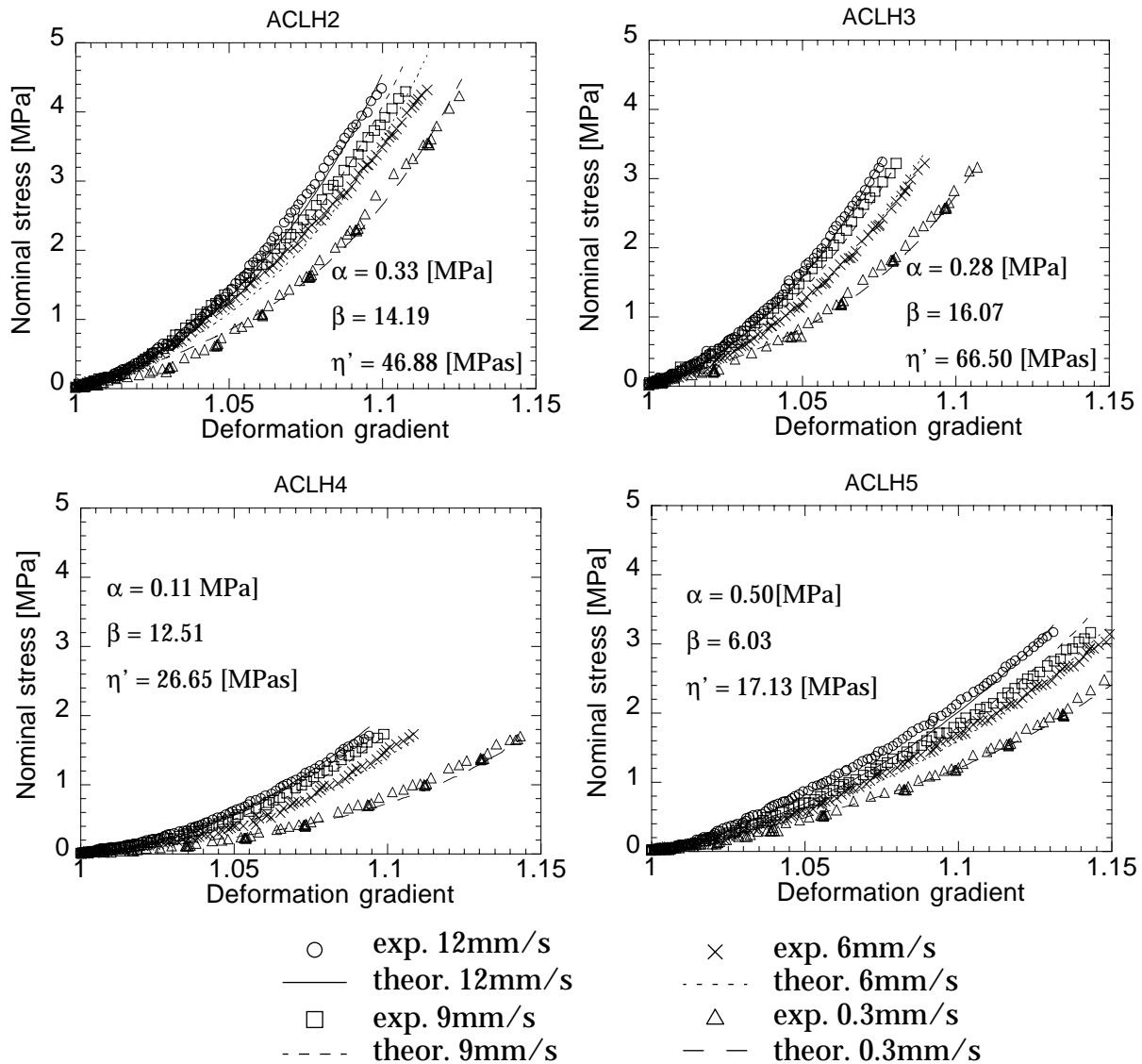
Elastic potentials tested in the compressible case

Type	Elastic potential	correct	incorrect
Poly.	$W = \alpha(I_1 - 3) + \beta(I_2 - 3)$	a,b,c,e	d
	$W = \frac{\alpha}{2}(I_1 - 3) + \frac{\beta}{2}(I_2 - 3) - (\alpha + 2\beta)(I_3 - 1)$	a,b,c,d	e
	$W = \frac{\alpha}{2}(I_1 - 3) + \frac{\beta}{2}(I_1 - 3)^2 + \frac{\gamma}{2}(I_2 - 3) + \frac{\varepsilon}{2}(I_3 - 1)$	a,b	d
	$W = \frac{\alpha}{2}(I_1 - 3) + \frac{\beta}{2}(I_1 - 3)^2 - \frac{\alpha}{2}(I_2 - 3)$	a,b	d
	$W = \frac{\alpha}{2}(I_1 - 3) + \frac{\beta}{2}(I_1 - 3)^2 + \frac{\alpha}{2}(I_2 - 3)$	a,b	d
Loga.	$W = \frac{\alpha}{2}(I_3 - \log I_3) + \frac{\beta}{4}(I_1 - 3)^2$	a,b	d
Expo.	$W = \frac{\alpha}{2\beta}\{Exp[\beta(I_1 - 3)(I_3 - 1)] - 1\}$	a,b,c,d	e
	$W = \frac{\alpha}{2\beta}\{Exp[\beta((I_1 - 3) - (I_3 - 1))] - 1\}$	a,b,c,d	e
	$W = \alpha\{Exp[\beta((I_1 - 3) - 2(I_2 - 3))] - 1\}$	a,b,c,d	e
	$W = \frac{\alpha}{2\beta}\{Exp[\beta(I_1 - 3)(I_2 - 3)] - 1\}$	a,b	d,e
	$W = \frac{\alpha}{2}\{Exp[\beta(I_1 - 3) + \gamma(I_2 - 3) - (\beta + 2\gamma)(I_3 - 1)] - 1\}$	a,b,d	e
	$W = \alpha Exp[\beta(I_1 - 3)](I_2 - 3)$		a
	$W = \alpha Exp[\beta(I_1 - 3)](I_3 - 1)$		a
	$W = \frac{\alpha}{2} Exp[\beta(I_1 - 3)]\{(I_1 - 3) - 0.5(I_2 - 3)\}$	a,b,c,d	e
	$W = \frac{\alpha}{2} Exp[\beta(I_1 - 3)]\{(I_1 - 3) - (I_3 - 1)\}$	a,b,c,d	e
LD Expo.	$W = \alpha\{\tilde{Exp}[\beta(I_1 - 3)] - 1\} - \frac{\alpha\beta}{2}(I_2 - 3)$	a,b,d,e	c
	$W = \alpha\{\tilde{Exp}[\beta(I_1 - 3)] - 1\} - \alpha\beta(I_3 - 1)$	a,b,d	c
	$W = \alpha\{\tilde{Exp}[\beta(I_1 - 3)] - 1\} - \alpha\beta((I_2 - 3) - (I_3 - 1))$	a,b,c,d	e

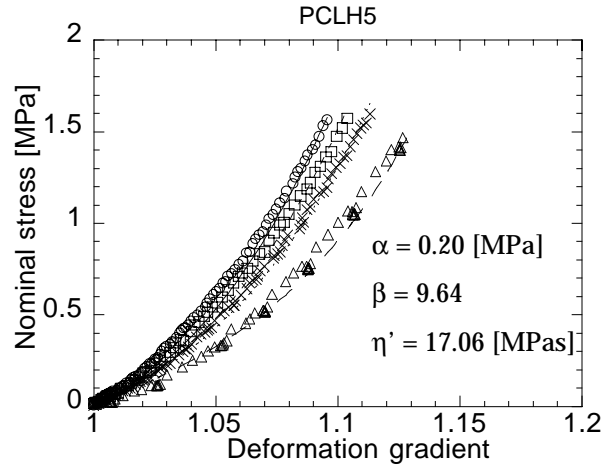
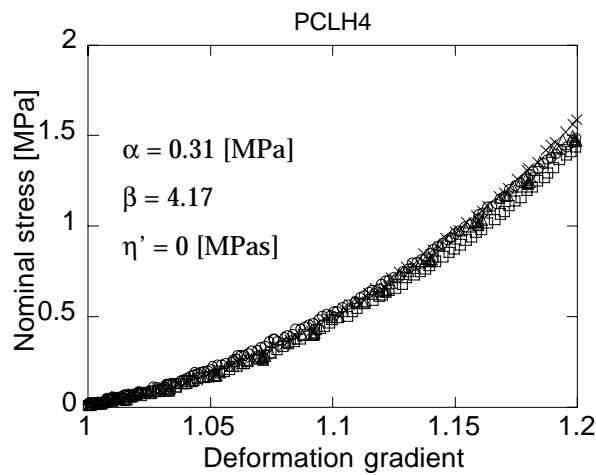
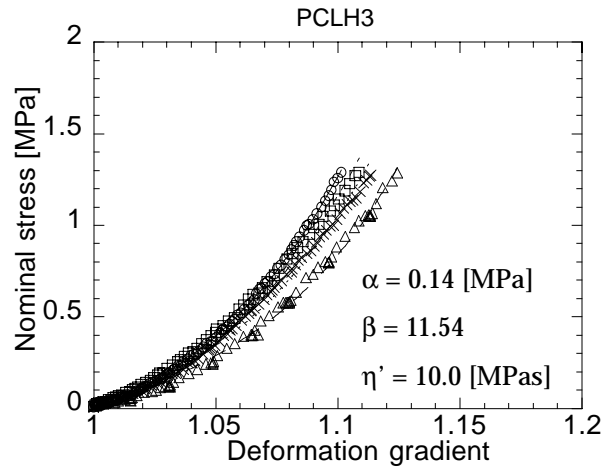
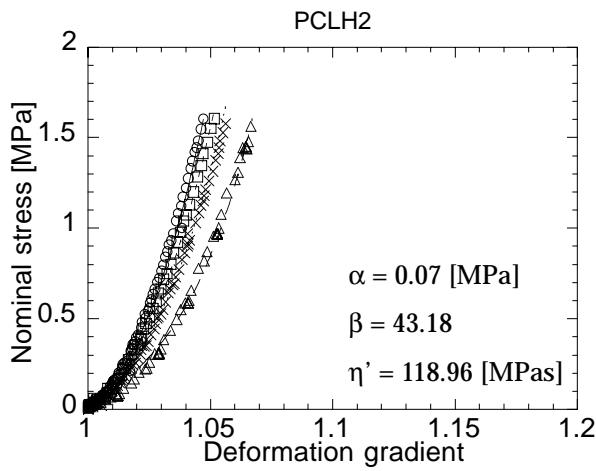
APPENDIX C *Elastic, short term memory effects and long term memory effects identification*

C. 1 Elastic and short term memory effects identification

C. 1.1 ACL

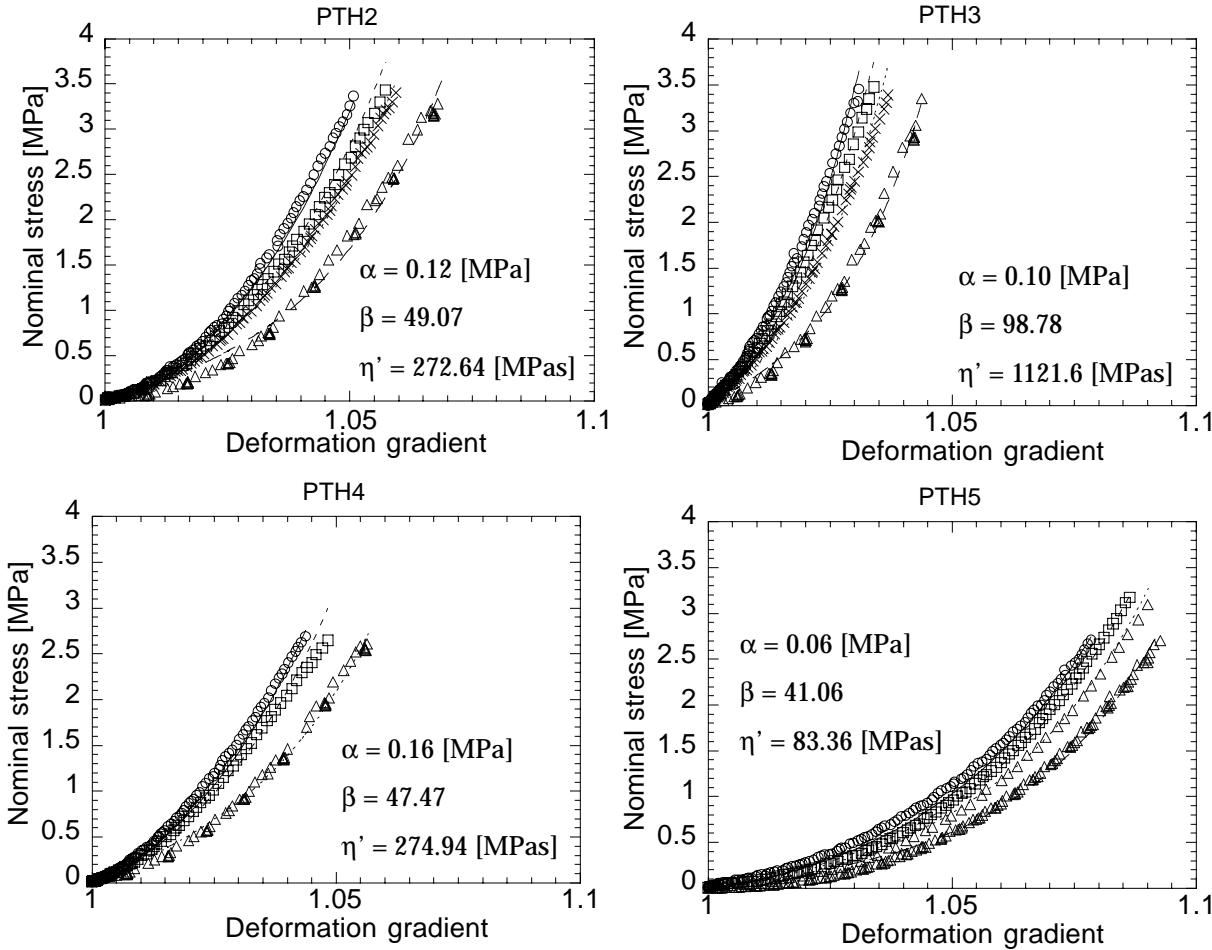


C. 1. 2 PCL



- exp. 12mm/s
- theor. 12mm/s
- exp. 9mm/s
- - - theor. 9mm/s
- × exp. 6mm/s
- · - · theor. 6mm/s
- △ exp. 0.3mm/s
- - - theor. 0.3mm/s

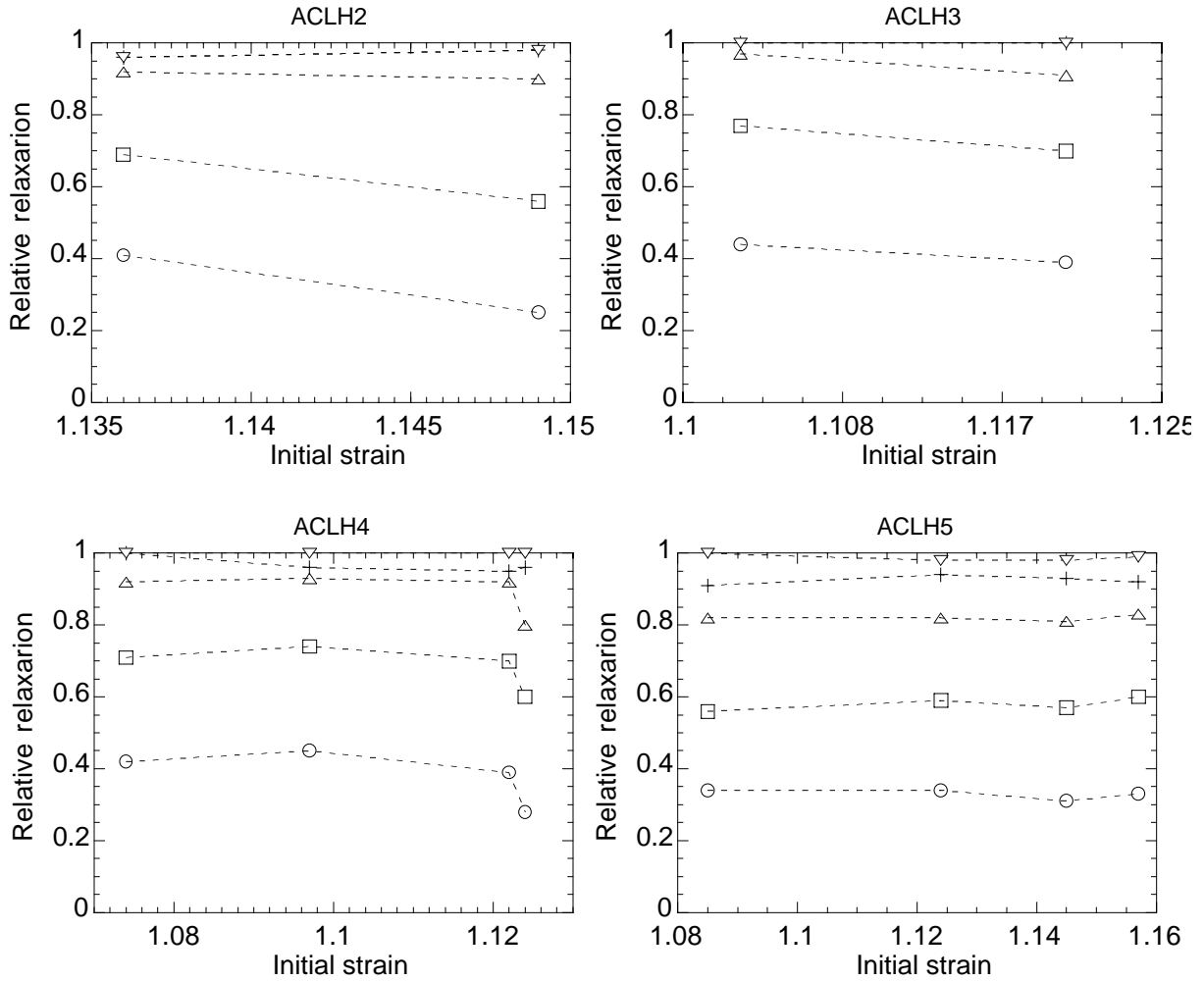
C. 1. 3 PT



- exp. 12mm/s
- theor. 12mm/s
- exp. 9mm/s
- - - theor. 9mm/s
- × exp. 6mm/s
- · - · theor. 6mm/s
- △ exp. 0.3mm/s
- - - theor. 0.3mm/s

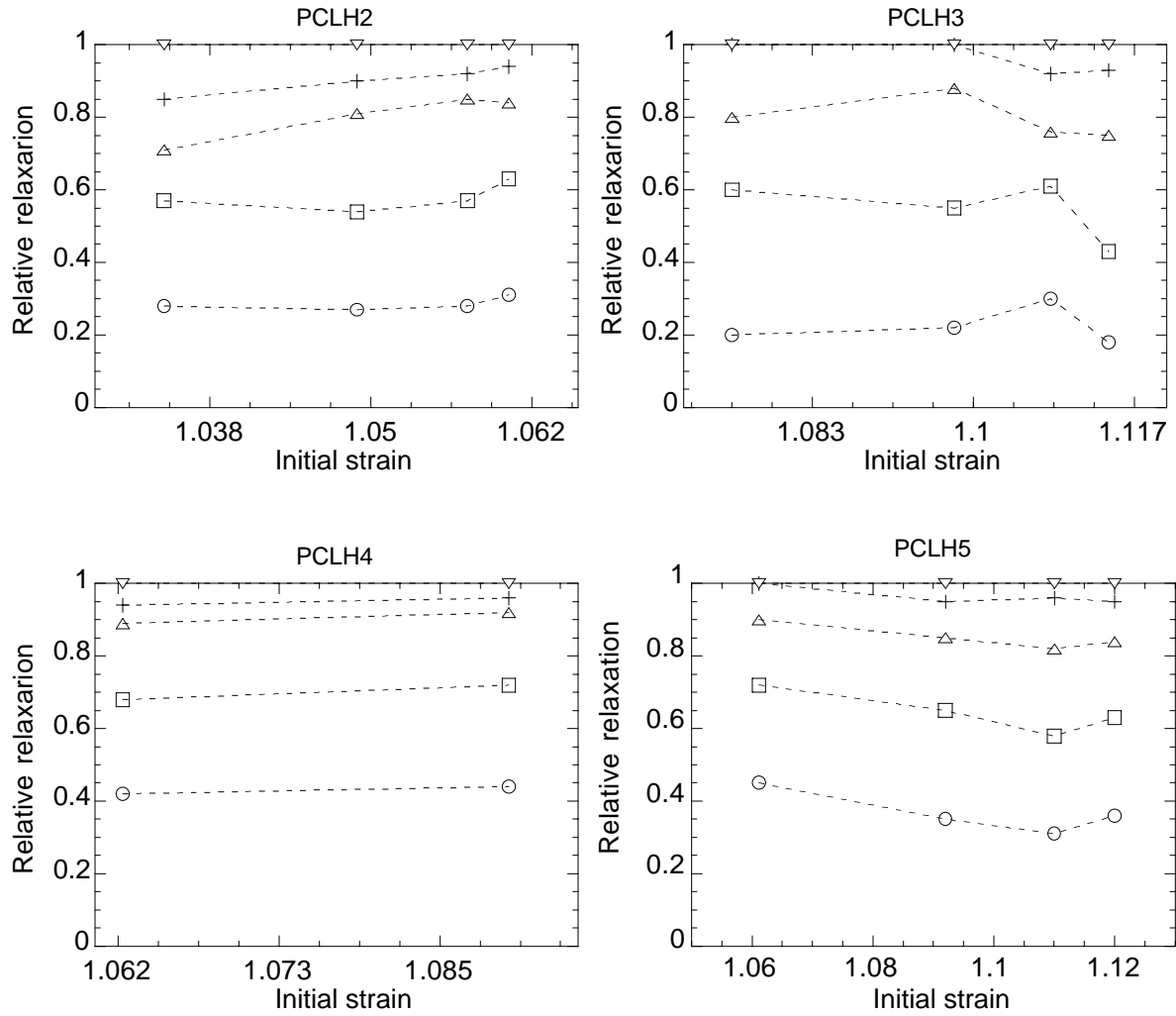
C. 2 Relative relaxation

C. 2.1 ACL



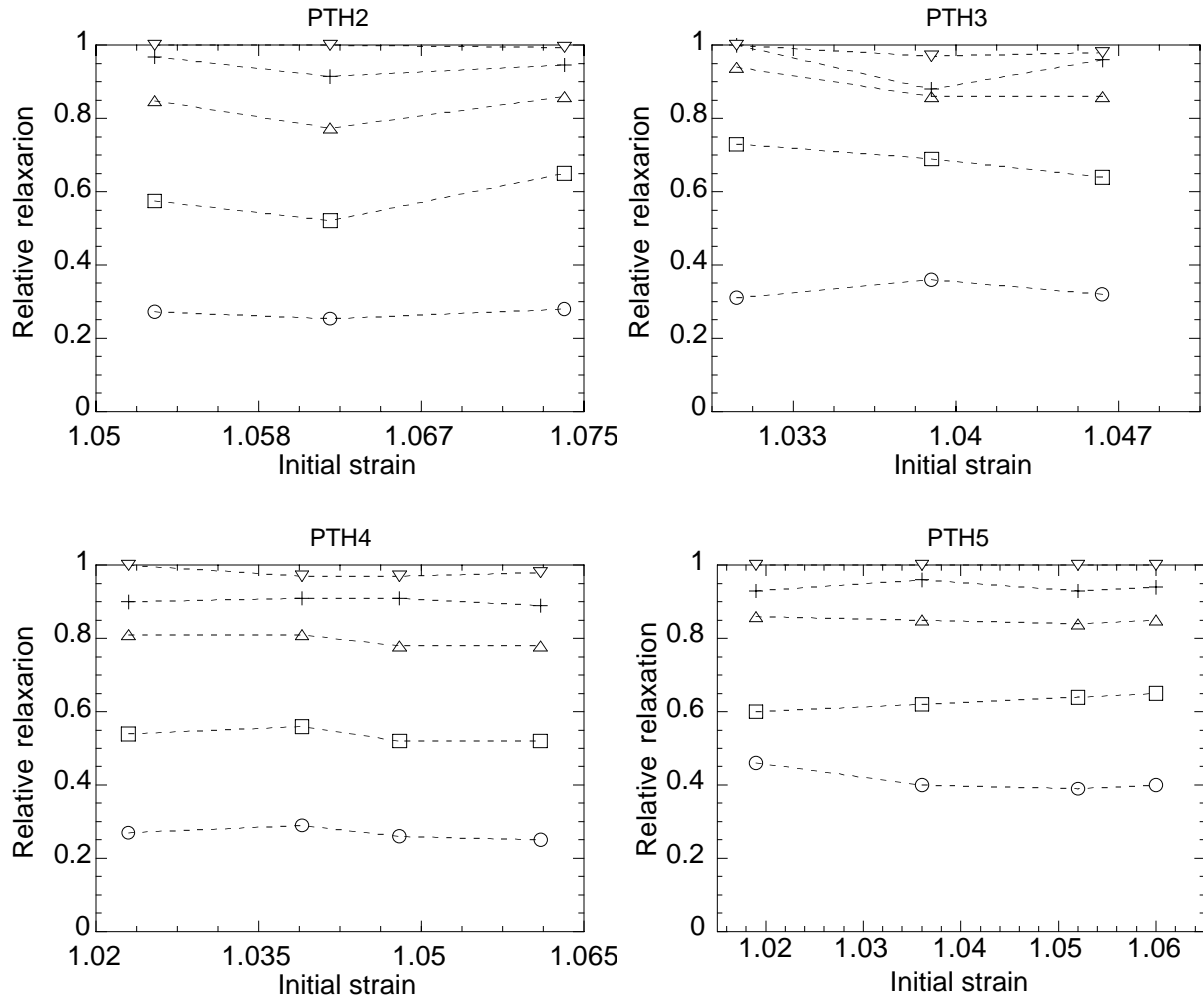
- t = 10 seconds
- t = 100 seconds
- △ t = 500 seconds
- + t = 1000 seconds
- ▽ t = 1500 seconds

C. 2. 2 PCL



- t = 10 seconds
- t = 100 seconds
- △ t = 500 seconds
- + t = 1000 seconds
- ▽ t = 1500 seconds

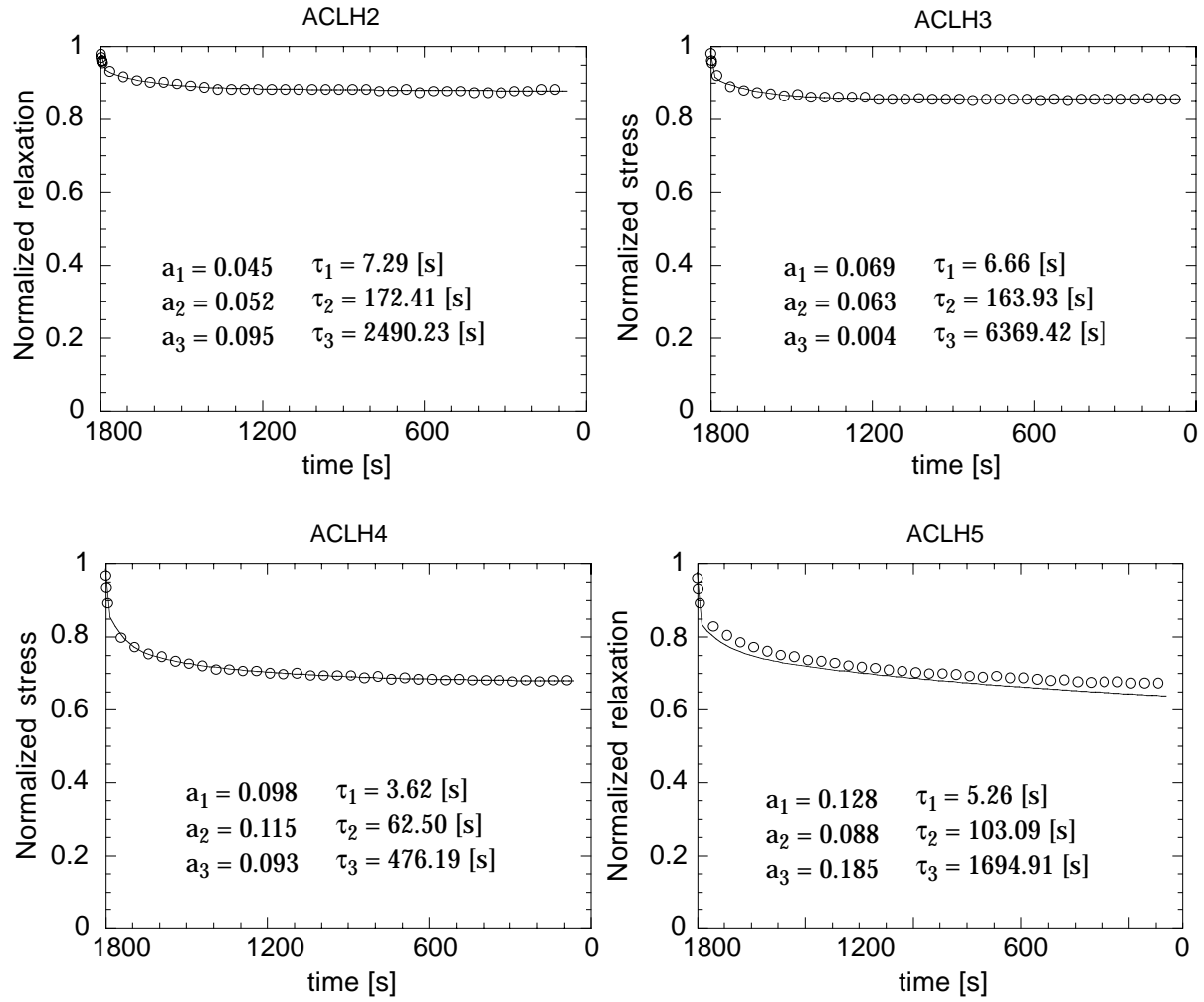
C. 2. 3 PT



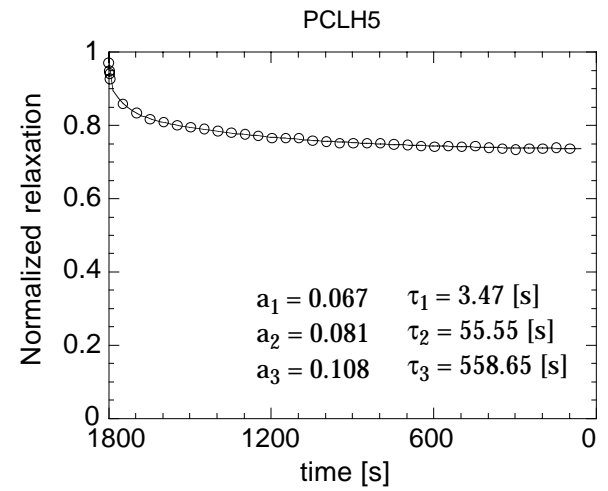
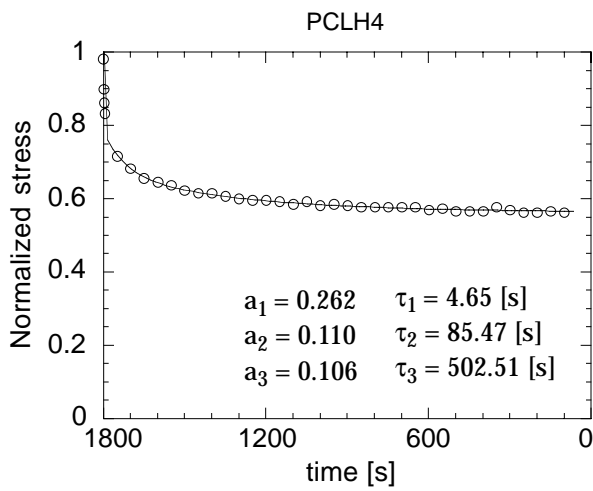
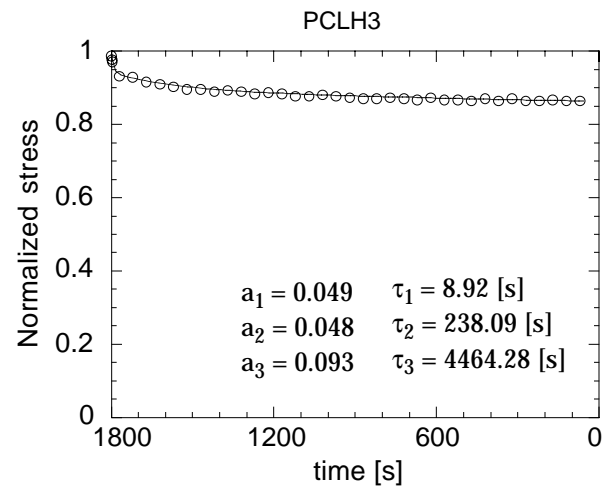
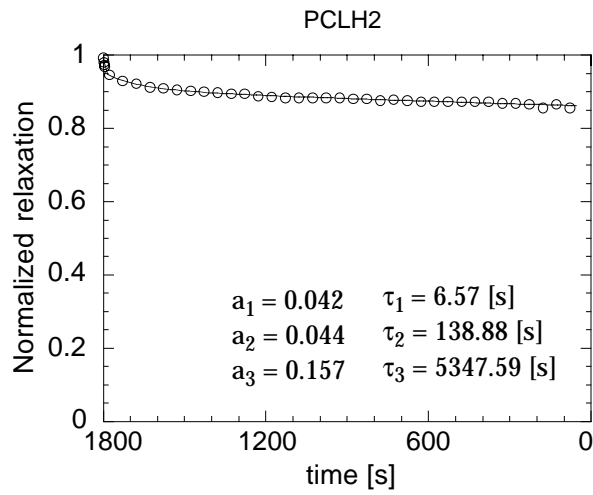
- t = 10 seconds
- t = 100 seconds
- △ t = 500 seconds
- + t = 1000 seconds
- ▽ t = 1500 seconds

C. 3 Long term memory effects identification

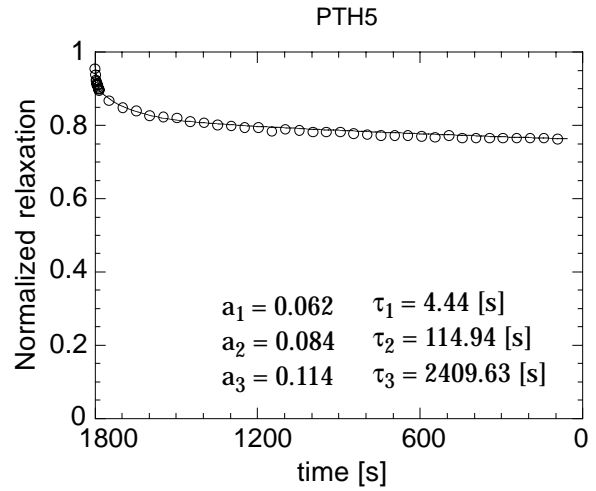
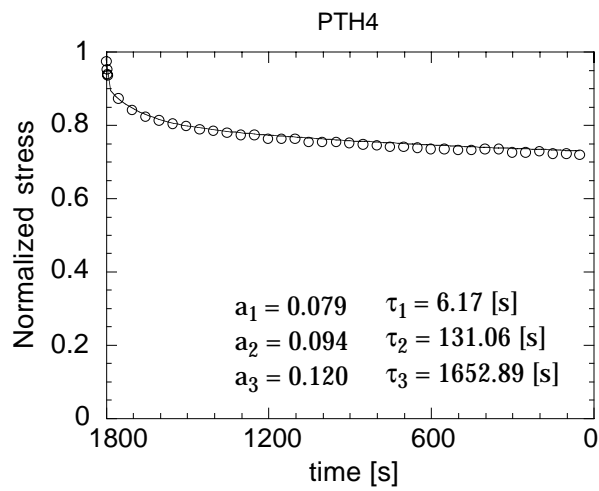
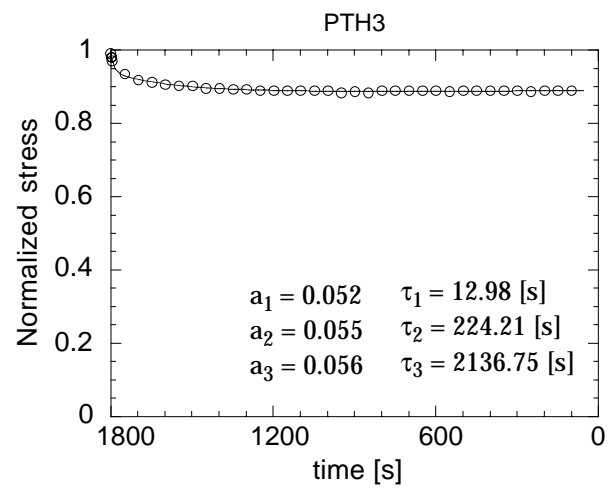
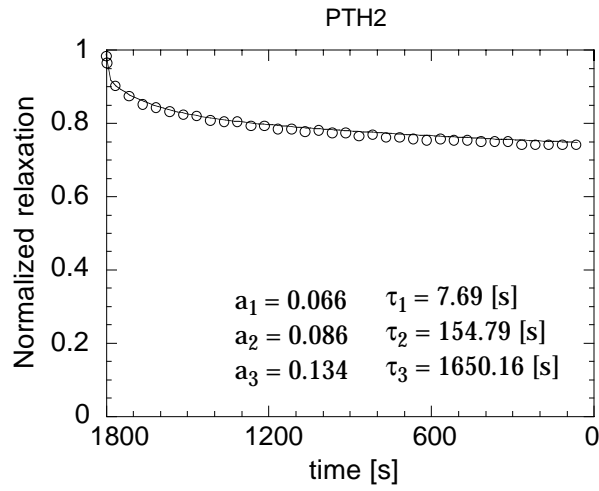
C. 3.1 ACL



C. 3. 2 PCL



C. 3. 3 PT



CURRICULUM VITAE

DOMINIQUE P. PIOLETTI

- Date de naissance : 31 août 1967
- Lieu de naissance : Lausanne
- Nationalité : suisse et italienne
- Etat civil : marié

Formation

- 1987 : Maturité Fédérale scientifique (Type C)
- 1992 : Diplôme d'ingénieur physicien (Dipl. phys. EPF)
Ecole Polytechnique Fédérale de Lausanne
- 1994 : Cours sur les Biomatériaux (Prof Aebischer, EPFL)
- 1994 : Cosmase Course on Computational Solid Mechanics Contact Mechanics
(Dr. Curnier, Prof. Klarbring, Prof. Wriggers)
- 1995 : Cosmase Advanced Course on Computational Fluid Dynamics (Prof. Farhat)

Activités professionnelles

- depuis février 1992 : Collaborateur scientifique à l'Hôpital Orthopédique de la Suisse Romande
- depuis février 1992 : Assistant au Laboratoire de Génie Médical de l'Institut de Physique Appliquée (EPFL)

Publications

- Pioletti DP, Heegaard JH, Rakotomanana RL, and Leyvraz PF. (1994). "Cinématique et élongation continue du ligament croisé antérieur." *Revue Médicale de la Suisse Romande*, 114, 161-169.
- Pioletti DP, Heegaard JH, Rakotomanana RL, Leyvraz PF, and Blankevoort L. (1995). "Experimental and mathematical methods for representing relative surface elongation of the ACL." *J. Biomech.*, 28(9), 1123-1126.
- Pioletti DP, Rakotomanana L, Gilliéron C, Leyvraz PF, and Benvenuti JF. (1996). "Nonlinear viscoelasticity of the ACL: Experiments and theory." in: *Computer Methods in Biomechanics and Biomedical Engineering*, ed.: J. Middletown, Gordon & Breach, 271-280.
- Pioletti DP, Rakotomanana L, Benvenuti JF, and Leyvraz PF. (1997). "Finite element model of the human anterior cruciate ligament." to be published in *Computer Methods in Biomechanics and Biomedical Engineering*, ed.: J. Middletown, Gordon & Breach.
- Pioletti DP, Rakotomanana LR, Benvenuti JF, and Leyvraz PF. (1997). "Visco-elastic constitutive laws of soft tissues: combination of short and long time memory effects." to be published in *IEEE Transaction of 16th Southern Biomedical Engineering*.
- Pioletti DP, Rakotomanana LR, Dahlgren P, Valloton J, and Leyvraz PF. (1997). "Intrinsic coordinate system for the tibial plateau." accepted with revision in *The Knee*.
- Pioletti DP, Rakotomanana LR and Leyvraz PF. (1997). "Strain rate effects on the mechanical behavior of the anterior cruciate ligament." submitted to *Annals of Biomed. Eng.*
- Lemaire P, Pioletti DP, Meyer FM, Meuli R, Dörfel J, and Leyvraz PF. (1997). "Tibial component positioning in TKA: bone coverage and extensor apparatus alignment." to be published in *Knee Surg Sports Traum Arthro*.
- Benvenuti JF, Rakotomanana L, Leyvraz PF, Pioletti DP, Heegaard JH, and Genton MG. (1997) "Displacement of the tibial tuberosity: effects of the surgical parameters", to be published in *Clin Orthop Rel Res*.

Abstracts

- Pioletti DP, Heegaard JH, Rakotomanana RL, Leyvraz PF, and Blankevoort L. (1993) "Surface relative elongation of the ACL." *Proc. 3rd EORS*, Paris, 66.
- Pioletti DP, Heegaard JH, Rakotomanana RL, Leyvraz PF, and Blankevoort L. (1994) "Relative elongation of the ACL surface." *Proc. 2nd World Congress of Biomechanics*, Amsterdam, 226a.
- Pioletti DP, Rakotomanana L, Gilliéron C, Leyvraz PF, and Benvenuti JF. (1994). "Propriétés viscoélastiques du LCA: approche expérimentale." *Arch. Physiol. and Biochem.*, Clermont-Ferrand, C104.
- Pioletti DP, Heegaard JH, Rakotomanana RL, Leyvraz PF, and Blankevoort L. (1994) "Relative elongation of the ACL surface." *Proc. 40th ORS*, New Orleans, 608.

Pioletti DP, Rakotomanana RL, Lauper F, and Leyvraz PF. (1995). "Modélisation et identification des propriétés viscoélastiques non linéaires du ligament croisé antérieur." *Arch. Physiol. and Biochem.*, 103(3), Lausanne, C51.

Pioletti DP, Rakotomanana RL, and Leyvraz PF. (1995) "Non linear viscoelastic model and experimental identification of the ACL." *ASME Bioengineering*, San Francisco, 35-36.

Pioletti DP, Rakotomanana RL, Leyvraz PF, and Benvenuti JF. (1995) "Ligament croisé antérieur: matériau élastique non linéaire." *55ème Congrès Société suisse d'orthopédie*, Genève, 35.

Pioletti DP, Lauper L, Rakotomanana L, and Leyvraz PF. (1996). "Viscosité à mémoire longue des ligaments croisés antérieurs: modélisation et identification expérimentale." *Arch. Physio. Biochem.*, 104(5), Nancy, 607.

Pioletti DP, Leyvraz PF, and Rakotomanana L. (1996) "Review of the biomechanical properties of the ligaments." *2nd Basel International knee congress and instructional course*, Bâle.

Pioletti DP, Meyer FM, Leyvraz PF, and Lemaire P. (1996). "Transepicondylar axis as rotational guide in TKA." *Acta. Orthop. Scand.*, 67(272), Bergen, 90.

Pioletti DP, Rakotomanana RL, Leyvraz PF, and Benvenuti JF. (1997). "Experimental measurement of static and dynamic tangent moduli of the ACL." *J. Bone Joint Surg.*, 79-B(Supplement I), Munich, 4.

Benvenuti JF, Heegaard JH, Rakotomanana LR, Pioletti DP, and Leyvraz PF. (1994) "Effects of shingle length and tubercle elevation in Maquet procedure on patella kinematics and interface peak pressure." *Proc. 2nd World Congress of Biomechanics*, Amsterdam, 296b.

Benvenuti JF, Leyvraz PF, Rakotomanana L, Pioletti D, and Heegaard JH. (1995). "Déplacement de la tubérosité tibiale: effets des paramètres chirurgicaux." *Arch. Physiol. and Biochem.*, 103(3), Lausanne, C56.

Benvenuti JF, Leyvraz PF, Rakotomanana L, Pioletti D, and Heegaard JH. (1995) "Déplacement de la tubérosité tibiale: effets des paramètres chirurgicaux." *55ème Congrès Société suisse d'orthopédie*, Genève, 31.

Benvenuti JF, Holm M, Rakotomanana L, Pioletti DP, and Leyvraz PF. (1996). "Description invariante des rotations: application à la cinématique in vitro du genou." *Arch. Physio. and Biochem.*, 104(5), Nancy, 665.

Benvenuti JF, Rakotomanana LR, Pioletti DP, Holm M, and Leyvraz PF. (1997) "Invariant description of rotations: application to the in vitro knee kinematics after ACL dissection." *Proc. 7th EORS*, Barcelone.

Heegaard JH, Leyvraz PF, Curnier A, Rakotomanana RL, Pioletti DP, and Huiskes R. (1994) "A mathematical model for articular biomechanics: application to the patello-femoral joint." *Proc. 40th ORS*, New Orleans, 88.

Heegaard JH, Leyvraz PF, Pioletti D, Rakotomanana L, and van Kampen A. (1994) "Patellar stability following Insall-Burstein knee replacement." *Proc. 2nd World Congress of Bio-*

mechanics, Amsterdam, 251b.

Lemaire P, Pioletti DP, Meyer FM, and Leyvraz PF. (1996) "Position du composant tibial dans une arthroplastie totale du genou: recouvrement optimal versus alignement sur la tubérosité antérieure du tibia." *56ème Congrès Société suisse d'orthopédie*, Berne, 53.

Lemaire P, Pioletti DP, Meyer FM, Leyvraz PF, and Benvenuti JF. (1996). "Tibial component positioning in total knee arthroplasty." *Acta Orthop Scand*, 67(272), Bergen, 90-91.

Leyvraz PF, Pioletti DP, and Lemaire P. (1996) "Rotational tibial component positioning in TKR." *2nd Basel International knee congress and instructional course*, Bâle.